Please do not adjust margins

Chemical Society Reviews

REVIEW

Aerosol processing: a wind of innovation in the field of advanced heterogeneous catalysts

Received 00th January 20xx,
Accepted 00th January 20xx

DOI: 10.1039/x0xx00000x

www.rsc.org/

Damien P. Debecker,[a,*] Solène Le Bras,[a] Cédric Boissière,[b] Alexandra Chaumonnot,[c] Clément Sanchez[b*]

Aerosol processing is long known and implemented industrially to obtain various types of divided materials and nanomaterials. The atomisation of a liquid solution or suspension produces a mist of aerosol droplets which can then be transformed via a diversity of processes including spray-drying, spray pyrolysis, flame spray pyrolysis, thermal decomposition, micronisation, gas atomisation, etc. The attractive technical features of these aerosol processes make them highly interesting for the continuous, large scale, and tailored production of heterogeneous catalysts. Indeed, during aerosol processing, each liquid droplet undergoes well-controlled physical and chemical transformations, allowing for example to dry and aggregate pre-existing solid particles or to synthesise new micro- or nanoparticles from mixtures of molecular or colloidal precursors. In the last two decades, more advanced reactive aerosol processes have emerged as innovative means to synthesise tailored-made nanomaterials with tunable surface properties, textures, compositions, etc. In particular, the "aerosol-assisted sol-gel" process (AASG) has demonstrated tremendous potential for the preparation of high-performance heterogeneous catalysts. The method is mainly based on the low-cost, scalable, and environmentally benign sol-gel chemistry process, often coupled with the evaporation-induced self-assembly (EISA) concept. It allows producing micronic or submicronic, inorganic or hybrid organic-inorganic particles bearing tuneable and calibrated porous structures at different scale. In addition, pre-formed nanoparticles can be easily incorporated or formed in a "one-pot" bottom-up approach within the porous inorganic or hybrid spheres produced by such spray drying method. Thus, multifunctional catalysts with tailored catalytic activities can be prepared in a relatively simple way. This account is an overview of aerosol processed heteroegneous catalysts which demonstrated interesting performance in various relevant chemical reactions like isomerisation, hydrogenation, olefin metathesis, pollutant total oxidation, selective oxidation, CO_2 methanation, etc. A short survey of patents and industrial applications is also presented. Our objective is to demonstrate the tremendous possibilities offered by the coupling between bottom up synthesis routes and these aerosol processing technologies which will most probably represent a major route of innovation in the mushrooming field of catalyst preparation research.

1. Introduction

Chemists have demonstrated that materials and nanomaterials with complex hierarchical structures and textures can be finely tailored through bottom-up and sometimes « bioinspired » chemical strategies.[1-5] The resulting advanced functional materials are playing an important role in the development of energy and environmental sciences and nanomedicine. Numerous fields are targeted, such as sensing, separation, sorption, electrochemical and photoelectrochemical devices for energy conversion and storage, controlled release, nanobiomaterials, smart therapeutic carriers, and of course heterogeneous catalysis.[6-8]

Porous materials presenting multimodal or multiscale porosity are of major interest, for catalysis, fuel cells, batteries, and separation processes, for which optimisation of the diffusion and confinement regimes is required.[9] In this context, the development of bottom-up strategies such as sol-gel chemistry routes, has open a land of opportunities.[10] Various templating strategies used to control the materials textural properties include cooperative self-assembly (with molecular or polymeric surfactants), multiple templating with submicronic or micronic objects (e.g.: latex,[11-13] biotemplates like bacteria, viruses, etc.[14-17]), dynamic templating (breath figures,[18, 19] organogelation,[20, 21] microphase separation,[22, 23] nanocasting).[24] However, conventional procedures used to process nanostructured porous nanomaterials mostly rely on multi-step and time-consuming batch operations.

Modern approaches coined "integrative chemistry",[1, 2, 25-27] where chemistry and process are strongly coupled, provide the ability to design materials at several length scales, with tuned functions and adjusted complex morphologies. These new approaches integrate synergistically template directed sol-gel chemistry with a large variety of processing methodologies

[a] Université catholique de Louvain. Institute of Condensed Matter and Nanoscience. Place Louis Pasteur, 1, box L4.01.09, 1348 Louvain-La-Neuve, Belgium
damien.debecker@uclouvain.be
[b] Sorbonne Université, Collège de France, PSL University, CNRS, Laboratoire de Chimie de La Matière Condensée de Paris LCMCP, F-75005 Paris, France
clement.sanchez@college-de-france.fr
[c] IFP Energies nouvelles, établissement de Lyon, Rond-point de l'échangeur de Solaize, BP 3, 69360 Solaize, France

Please do not adjust margins

Please do not adjust margins

producing efficient materials with multiscale textures. The main processing methods reported to date concern inkjet printing,[28-32] electrospinning,[33-35] foaming,[36-40] dip-pen lithography,[41] TPA lithography,[42] multilayers deposition (via dip- or spin-coating),[43-46] 3-D printing,[47-49] and finally, aerosol processing.[50-56]

Around the year 2000, the coupling between (i) sol-gel chemistry, (ii) evaporation-induced self-assembly, and (iii) aerosol processing was envisaged as a practical way to prepare porous materials.[50, 57, 58] In such aerosol-based synthesis, the dynamic coupling between chemical and processing conditions is an important factor that controls materials on both the micro and nanostructures. In contrast to the classical solution pathways, the "aerosol-assisted sol-gel process" (AASG) involves a very limited number of preparation steps, produces material in a continuous mode, allows for a simple collection of the powder and generates low amounts of waste. Moreover, the kinetic quenching associated with droplet formation and fast drying allows for the "freezing" of materials into metastable states, which are hardly achievable by the usual precipitation method, because condensation/dissolution equilibrium usually favours the formation of the thermodynamically stable material.[59] The very short thermal treatment at relatively low temperatures associated with the aerosol process is compatible with the use of fragile organic moieties.[54] Moreover, a control over particle localisation can be achieved through an adequate functionalisation of nanoparticles and accurate control of the spray drying processing parameters.[60]

Understandably, heterogeneous catalysis is a field which takes advantage of such preparation technique that offers so many degrees of freedom to tune the properties of the materials at the nanoscale.[61] Continuously, important effort is indeed being made to develop a variety of innovative nanostructured materials which regularly open up new perspectives in catalysis.[61-69] In fact, the preparation of advanced catalytic materials by aerosol processes (spray drying, flame-aerosol processes, etc.) was already long recognised as a prime method for commercial catalyst synthesis. However, the on-purpose and controlled coupling between aerosol techniques and sol-gel chemistry is much more recent. The literature records in the past two decades evidently show that the peppy field of heterogeneous catalysis has been strongly impacted by the development of new and advanced aerosol-based methods.

In this review, we cover some historical aspects of the development of aerosol-based methods for the preparation of nanomaterials and we propose some perspectives to this mushrooming field. We first present the different types of aerosol-based preparation methods and we propose a classification: (Type I) simple drying, (Type II) precipitation, (Type III) reactive aerosol processes, and (Type IV) micronisation of metal melts. We discuss the – sometimes fuzzy – frontiers between these types of processes, and we rationalise our proposition to focus on some of these types of aerosol processes. Then, we present and discuss a comprehensive list of aerosol-made catalysts which have been successfully applied in the fields of environmental catalysis, biomass conversion, organic synthesis, petrochemistry, photocatalysis, electrocatalysis, etc. Systematically, we cover the details of the aerosol preparation procedures and we highlight the decisive properties of the aerosol-made catalysts which explain their performance.

2. Aerosol processing

2.1. The rise of aerosol processes in materials science

Aerosol processes encompass all procedures which involve the production of an aerosol, i.e. a gas-transported "mist" of liquid particles. The nature and composition of the starting material, the subsequent processing of the aerosol and the targeted final materials can differ and this gives rise to a relatively wide range of subclasses of aerosol processes (vide infra).

Spray drying has long been used to dry solid materials that are present in a liquid suspension and obtain fine or aggregated dry particles or to encapsulate active molecules.[70-73] Such techniques are widely used industrially, especially in the food industry, for example for the microencapsulation of flavours and other food ingredients[74-78] or for the production of milk or fruit juice powders,[79-82] for example. Spray drying is also used for the preservation of micro-organisms,[83-89] in the manufacture of pharmaceuticals,[90-93] or even in the large scale production of burning rate modifiers for propellants.[94] Spray drying is a traditional unit operation in chemical engineering with an important know-how about its design, automated control and scaling up.[60] Often, it can be operated at low-cost and in environmentally benign conditions.

Another particular example of aerosol process is the "gas atomisation" (and derived processes) of metals and metal alloys.[95-99] In this case, a melt stream is sprayed through a nozzle and disrupted by an inert gas to produce fine liquid droplets, which are rapidly cooled and solidified to give small spherical particles of metals or alloys. Rapid solidification allows obtaining fine microstructures, avoiding segregation effects and exploiting the possibility to produce metastable phases.

Aerosol techniques used for the synthesis of solid materials were claimed by Govers as early as in 1924,[100] and then by Behrman Abraham in 1930[101] for the preparation of divided siliceous materials. Then Ebner *et al.* in 1939 claimed a spray method for the thermal decomposition of mixtures of salts.[102] In the late 1970s, important advances were made in the field of high performance ceramics, electronic materials, and super-conducting oxides.[103] In the early development of aerosol technologies for materials synthesis, the main method was alternatingly called evaporative decomposition of solutions (EDS), spray pyrolysis (SP), flame spray pyrolysis (FSP), liquid-feed flame spray pyrolysis, (LF-FSP), high temperature aerosol decomposition (HTAD), mist decomposition (MD), aerosol thermolysis (AT), or aerosol high temperature decomposition (AHTD). It generally implied the atomisation of metal salt solutions and the rapid decomposition of the molecular precursors in a high temperature furnace or in a flame. The decisive advantage was the possibility to initiate the process

 This journal is © The Royal Society of Chemistry 20xx

Please do not adjust margins

Please do not adjust margins

with a homogeneous – aqueous or organic – solution of various metal salts (nitrates, chlorides, acetates, hydroxides, etc.), generating highly divided solid particles with controlled composition. Such techniques are currently used to prepare a range of nanomaterials at the industrial scale for various applications (including catalysts), as reviewed recently by Buesser and Pratsinis.[56] For example, flame aerosol-processed fumed silica particles serve as excipient materials in drug tablets. Similarly, the white nanoparticles of titania used as an opacifying agent in most paints are also produced by flame aerosol technology. In fact, the method provides an access to a large range of single and mixed oxide nanopowders with various morphologies.[104] As far as heterogeneous catalysts are concerned, one interesting feature of the flame aerosol technology is the fact that the most refractory oxides condensate first in the flame, while other components get dispersed at the surface of the particles, thus accessible for surface reactions.[105]

Independently, the advent of sol-gel chemistry led to the development of new types of inorganic or hybrid materials with tailored structural, textural and surface properties. Sol-gel routes can be defined as the synthesis of solid materials such as metal oxides starting from a solution of molecular precursors which evolve towards a suspension (sol) and then reticulate to form a gel via inorganic polycondensation reactions.[106, 107] Synthesis is typically performed at a moderate temperature (< 200°C) and upon long reaction times. Importantly, the introduction of sacrificial templating agents in the synthesis mixture allows generating a variety of textural features, essential for heterogeneous catalysis preparation.[2, 108]

Thus, a rather recent development in aerosol-processes which builds upon the progress made in sol-gel chemistry is the so-called "aerosol-assisted sol-gel" process (AASG). The concept of the AASG process is to merge the two fields of (i) sol-gel chemistry and (ii) aerosol processing. In 1997, Bruinsma *et al.* were the first to report the synthesis of mesoporous silica powders by spray drying of alkoxide-surfactant solutions.[58] They atomised an aqueous solution of hydrolyzed tetraethylorthosilicate (TEOS) containing also cetyltrimethylammoium chloride as the surfactant, dried the aerosol, and calcined the obtained powder. The resulting solid was made of hollow spherical particles of silica with a mesoporous texture. In 1999, Brinker *et al.* proposed an aerosol-based process for synthesising solid, well-ordered, and spherical silica particles with stable pore mesostructures.[43, 50] Datye *et al.* described the actual impact of preparation parameters like the temperature of the drying zone, the surfactant-to-TEOS ratio, the pH, etc. on the final properties of the mesoporous silica.[57] Like other classical templated sol-gel syntheses, the method relies on the evaporation-induced self-assembly (EISA) of surfactant molecules, and on the concomitant condensation of the silica precursors. However, the whole process is confined to individual spherical aerosol droplets and occurs during the very short time (typically 1 or a few seconds) needed to dry the particle.

Since then, the method has been adapted to the preparation of various nanostructured materials which accommodate different types of textural features and a large range of chemical formulations.[54] Indeed, an infinite number of combinations arise when the template-directed sol-gel chemistry is coupled with aerosol processing methods. This scientific orientation was consolidated by the better understanding of the coupling between sol-gel chemistry and aerosol processing provided by the use of in situ characterisation techniques that can follow, in real time, aerosol droplets formation and structuration from the molecular precursor solutions to the final stabilised powder.[109, 110] Examples of the use of such AASG techniques for the preparation of heterogeneous catalysts have flourished in the past two decades, as it will be shown in details in the present review.

2.2. Classification of aerosol techniques used for the preparation of solid materials

A range of techniques based on the processing of aerosols has been developed for the preparation of divided materials. Names commonly encountered include spray drying, atomisation, aerosol-assisted sol-gel, gas atomisation, flame aerosol methods, aerosol-assisted self-assembly process, etc. All of these techniques start with the atomisation of a liquid sample in the form of a mist of micronic or submicronic droplets. Several types of atomisation techniques are available, which use either pressure, centrifugal, electrostatic or ultrasonic energy to generate dispersed and gas-transported droplets. The processes, however, differ (i) on the nature and properties of the sprayed solution or colloidal suspension and (ii) on the treatments that are subsequently applied on the aerosol. Based on this, we propose a classification of aerosol processes, in four categories: Types I to IV (**Scheme 1**).

Type I – Drying of pre-formed solid particles

The starting point is a suspension of solid particles and the spray processing is only used to dry pre-existing solid materials (i.e. pre-formed particles). The process yields new solid particles of the same chemical composition and nature as the starting materials but different in the aggregation form, humidity content, size, etc. The obtained materials are often subsequently sintered by thermal treatments to ensure the cohesion of the aggregates. Note that in some case, additives (binders) are introduced to tune the aggregation behavior.[111] Such binder can itself be reactive in some cases, which complicates the classification as a "simple drying" process. Additionally, active compounds can be added to the starting mixture and get deposited onto the preformed solid particles upon drying. Nevertheless, if the final solid is mainly composed of the pre-formed solid particles used as a starting point (> 50 wt.%), we propose to put them in the Type I category.

For heterogeneous catalysis, Type I aerosol techniques are used to shape aggregates of small catalytic particles so that larger particles can be used in the catalytic process, allowing for an easier catalyst recovery or for the design of flow processes in fixed beds.[112] Also, spherical aggregates typically obtained via such spray drying process usually display improved attrition

Please do not adjust margins

Please do not adjust margins

resistance which makes them highly interesting for applications in fluidised bed reactors.[113]

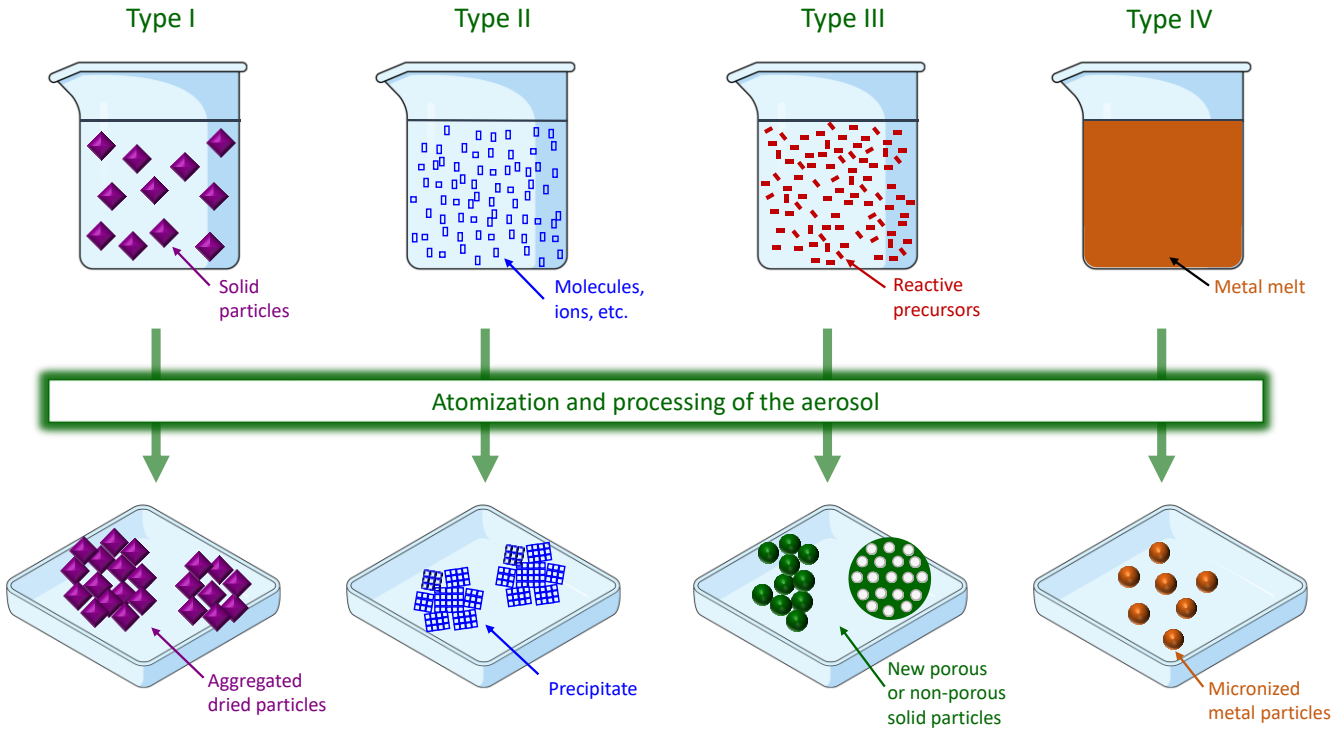

Scheme 1. Classification of aerosol processes for the preparation of solid particles in 4 categories. (Type I) Simple drying of pre-existing particles in suspension leading to particles aggregates (binders, sacrificial texturing agents may be added). (Type II) Molecules in solution are dried by aerosol and precipitate under the effect of solvent evaporation (binders or sacrificial texturing agents may be added). (Type III) Molecular precursors in solution react via inorganic polycondensation reactions during the aerosol processing to yield a solid which is chemically different from the starting compounds. Depending on the aerosol processing technique – which includes flame processing, high temperature thermal decomposition or mild thermal treatment – we define three sub-types for Type III processes (see text). In the presence of sacrificial texturing agents, porous particles can be obtained. (Type IV) A metal melt – usually obtained from a mixture of different metals – is atomised and cooled to yield micronized metal particles. Note: the frontier between Types I and III or between Types II and III may be blur in the cases where the starting system contains both reactive precursors and for example preformed nanoparticles or non-reactive molecular species. We propose to put such processes in the most relevant category, based on the main phenomena (simple drying or precipitation or reactive inorganic polycondensation) which leads to at least 50 wt.% of the final solid.

Type II – Precipitation

The starting solution contains molecular species (e.g. salts, organic molecules, organometallic complexes, biomolecules, etc.) which will dry and precipitate under the effect of increasing concentration, as the solvent evaporates. Thus, molecular species in solution form solid particles by simple precipitation. There are no inorganic polycondensation reactions and no decomposition of the starting molecule. The chemical nature of the initial species can be either totally preserved (e.g. in the case of a single salt, a protein, etc.) or a new kind of solid may be formed from their combination (e.g. precipitation of a mixture of salts yielding a new crystalline compound). The composition, size, crystallinity, humidity, texture depend on the composition of the starting solution and on the parameters of the drying. In some cases, seeds of the desired crystal may already be present in the precursor solution. Additives and sacrificial texturing agents may be added in the process to help control the physical properties of the final solid particles. Such drying by atomisation is often applied in the pharmaceutical and in the food industry.[114-116] In heterogeneous catalysis, such technique was used for example to produce microspheres of sodium aluminate used as basic catalysts for biomass upgrading,[117] or intimate mixtures of metal salts which are then thermally treated to yield complex oxide catalysts active in selective oxidation reactions.[118]

Type III – Reactive aerosol processes

The solution contains reactive molecular precursors which react during the aerosol processing to give new solid compounds by decomposition or by inorganic polycondensation reactions. The solid formed is chemically different from the species initially present in the solution. For example, metal oxides are formed starting from molecular precursors (metal alkoxydes, metallic salts, etc.) or metal nanoparticles are obtained through thermal or reductive processing of metal halides. Depending on the conditions used to trigger the chemical reactions during aerosol processing, we define three sub-categories.

Type IIIa – Flame-aerosol synthesis

This journal is © The Royal Society of Chemistry 20xx

Please do not adjust margins

Please do not adjust margins

The precursor solution – or less frequently a suspension – is atomised and the aerosol is injected into a flame, where fast thermal decomposition and condensation occur.[56, 104, 105, 119-122] The temperature in the flame can be as high as ~3000°C.[120] The sprayed solution usually includes a combustible and the process yields non-porous particles. Depending on the parameters of the process, primary particles can form loose agglomerates or aggregates,[56] where porosity arises from the interparticle voids. Particles can be heterogeneous in composition because more refractory materials condense first in the flame, forming the core of the particles, while less refractory species are found at the surface. This technique is widely applied for the preparation of various kinds of nanomaterials, both at the research level and in large industrial processes.[119, 123, 124] As far as the preparation of heterogeneous catalysts is concerned, flame-aerosol processes have already been identified as highly efficient and versatile routes to produce catalysts such as, for example V_2O_5/TiO_2 for pollutant total oxidation catalysts,[125] BiMo complex oxides for selective oxidation of light hydrocarbons,[126], MoO_3/SiO_2-Al_2O_3 olefin metathesis catalysts,[127] $CoMo/Al_2O_3$ catalysts for hydrotreatment,[121] Pt-Sn/Al_2O_3 catalysts for light alkane dehydrogenation,[128] Pt/Al_2O_3 and Pd/SiO_2 catalysts for hydrogenation reactions,[129, 130] etc.

Type IIIb – High-temperature thermal decomposition

The precursor solution – or less frequently a suspension – is atomised and the aerosol is processed in a high temperature reactor where precursors are thermally decomposed. So the process is very similar to Type IIa, but no flame is used. Typically, the reactor temperature is around 1000°C. The process leads to non-porous particles with various degrees of aggregation. In heterogeneous catalysis, such high-temperature decomposition is typically applied to obtain formulations based on a metal dispersed at the surface of a refractory oxide, like for example Ru/TiO_2 methanation catalysts,[131] or doped TiO_2 photocatalysts.[132]

Type IIIc – Aerosol-assisted sol-gel processes (AASG)

The precursor solution is atomised and the aerosol is processed to dry in relatively mild conditions, triggering inorganic polycondensation reactions. Here, the typical strategies of sol-gel chemistry are exploited during aerosol processing (see below, section 3.1.). The spray is processed in mild conditions, to activate chemical reactions from the precursors under the effect of increasing concentration, of a variation of the pH, etc. The method often takes advantage of the presence of organic species in the starting solution to tune the textural properties of the final material. Thus, the starting precursors solution often includes templating agents which can be either pre-formed (e.g. beads or rods of polymer or biopolymers) or can self-assemble during the drying process (i.e. surfactants forming micelles). The aerosol-assisted sol-gel process is frequently followed by a separate thermal or chemical post-treatment to remove the templating agent and release the porosity, or to modify the obtained solid (e.g. reduction to metal nanoparticles, conversion of amorphous materials to crystalline, etc.). Often, the starting solution is exclusively composed of molecular species (no solid particles), which co-condense and self-assemble in a strictly bottom-up fashion during the drying process.[133] In some cases, however, polycondensation and/or self-assembly is initiated before atomisation and the droplets already contain inorganic oligomers and/or organic micelles. Also, the starting system can contain a suspension of pre-formed objects (e.g. particles, nanoparticles, polymer beads, zeolite seeds, colloids, enzymes, viruses, cells, etc.) in addition to the main reactive chemical species which condenses during the process.[134] In this case, the frontier with Type I process performed in the presence of a reactive binder is blur. If the majority (in mass) of the material is obtained through reactive inorganic polycondensation, we propose to position the process in the Type IIIc category.

Type IIIc aerosol processes have offered tremendous new opportunities for the design of advanced heterogeneous catalysts in the last two decades, yielding a wide range of catalysts with tailored properties (texture, composition, surface functionalities). These will be an important focus of the review (see below).

Type IV – Gas atomisation of metals and alloys

In this technique, also called “micronization”, a metal or a mixture of several metals is melt at high temperature and atomised in the form of small droplets. The aerosol is processed to cool and generate small spherical particles of metal or metal alloys which can be exploited as heterogeneous catalysts.[135] Gas atomisation was used to produce Raney-type catalysts and other Ni-based alloys for hydrogenation reactions,[136-140] and mixed metallic glasses for the catalytic degradation of dyes,[141] for example.

2.3. Process – morphology – performance relationship

One crucial aspect of particles synthesis is the possibility to control the particles size and morphology. In all above-mentioned aerosol processes, this can be achieved with a certain degree of versatility, by tuning the process parameters. Nandiyanto and Okuyama have recently covered the technical aspects of such control on particle morphology and size, mainly for spray drying techniques (Type I processes).[142] In many of the applications covered in the present review, the particle morphology is in fact one key property of the new catalyst which can participate in the enhanced catalytic performance.

The size of the particles is primarily governed by the size of the aerosol droplets and by the composition of the starting suspension or solution, i.e. by the proportion of volatile solvent vs. non-volatile species which produce the final solid material.[143] Indeed, in aerosol processes, a single droplet produces one particle. Depending on the type of atomiser used, a range of droplets size can be selected: ~200 µm (rotary disks), 10-1000 µm (two-fluid nozzles), or 1-10 µm (ultrasonic nebuliser).[144] Apart from the choice of the atomiser type and concentration, the operating parameters (precursor temperature, spray volume rate, drying gas volume rate) and the physical properties of the starting solution or suspension (surface tension, viscosity, density) can be used as control

Please do not adjust margins

Please do not adjust margins

parameters to tune the particle size.[145] Empirical correlations are available to help the engineers in the design of their process.[142]

Particle morphology can be adjusted as well, and many different types of particle ultrastructures have been described in the literature.[54, 142] These can be obtained on purpose by carefully selecting the drying conditions (type of drying gas, temperature, relative humidity, residence time, co-current or counter-current, etc.). As particles formation results from the drying of liquid droplets – for which the spherical shape is the most stable – aerosol processes typically produce spherical particles. Yet, depending on the rate of mass and heat transfer during the drying, different particle morphologies can be obtained.[146] If the drying occurs fast at the droplet surface, a solid skin can rapidly form and result in hollow particles. Changes in the hydrodynamics and structural stability of the droplets during drying can allow the transformation of spherical droplets into convex structures which yield donut-like particles. Obviously, when using a suspension of preformed particles or sacrificial nano-objects used as templating agents, the size of the latter will dictate particle roughness and porosity.

When looking specifically at heterogeneous catalysts, it is evident that the size and microstructure of the particles have a tremendous importance and can – to some extent – dictate the level of catalytic performance reached by the material. In particular, diffusion phenomena are governed not only by the size of the pores but also by the path that the reactants and products have to follow to enter and exit the catalyst particles. In this context, small or hollow particles may be advantageous because they imply shorter diffusion distances.[147] Looking at catalytic applications using fixed beds in flow mode, larger particles can be more interesting because they develop lower pressure drops. Finally, resistance to attrition is an important factor as well, especially in fluidised bed applications or in batch mode when intense stirring is required.[148] In those cases, dense and spherical particles appear more practical than anisotropic or hollow microstructures. The process operating parameters also govern the particle size distribution, which has a tremendous importance for many catalytic applications.

Finally, catalytic performance is largely governed by the chemistry of the solid (nature of the surface species, degree of dispersion of the active element, etc.). These aspects will be covered specifically for each categories of materials covered in the review.

2.4. Focus of the review

The methods described above are developed for the synthesis of a variety of divided materials with a huge diversity of potential applications for the obtained materials. This review, however, is focused exclusively on heterogeneous catalysis as the targeted application. The purpose is to provide a wide-ranging overview of the recent (~ last two decades) developments that have been made in the field of the synthesis of heterogeneous catalysts using aerosol techniques.

The frontiers between the different types of processes as defined above are somewhat arbitrary. Yet, this classification should allow the community to identify more clearly the principles behind the formation of solid catalysts when discussing the scientific literature.

Here, we purposely excluded from the review the catalysts obtained by aerosol-flame techniques (Type IIIa) and those prepared from metal melts (Type IV). Indeed, Type IIIa and IV rely on very specific high-temperature equipment and technology. As such, they should be discussed separately. As far as flame-made heterogeneous catalysts are concerned, the reader can find a number of recent reviews which comprehensively cover both the technological and fundamental aspects of the methods.[56, 104, 105, 119, 120, 122, 149, 150]

Thus, the present review covers systematically the heterogeneous catalysts prepared using Type II, Type IIIb and Type IIIc processes. In other words, the review is an account on preparation methods starting from solutions or suspensions containing molecular precursors which undergo polycondensation, decomposition or precipitation during the processing of aerosol droplets, under the effect of mild or moderate thermal treatment (no flame), often exploiting templating strategies to control the textural properties of the materials. For these processes, no systematic and comprehensive review of the literature is available to date. While Type I processes are important in the field of heterogeneous catalysis, they rather consist in shaping techniques than actual synthesis of heterogeneous catalysts. The literature on these processes is vast and we chose to select a few examples to illustrate the role of aerosol techniques in the aggregation of powdery catalyst particles.

3. Review of successful catalyst development by the aerosol process

In this section, the preparation of heterogeneous catalysts using aerosol techniques is reviewed. The synthesis conditions, the specific textural, structural, chemical, physical properties of the obtained catalytic materials are discussed, together with the performances. When possible, we attempt to highlight the decisive advantage that the aerosol process offers as compared to a more classical preparation route.

In the first section, the syntheses based on the aerosol-assisted sol-gel process (AASG, Type IIIc) are systematically covered. This category of synthesis appears to be the most innovative and promising for the design of advanced heterogeneous catalysts. Indeed, Type IIIc processes can combine the versatility of sol-gel approaches to obtain tailored chemical formulations and functionalities, along with an array of strategies that allow designing tailored textures. In the second section, the preparation of catalysts using high-temperature decomposition (Type IIb) is covered. This category is particularly interesting for the synthesis of non-porous catalyst particles exploited mainly as photocatalysts, or possibly decorated with metal nanoparticles active in various redox reactions. In the third section, the preparation of catalysts through precipitation is covered. In this case, the starting molecules or salts are simply dried to yield a crystalline solid.

 This journal is © The Royal Society of Chemistry 20xx

Please do not adjust margins

Please do not adjust margins

The latter can be used directly as a catalyst of further thermally treated to yield active phases. In the fourth section, a non-exhaustive overview of Type I processes is proposed to illustrate the importance of aggregation and shaping in heterogeneous catalysis.

3.1. Porous catalysts obtained by the aerosol-assisted sol-gel process with a texturing template

Metal oxides and mixed metal oxides are an important class of heterogeneous catalysts and catalyst supports, for which bottom-up approaches – including Type IIIc aerosol processes – have proven to be useful in the development of high catalytic performance.[61] Catalytic activity is often brought about by the formation of unbalanced bonds between the different partners of the mixed oxides, resulting in the formation of acid or basic surface sites, like in the case of SiAl mixed oxides used in cracking and isomerisation reactions,[151-153] or like MgAl mixed oxides obtained from alkaline clays and used in condensation or cycloaddition reactions.[154-156] The dispersion of isolated metal oxide species with specific coordination leads to the formation of selective redox sites, like for example in the case of Ti-Si mixed oxides used in epoxidation reactions.[157-160] Thus, sol-gel processes are recognised as a versatile way to prepare mixed metal oxide catalysts because they allow to make dispersed materials through the growth of metal-oxo polymers in a solvent.

Inorganic (mixed) metal oxides are obtained as amorphous or crystalline network or as metal-oxo clusters via inorganic polycondensation of metal organic precursors (such as alkoxides) or metallic salts.[8, 10] Sol-gel polymerisation can be driven through hydrolysis reactions (eq. 1 in Scheme 2) to form reactive M-OH species which then condense through oxolation or olation to generate metal-oxo polymers assembled via M-O-M and/or M-OH-M bridges (reactions (2) and (3) in Scheme 2). A large variability of materials morphology can be obtained depending on the many different ways in which these inorganic oligomers and polymers can be linked and organised when they are dispersed in a solvent. By controlling the structure of these oxo polymers, it is possible to tailor the final properties of the materials. This is typically achieved by tuning synthesis parameters (pH, hydrolysis ratio, temperature, use of a catalyst, use of complexing ligands, nature of the solvent, etc.).

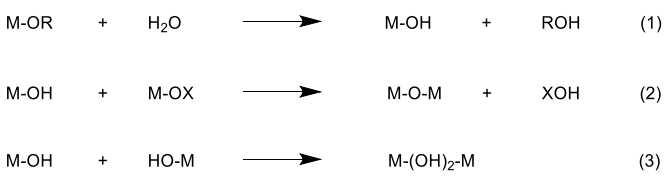

Scheme 2. Classical sol-gel chemistry is based on inorganic polymerisation reactions usually involving metal alkoxides (M = Ti, Zr, Al, etc. and OR = alkoxy group). For Si, only reactions (1) and (2) apply. Upon hydrolysis (equation (1)), reactive hydroxyl groups are created, which can then polymerise via (2) oxolation or (3) olation reactions to yield a polymer or branched polymer with a metal oxo based skeleton. X = H or alkyl group.[8]

In aerosol-assisted sol-gel processes, these reactions occur very fast during the processing of the liquid droplets. In fact, sol-gel reactions can already start to proceed in the precursor solution; in particular, alkoxide pre-hydrolysis is often carried out before atomisation and the formation of the first small oligomers can also happen at this early stage. Yet, the consolidation of the solid oxide occurs during the aerosol processing.

In many cases, the aerosol process has proven to be advantageous over other more classical preparation techniques either because of higher production yields or because the properties of the catalytic materials were significantly improved. Indeed, though often satisfactory, classical preparation methods also suffer from important limitations. Heterogeneous catalysts are usually prepared by one of the three classical routes: (i) impregnation or grafting of active species on preformed supports, (ii) co-precipitation or (iii) hydrolytic sol-gel.[68, 161-163] Impregnation and grafting methods ensure that the active phase is deposited at the surface of the preformed support, where it can act in the catalytic process. However, they are multi-step procedures and a challenge is to ensure that the active phase gets evenly dispersed over the available support surface. The texture is often altered during impregnation procedures (e.g. pore plugging). The workability of these methods is somewhat limited by the nature and quality of the interactions between the active phase precursors and the supports. In co-precipitation and classical sol-gel methods where several precursors are to be used simultaneously, one challenge is to ensure a truly homogeneous composition throughout the materials. Indeed, precipitation or hydrolysis/condensation rates can vary significantly from one precursor to another, resulting in segregated phases and lack of control on the composition and texture. These issues may be the cause for limited catalyst activity, selectivity or stability.

The technical features of the aerosol-assisted sol-gel process make it particularly well-suited for the preparation of a range of tailored heterogeneous catalysts (Table 1). In particular, the Type IIIc processes where a template is used to generate porosity take advantage of the so-called EISA phenomena. More precisely, the process relies on three key features, which are schematically illustrated in Scheme 3 and detailed here:

(1) The starting solution (or suspension) is relatively dilute and is metastable over the timespan of atomisation. No gel or precipitate is formed spontaneously before aerosol formation; the solutions remains homogeneous. As a result, each droplet of aerosol produced from the starting solution (or suspension) has exactly the same composition. This is the key to the control of composition and particle-to-particle homogeneity throughout the obtained solid product.

(2) If a surfactant is used as a templating agent, operating conditions can be selected so that the evaporation-induced self-assembly of surfactant to form micelles occurs earlier than or together with the formation of the inorganic network through inorganic polycondensation reactions. Consequently, micelles are trapped in the inorganic material and will leave calibrated

Please do not adjust margins

Please do not adjust margins

pores upon calcination or washing. This templating action is the key to the formation of controlled textural properties.

(3) Upon evaporation, heating and concentration, components with high sol-gel reactivity (e.g. pre-hydrolyzed metal alkoxides) rapidly form an inorganic network via polycondensation reactions, trapping other species with low or no reactivity (e.g. salts or metal nanoparticles).[60, 133] This "kinetic quenching" is the key to obtain metastable solid phases, which feature a homogeneous dispersion of the different components throughout the material that is difficult to obtain with other classical synthesis routes.

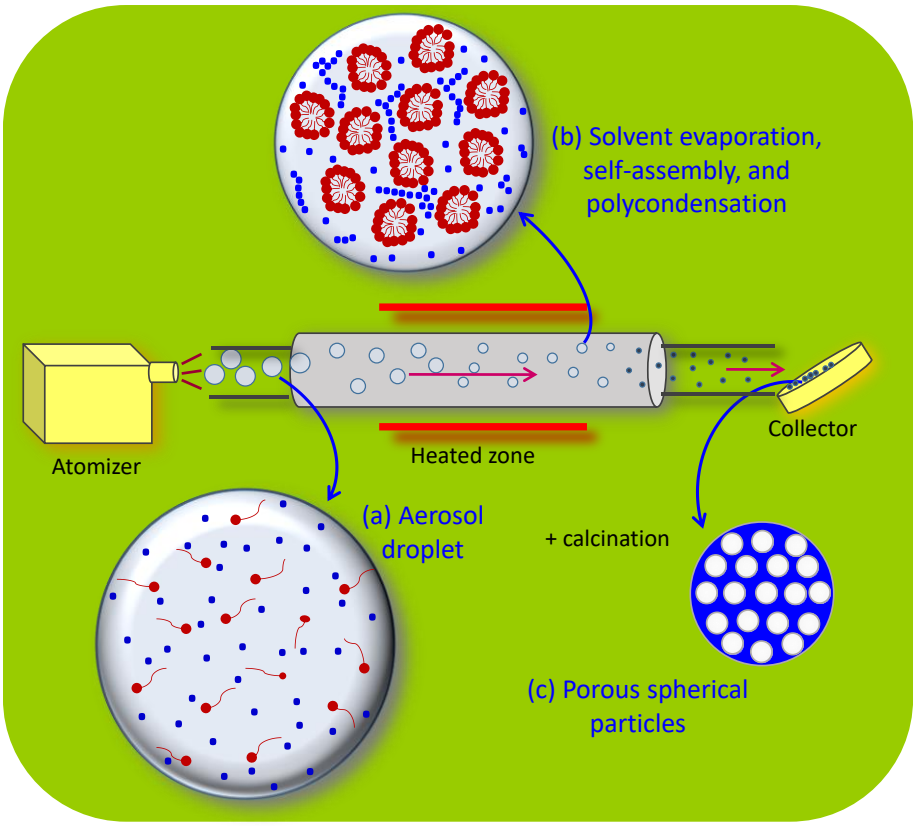

Scheme 3. Schematic view of the aerosol-assisted sol-gel process (Type IIIc) in the case where a surfactant is used as sacrificial texturing agent.[54] The one-pot reactive medium containing all precursors is sprayed in the form of an aerosol. (a) Each of the formed droplets has the same composition (provided the starting solution is stable during in the timespan of the spraying) and contains a mixture of molecular precursor monomers (blue dots) and a surfactant (in red). For the sake of clarity, only monomers are depicted but in some cases, a partial polycondensation may already be initiated before atomisation. (b) The aerosol droplets are dried by passing in a heated zone (this can be a glass or quartz tube inserted in a tubular furnace or a cyclone separator fed with hot drying gases, for example). Upon solvent evaporation, the concentration of non-volatile species increases and two phenomena take place: (i) the evaporation-induced self-assembly of surfactant molecules to form micelles and (ii) inorganic polycondensation reactions leading to the formation of an oxide matrix, surrounding the micelles. (c) Dried particles are collected on a filter of via cyclone separation for example and calcined (or washed) to eliminate the surfactant and release the calibrated porosity. Depending on the precursors used, complex formulations can be obtained including mixed oxides, hybrid materials bearing (multi)-functional groups, etc.

As it will be demonstrated individually for most of the following examples, such aerosol-assisted sol-gel approach often allows to adjust the process parameters to fine-tune some of the most important catalyst properties (structure, morphology, homogeneity, dispersion, surface properties, texture, etc.) and in turn to develop catalysts with enhanced performance. Generally speaking, one may underline three reasons for improved catalytic performance (activity, selectivity, stability) that are directly linked to the control on the aerosol-assisted sol-gel preparation process.

First, the method is run at moderate temperature (as compared to flame processes for example). This opens up the possibility to use a wide range of structuring and functionalization strategies: templating with organic species (self-assembly, phase separation, polymer beads, etc.), fabrication of nanocomposites, or preparation of hybrids. This control on texture and surface chemistry opens important opportunities for the production of heterogeneous catalysis with tailored reactivity and performance.

Second, the fast drying implies a fast polycondensation process and results in the kinetic quenching of metastable

 This journal is © The Royal Society of Chemistry 20xx

Please do not adjust margins

Please do not adjust margins

phases which can exhibit improved catalytic performance. In fact, in sol-gel processes, the small oxo-clusters formed via polycondensation reactions are in dynamic equilibrium with the solid phases formed. Yet, unlike for classical sol-gel processes in which the most stable formulation is ultimately obtained after long reaction times, the aerosol-assisted sol-gel allows to freeze the system in "local minimum states" that are different from the thermodynamically favoured one. For example, the degree of crystallisation of metal oxides can be tuned, allowing to reach amorphous materials that mimic crystalline ones but with a composition that does not correspond to the thermodynamically stable one and with open texture (e.g. mesoporous aluminosilicate[164] or titanosilicates[165] with high concentration of heteroelement incorporated in the silica network). Such metastable states may feature specific molecular structures in which the coordination and/or the angles between the elements are different from the most stable formulations, resulting in different levels or types of reactivity.

Third, the process offers the possibility to place specific constituents preferentially at the pore surface or in the walls of porous materials. This was shown for example with hydrodesulfurisation catalysts where the interaction between the Co or Mo precursors and the surfactant could be tuned by adapting some parameters of the synthesis, allowing to force the localisation of the active components at the internal surface of the pores.[166] Another successful example was reported with Fe/carbon composites, for which the processing temperature allowed to either disperse Fe oxide nanoparticles at the surface or inside of carbon nanospheres.[167]

Finally, the process can be adjusted to yield different particles morphologies (e.g. hollow spheres, plain spheres, donut-shape particles, core-shell particles, etc.) which can – in many cases – have a decisive impact on catalytic performance, as discussed in Section 2.3.

Table 1. Porous catalysts obtained by the aerosol-assisted sol-gel process with a texturing template

Catalyst	Templating / structuring agent	Pore diameter (nm)	Specific surface area ($m^2.g^{-1}$)	Pore volume ($cm^3.g^{-1}$)	Reaction	Key chemical property	Reference
SiO_2-Al_2O_3	F127 / TPAOH	5-16	240-900	0.27-0.97	m-xylene isomerisation	Increased acidity in comparison to classical LAB	168
SiO_2-Al_2O_3	F127 / TPAOH	6.3-26	240-880	0.27-1.23	m-xylene isomerisation	Microporous surface seems to be a relevant structural parameter	60
SiO_2-Al_2O_3-MoO_3	Brij58	1.9-2	480	0.23	Olefin metathesis	High dispersion of MoO_x species, high acidity	133
SiO_2-Al_2O_3-WO_3	P123	5.3	530	0.7	Olefin metathesis	High dispersion of WO_x species, high acidity	169
SiO_2-WO_3	Brij58	2	490-570	0.25-0.28	Olefin metathesis	High dispersion of WO_x species	170
CoMo-SiO_2	P123	8	280	0.42	Hydrotreatment (hydrogenation catalyst)	Homogeneous distribution of active species	166
Sn-Si	P123	6	360	0.5	Synthesis of alkyl lactate	Incorporation of Sn as single sites	171
Metal (Ce, Mn, Cu, Al) /SiO_2	CTAB	2.4-4.56	230-1150	0.24-0.9	Catalytic oxidation of VOCs (acetone)	Synergetic effect of Ce-Al	172
Metal (Ce, Mn, Cu, Al) /SiO_2	CTAB	2.4-3.05	550-1150	0.49-0.9	VOC	Increased stability (96h) and acetone destruction at 250°C with Ce	173
V_2O_5-TiO_2	P123	6.6-14.2	55-140	0.24-0.458	Catalytic oxidation of 1,2-DCB	Increased fraction of vanadium active sites exposed to the pores surface involved	174
SiO_2-TiO_2	α-chitin nano-rods	5-6	70-450	0.1-0.44	Oxidation of MPS and DBT	Amount of Ti accessible sites controlled by initial chitin volume fraction	175
SiO_2-TiO_2	CTAB and TPAOH	Micro and mesopores	720-760	0.42-0.47	Cyclohexene epoxidation	Hierarchical porosity, high Ti loading and formation of TS-1	165
TiO_2	F127	3.2-9.3	2.5-88	0.014-0.084	Photodegradation of acetaldehyde	Photocatalytic performances enhanced by controlling crystallinity and microstructure	176

Please do not adjust margins

Please do not adjust margins

Metal(Pd,Rh,Ru)-PMO	CTAB	2.7-7.8	780-1670	0.64-0.9	Barbier reaction, Sonogashira reaction, terminal alkyne acylation, Suzuki reaction, isomerisation, Miyaura-Michael reaction	Presence of cavities chamber enhances both activity and stability against damage of the mesostructure and leaching of metals	177
Pd@MOF	-	1.3	180-1400	0.07-0.54	Alkene hydrogenation	Homogeneous dispersion of Pd nanoparticles inside the MOF structure	178
Amorphous Metal Oxides (Fe-Ni-Ox)	P123	n.r.	n.r.	n.r.	Photocatalytic oxygen evolution and gas sensing	Easier synthesis of amorphous metal oxides than with the PMOD route	179
Metal oxides	P123 / F127	5-12	18-190	0.04-0.52	Photocatalytic oxygen evolution and gas sensing	Easy doping of multimetallic oxides than with conventional wet-chemistry of solid-state preparation methods	180
$NiFe_2O_4$	F127	3.7-7.1	120-280	0.33-0.84	Photocatalytic H_2 evolution from H_2O with CH_3OH	Increases catalytic activity and robustness	181
Au/Al_2O_3 and Au/CeO_2	CTAB / P123	n.r.	n.r.	n.r.	Hydrogenation of 4-nitrophennol	Nanoparticles small size maintained and H_2 reduction avoided	182
Au, Pt, Pd / Al,Ti,Zr oxide	F127	5.1-13.6	150-190	n.r.	Catalytic reduction of 4-NP to 4-AP	Nanoparticles well distributed inside entire oxide microspheres	183
Au(Al,Co)/SiO_2 (TiO_2)	CTAB	2.7-2.9	450-480	n.r.	CO oxidation	Limited pore connectivity, resistance to sintering for Au	184

n.r. stands for “not reported”

3.1.1. Amorphous aluminosilicates and zeolites for hydrocarbon cracking

Refining catalysts are required for transforming heavy petroleum fractions into fuel.[185] As commonly used structured aluminosilicates (zeolites) present narrow pores that limit the diffusion of heavy molecules, the quest for alternative large pore acid catalysts is important. In this perspective, syntheses strategies rely on multi-step grafting procedures or on the assembling of preformed zeolitic particles.[186-188] The aerosol-assisted sol-gel process offers a cost-effective alternative for the production of mesostructured aluminosilicates, with controlled morphology. For examples, Fiorilli *et al*. reported on the preparation of mesoporous aluminosilicates, under mild acidic aqueous conditions starting from either aluminum isopropoxide or aluminum chloride as Al source.[189] The microspheres were rather monodisperse in size, and characterised by high surface areas (up to 640 $m^2\ g^{-1}$) and narrow pore size distributions (centred at 2.5 nm). Their surface acidity makes them attractive materials for applications in catalysis.

Earlier, aluminosilicates with large mesopores and high acidity were successfully produced by Pega *et al.* using the aerosol-assisted sol-gel process (Type IIIc) and exploited as catalysts for the cracking of large-molecules.[60, 164] The acronym “LAB” was coined, standing for “large-pore aluminosilicates made in basic medium”. The precursor solution contained aluminosilicate precursors (pre-hydrolysed TEOS and aluminium sec-butoxide), pluronic F127 block copolymer as the templating agent, and tetrapropylammonium hydroxide (TPAOH) as the microstructure-directing agent. The obtained mesostructured particles were calcined to obtain amorphous mesoporous spherical particles (Figure 1).

Depending on the Si/Al molar ratio, on the amount of TPAOH added in the preparation, and on the precursor solution ageing time before spray drying, texture can be tuned in a certain range. The Si/Al molar ratio fixed in the initial solution between 6 and 50 was strictly preserved in the powder. The Al-O-Si network in the LABs was completely amorphous; nanozeolitic nuclei were not observed in XRD and the characteristic FTIR signature of ZMS-5 zeolite was not observed either. Yet, echo MAS-1H-NMR experiments performed on dehydrated samples exhibited resonance signals similar to those of zeolitic Si-(OH)-Al acid sites.[190] The strength of the active acid sites was higher than in classical amorphous aluminosilicates (Al-SBA-15 sample with a Si/Al atomic ratio of 12), but lower than in a Y-zeolite (Y/Al_2O_3 reference sample with a Si/al atomic ration of 16.7). Using a (^{27}Al)-1H TRAPDOR effect, it was shown that these protons are in close proximity with aluminium centres. The presence of such “zeolitic” protons could explain the strong Brønsted acidity of LABs similar to that observed for improved mesostructured materials prepared from zeolite seeds.[191-195] LAB have demonstrated higher

 This journal is © The Royal Society of Chemistry 20xx

Please do not adjust margins

Please do not adjust margins

catalytic activities with much lower coke formation for the m-xylene isomerisation process than a 10 wt% Y-zeolite industrial reference (Figure 1). The high microporous volume of LAB materials (up to 0.2 $cm^3.g^{-1}$) seems to be the relevant structural parameter dictating their catalytic properties in m-xylene isomerisation.

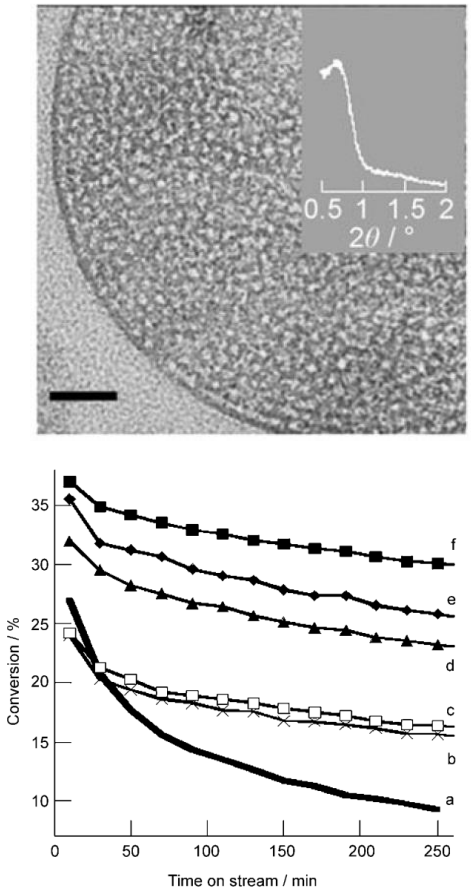

Figure 1. (top) TEM pictures of the mesostructured sub-micrometric spheres (scale bar: 50 nm), (bottom) m-xylene conversion as a function of the time on stream for a) Y/Al_2O_3 (Y-Zeolite with Si/Al = 16.7), b-f) LAB catalysts with variations in the preparation method. Reproduced with authorisation from Pega *et al.* [60]

3.1.2. WO_3- and MoO_3 based catalysts for olefin metathesis

Olefin metathesis is of crucial importance in the petrochemical industry as it allows the on-purpose production of highly demanded propene from cheaper butenes and ethene.[196-199] The reaction can be catalysed with Mo-, Re-, or W-oxide based heterogeneous catalysts.[199-205] MoO_3-based catalysts offer a good compromise in terms of activity, stability, and price. Classically, molybdenum oxide is deposited on the surface of a preformed support by means of impregnation methods or by thermal spreading.[206-208] Silica-alumina supports are preferred to silica or alumina because their moderate acidity significantly enhances the metathesis activity of the deposited MoO_x species.[209, 210] Excessive acidity, as typically encountered in zeolites should be avoided because it favours isomerisation and alkylation over metathesis reactions.[211] One difficulty with impregnation, thermal spreading or grafting methods is to effectively disperse MoO_x species over the whole available surface of highly porous supports. Inhomogeneous deposit, pore plugging and formation of MoO_3 crystals are often encountered, thereby limiting the catalytic performance of catalysts prepared in two steps.[206] Therefore, one-step preparation techniques, allowing the dispersion of MoO_x species at the molecular scale onto/into a silica-alumina matrix are desired. Three successful one-step preparation methods have been reported recently: (i) non-hydrolytic sol-gel route (NHSG),[212, 213] (ii) flame spray pyrolysis (FSP),[127] and (iii) the aerosol-assisted sol-gel process.[133]

In the aerosol-assisted sol-gel process, an aqueous solution containing ethanol, pre-hydrolysed TEOS, a Mo Keggin salt (or Mo chloride), Al chloride and a block copolymer (Brij58) was sprayed and dried rapidly by passing through in a tubular furnace set at 450°C. The recovered powder was then calcined at 550°C. Spherical particles were generated with a nanoscale organisation of super-microporous pores of ca. 1.9 nm (Figure 2). The specific surface area reached 480 $m^2.g^{-1}$ and molybdenum was effectively dispersed. This catalyst performed very well in the metathesis of ethene and 2-butene to propene. In Figure 2, it is compared to series of catalysts prepared by the other one-step preparation methods (FSP and NHSG). One catalyst prepared in two-step via an improved impregnation method – using molybdenum hydrates as precursors[214] – is also plotted as a reference. In FSP catalysts, Mo is condensed solely at the surface of non-porous silica-alumina particles. As the available surface is low, polymolybdates and MoO_3 crystals form as the loading increases and this relates to poor specific metathesis activity.[127] The Mo-Si-Al mixed oxide obtained by NHSG have a high surface area (470-500 $m^2.g^{-1}$) and feature high Mo dispersion, even at high loading. This makes NHSG catalysts highly active olefin metathesis catalysts, even if part of the Mo is obviously lost in the bulk of the materials and not available at the surface.[213] Nevertheless, the aerosol catalyst was even more active than the corresponding NHSG catalyst (10 wt.% MoO_3). In terms of apparent turn over frequency, the aerosol is also more active than the most active NHSG catalyst (13 s^{-1} vs. 9 s^{-1}). This shows that the dispersion of surface molybdate species in aerosol catalysts is at least as good as in NHSG catalysts.

Convincing results have also been obtained with aerosol-made super-microporous WO_3-SiO_2 metathesis catalysts.[170] Such tungsten-based metathesis catalysts require higher reaction temperature but are known to be more stable on stream.[215] When prepared through classical impregnation on preformed porous silica supports, inactive crystallites of WO_3 form readily from a relatively low tungsten oxide loading. When prepared by the Type IIIc aerosol process, high tungsten oxide loading can be achieved while keeping a high degree of dispersion. It can be noted that calcination plays a double role here. In addition to removing the surfactant, calcination also triggers the partial migration of W oxide species towards the surface of the catalyst (as proven by XPS measurements).[170] Thus calcination was identified as a key step that must be optimised for the design of a highly active WO_3-based metathesis catalyst. Also mesoporous WO_3-SiO_2-Al_2O_3

Please do not adjust margins

Please do not adjust margins

metathesis catalysts have been prepared starting from an alkaline sol-gel medium, with TPAOH used as a structure-directing agent and Pluronic P123 as templating agent.[169] These catalysts performed significantly better than corresponding catalyst prepared by impregnation, confirming again that the dispersion of the active oxide species was the key to obtain high olefin metathesis performance.

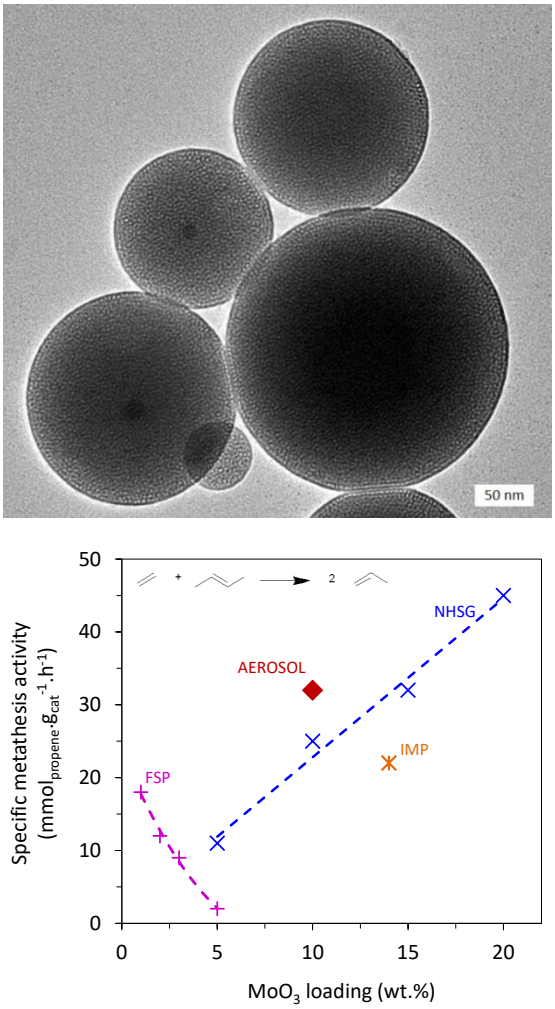

Figure 2. (Left) MoO_3-SiO_3-Al_2O_3 mixed oxide catalyst[133] prepared by the aerosol process as observed in TEM. (Right) Comparison of the performance of this aerosol catalyst with other metathesis catalysts prepared by various methods (FSP = flame stray pyrolysis, IMP = wet impregnation with molybdenum oxide hydrate, NHSG = non-hydrolytic sol-gel) and tested in the cross-metathesis of ethene and 2-butene to propene at 40°C.

3.1.3. Co- and Mo-based catalysts for hydrocarbon hydrotreatment

Among the different catalytic processes that take place in petroleum refining, hydrotreatment is a key process since it enables the elimination of heteroatoms, responsible for environmental issues and facilities damages.[216, 217] Conventional hydrotreating catalysts are usually obtained by impregnation on porous oxide of the oxometallic elements precursors (e.g. Co and Mo salts), which are the precursors of the promoted active phase (e.g. Co-MoS_2) itself obtained after calcination and sulfidation treatments.[218-220] This multistep preparation processing suffers from different drawbacks and in particular, the amount of oxo-species and their localisation must be optimised to avoid crystallisation of bulk $CoMoO_4$ or MoO_3, which are refractory to sulfidation.[221] Although sol-gel method allows a good dispersion of metal oxo-species within the catalyst, their localisation into the wall of the support may hinder their accessibility and then decrease the final catalytic activity.

In a recent work,[166] an original and low-cost aerosol method was developed for synthesising mesoporous $CoMo/SiO_2$ composites that demonstrate a good compromise between metal oxo-species localisation and catalyst activity. In a typical synthesis, an aqueous solution of hydrolyzed tetraethyl orthosilicate (TEOS) is blended with a solution of a molybdic heteropolyacid ($H_3PMo_{12}O_{40}$) with $Co(OH)_2$ (Co/Mo = 0.36 mol) and a solution of block-copolymer Pluronic P123. The resulting solution was sprayed with a Büchi B-290 spray drier and the material was then calcined under static air (350 °C for 12 h) to remove the surfactant. By promoting the co-location of the precursor nearby the micelles of non-ionic structuring agent during the evaporation of aerosol droplets, the active phase of the mesostructured catalyst for sulfidation of molybdenum centres was made more accessible. This co-location could be obtained by adjusting the interaction between the heteropolyacid precursor and the surfactant as well as the kinetics of hydrolysis-condensation of the silica matrix. Aerosol-processed mesoporous $CoMo/SiO_2$ catalysts had a spherical shape with a diameter ranging between 0.1 and 20 µm (Figure 3-A). Mesostructuration is clearly observed on the TEM micrographs (Figure 3-B) and was also confirmed by small angle X-ray scattering measurements. Nitrogen physisorption isotherms exhibited the characteristic features of mesoporous materials showing periodic porosity. The simultaneous presence of oxo-species of Mo and Co did not trouble the mesostructuration indicating that the localisation of the oxo-metallic phase is not in the silica wall matrix. The resulting mesoporous microspheres of $CoMo/SiO_2$ composites exhibit 8 nm pore size, BET surface area of 278 $m^2.g^{-1}$ and porous volume of 0.42 $cm^3.g^{-1}$. SEM-EDX cartography of the one-pot aerosol synthesised $CoMo/SiO_2$ materials, confirmed that the dispersion obtained by spray drying was homogeneous. After sulfidation, the presence of highly dispersed entangled MoS_2 slabs inside the pores is clearly observed by TEM (Figure 3-C) indicating that the spray drying process has the very favourable effect to produce particles with homogeneous repartition of metal centres, as well as to allow the co-location of both molybdenum precursor and cobalt promotor at the pore surface.

 This journal is © The Royal Society of Chemistry 20xx

Please do not adjust margins

Chemical Society Reviews

REVIEW

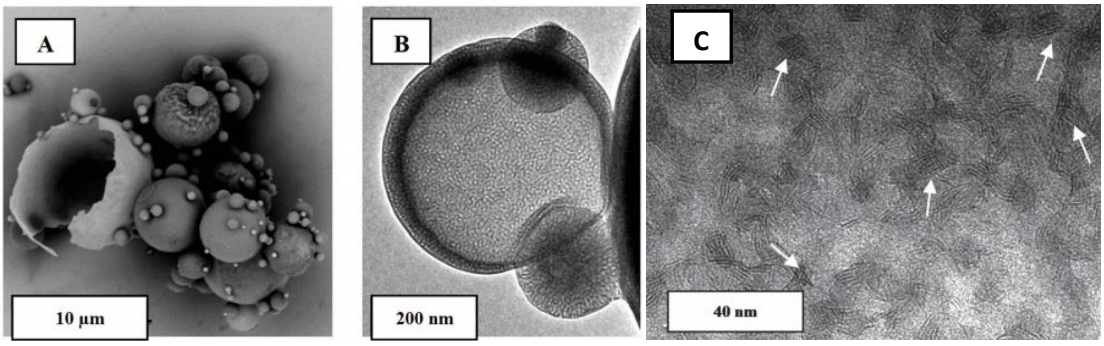

Figure 3. CoMo/SiO_2 composites obtained by the aerosol process, observed in (A) SEM and TEM (B) before and (C) after sulfidation (white arrows point out entangled MoS_2 slabs). Reproduced with authorisation from Colbeau-Justin *et al.* [166]

The catalysts were tested in the model reaction of toluene hydrogenation and showed higher activity on the basis of the Mo content (Figure 4) than the catalysts prepared by impregnation at equivalent composition and also outperform the industrial catalyst by 50%.[166] This enhancement of hydrogenation activity is likely related to the facts that MoS_2 crystallites are forced to grow within an interconnected vermicular network of mesopores. This favours both the formation of anisotropic morphology of the slabs that is expected to increase the number of edge sites in comparison with an isotropic slab and the formation of entangled slabs as observed in TEM. Defects being the quality of catalysts, these structural features certainly promote the better catalytic activity observed for these new catalysts.

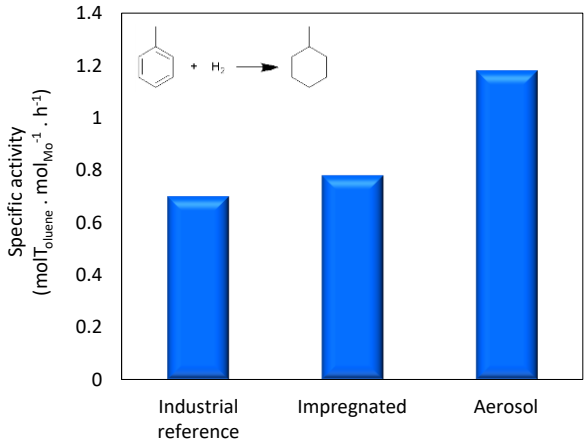

Figure 4. Catalyst performance in toluene hydrogenation (model reaction for hydrotreatment catalysts). The one-pot aerosol CoMo@SiO_2 catalyst is compared to an industrial reference and to a catalyst with the same bulk composition (10 wt.% MoO_3 and a molar Co/Mo ratio of 0.36) prepared by impregnation.[166]

3.1.4. Stanosilicate for the synthesis of alkyl lactate

Since the advent of biodiesel, the upgrading of glycerol – a by-product of the transesterification of triglycerides – has become a major field of research in heterogeneous catalysis. One proposed pathway is to first oxidise glycerol into dihydroxyacetone (DHA) which then reacts with an alcohol to produce alkyl lactates or lactic acid. Note that DHA can also be obtained from sugars and enter the same upgrading routes.[222] Lactates are important bio-based building blocks for biodegradable plastic material (polylactates).[223-226] Lactic acid and lactates also find applications in the pharmaceuticals, chemical, and cosmetic industries.[227, 228] In the recent years, Sn-silicates emerged as highly active heterogeneous catalysts for the direct conversion of DHA to ethyl lactate.[229-233] In these catalysts, the dispersion of tin in the form of single sites is the key to obtain high activity. Also, the activity of the catalysts can be improved by tuning the pore size in the mesoporous range and using smaller particles, to facilitate mass transfer.[230]

Thus, Godard *et al.* have proposed the aerosol preparation of mesoporous Sn-silicate, using TEOS and $SnCl_4$ as precursors and Pluronic P123 as a templating agent.[171] After calcination, the catalysts consisted of porous spherical particles in the range of 100-400 nm (Figure 5-top) and had advantageous textural properties (SSA = 360 $m^2.g^{-1}$, V_p = 0.5 $cm^3.g^{-1}$; D_p = 6 nm). Aerosol-made SnSi mixed oxides displayed record activity in the synthesis of ethyl lactate from DHA and ethanol, reaching a TON of 173 after 6 hours of reaction at 90°C (to be compared with a TON of 113 for a previously reported highly active sol-gel catalyst[230]). This high activity was correlated to the excellent dispersion of Sn centres in the aerosol catalyst, as compared to other reported methods. Indeed, no crystalline phase was detected in XRD and ^{119}Sn-MAS-NMR showed unambiguously the presence of intra-framework Sn(IV) connected to four silicon atoms[234] and the absence of extra-framework Sn(IV) that

Please do not adjust margins

would be easily detected in the presence of SnO_2 microcrystallites[235] (Figure 5-bottom). Such effective insertion of Sn into the silica framework allowed for the formation of abundant and strong acid sites, which are responsible for the catalytic activity in the synthesis of alkyl lactates.

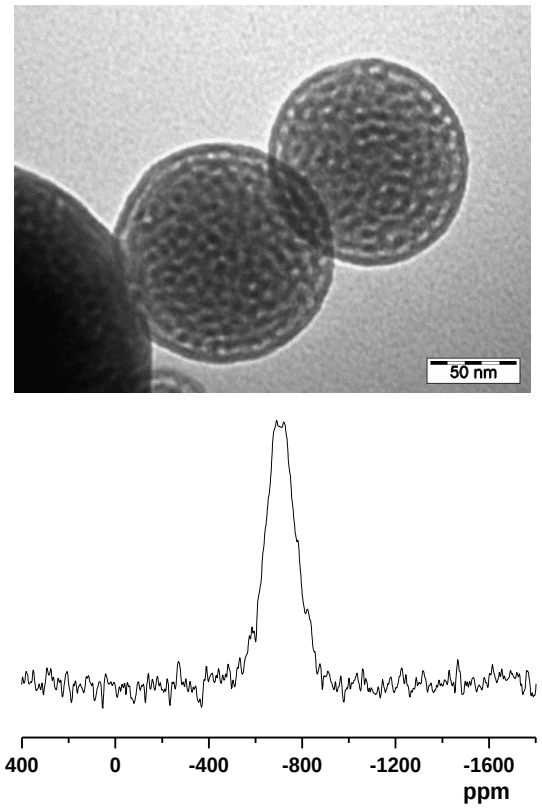

Figure 5. (a) TEM micrograph and (b) Solid state ^{119}Sn static NMR of a SnSi mixed oxide catalyst prepared by the aerosol assisted sol-gel process (Si/Sn molar ratio = 74) Adapted with authorisation from Godard *et al.*[171]

3.1.5. Transition metal-doped silica and titania for the total oxidation of volatile organic compounds

Volatile organic compounds (VOCs) constitute a major environmental concern and intense efforts are paid to limit industrial emissions.[236-238] The total oxidation of VOCs can be catalysed by noble metal catalysts[239, 240] or transition metal-based catalysts.[241] While the former can work at lower temperature and show good stability and selectivity in most reactions, the latter is much cheaper and can be preferred in some specific cases.[242, 243] In this application, a key parameter is the pollutant adsorption behavior,[244-247] and therefore the available catalyst surface area and its affinity for the pollutant have to be tuned.

Wang and Bai used the aerosol process to prepare transition metal-doped mesoporous silica catalysts for the total oxidation of acetone.[172] CTAB was chosen as a templating agent. Five metal dopants – Ce, Mn, Cu, Fe, and Al – were tested as the active species, with Si/metal molar ratios varying from 10 to 200. The catalysts were compared to MCM-41-based materials of identical composition, obtained by a classical hydrothermal method. In the proposed aerosol process (Type IIIc), two furnaces were used in series at 150°C and then 550°C. The dried powder was then calcined at 550°C for 6h.

The method allowed for the production of doped mesoporous silica materials with interesting texture and high sorption capacity. The CeO_2-doped catalyst with a Si/Ce molar ratio of 25 was the most active (Figure 6). This catalyst had pores around 2.5 nm in diameter and displayed large specific surface area (950 $m^2.g^{-1}$) and pore volume (0.7 $cm^3.g^{-1}$) (Table 1). This result was related to the good dispersion of CeO_2 particles and to its high specific surface area. Several bimetallic catalysts were also studied,[173] and the mesoporous silica particles doped with both Ce and Al seemed to display a synergetic effect on the acetone removal as compared to the respective formulations with only one dopant. High catalytic activity was reached as long as the mesoporous structure could be maintained with high BET surface area and small CeO_2 particles sizes. These catalysts also showed good stability during a 24h test reaction at 250°C.

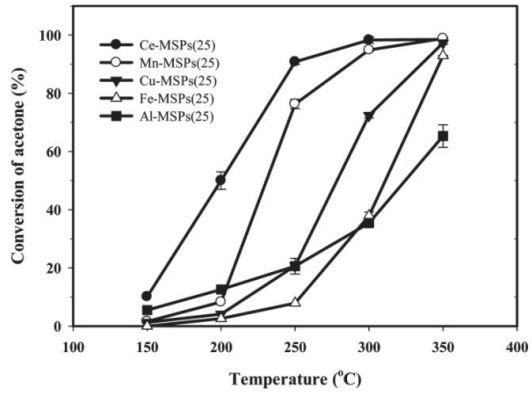

Figure 6. Acetone light-off curves obtained with transition metal-doped mesoporous silica catalysts prepared by the aerosol process, at a Si/metal molar ratio of 25 (acetone inlet concentration = 1000 ppmv, GHSV = 15000 h^{-1}). Reproduced with authorisation from Wang and Bai.[172]

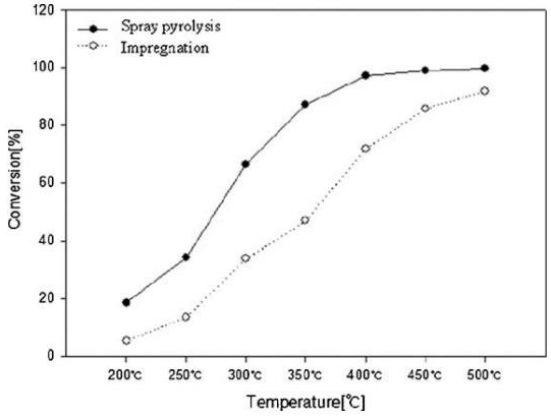

Figure 7. Comparison of two V_2O_5/TiO_2 catalysts respectively prepared by the aerosol-assisted sol-gel process (Type IIIc, here denoted "spray pyrolysis" by the authors) and impregnation method in the total oxidation of 1, 2-dichlorobenzene. Reproduced with authorisation from Jung *et al.*[174]

 This journal is © The Royal Society of Chemistry 20xx

Please do not adjust margins

Please do not adjust margins

Another common catalyst for the oxidation of chlorinated organic pollutants is V_2O_5-TiO_2.[125, 158, 238, 248-253] It has been demonstrated that its catalytic activity and selectivity strongly depend the dispersion of vanadia species, on the support crystallinity and on the catalyst texture.[254, 255] Jung *et al.* compared two V_2O_5/TiO_2 catalysts prepared by different methods and tested their catalytic performances in the conversion of 1,2-dichlorobenzene (1,2-DCB).[174] In the aerosol method, a mixture of titanium tetra-isopropoxide (TTIP), NH_4VO_3 and P123 was spray-dried in a two-zone electrical oven heated at 200 and 500°C, and then calcined at 450°C. In the conventional impregnation method (incipient wetness), the TiO_2 P25 from Degussa was used as the support. The V_2O_5/TiO_2 particles obtained by the spray method was mesoporous (Table 1) and presented anatase and rutile TiO_2 as the major and minor crystalline phases respectively. The rutile content increased with the increase of V_2O_5 loading, together with the catalytic activity. The best catalyst was obtained at 7 wt.% V_2O_5 and with a P123/Ti molar ratio of 0.05. This catalyst was much more active than the one prepared by impregnation (Figure 7). Such excellent catalytic behaviour in the total oxidation of chlorinated VOC can be ascribed to the stabilisation of highly dispersed VO_x crystallites of less than 4 nm, earlier identified as the more active than both isolated VO_x species and bulk V_2O_5 crystals.[125]

3.1.6. Silica-titania for selective oxidation reactions

Silica-titania materials are long-known as excellent catalysts for the oxy-functionalisation of alkanes.[256-258] Introducing mesopores in titanosilicate allowed to target the mild oxidations of bulky molecules, and particularly of sulphur-containing products.[256-258] Nevertheless, the textural properties of the mesoporous Si-Ti materials obtained with classical synthesis methods, such as the direct hydrothermal synthesis of ordered mesoporous materials (e.g. Ti-MCM-41, Ti-MCM-48, etc.),[259, 260] the grafting of Ti species onto mesoporous silica,[261, 262] or the hydrolytic[157] and non-hydrolytic sol-gel routes,[263] usually offer limited accessibility for large molecules.

Alonso *et al.* proposed to use α-chitin-nanorods as a natural template combined with sol-gel chemistry and spray drying process to obtain silica particles with large pores (Type IIIc).[134, 264] The idea was to simultaneously achieve optimum pore sizes and address the issue of the high cost of synthetic templating agents. To obtain Ti-Si catalysts with a similar texture, an ethanolic suspension of siloxane oligomers (3 nm) was first mixed with different quantities of $Ti(OiPr)_2(acac)_2$ and then with an aqueous chitin suspension (Figure 8).[175] Thus, in this case, one of the precursor for the sol-gel polycondensation reaction is already partly condensed. The resulting sol, presenting Si/Ti molar ratios from 19 to 70, was exchanged with ethanol before the spray drying (heated zone set at 120°C). The recovered powder was dried in an oven at 60°C for 72h and calcined at 550°C for 8h. Unlike the precipitation route, the aerosol-assisted sol-gel process enabled to recover – after calcination – the total amount of titanium introduced. These catalysts performed at high rates in the mild oxidation of methyl-phenyl sulfide (MPS). Interestingly, activity was almost linearly dependent on the pore volume.[175] In fact, the amount of accessible Ti sites was controlled by the initial chitin volume fraction. Thanks to the network of well-defined and interconnected mesopores obtained with the use of chitin as a sacrificial templating agent, the mass transfer was enhanced. Activity normalised by the surface area increased three-fold, compared to a Ti-MCM-41 catalyst and a SiO_2-TiO_2 non-hydrolytic sol-gel material.

Another application of the aerosol-assisted sol-gel process for the production of titanosilicate catalysts was proposed by Guo *et al.*[165] In this case, the TS-1 zeolitic structure was targeted for its well-known high activity in olefin epoxidation. Two different strategies were proposed in order to obtain spherical particles made of the TS-1 structure. In the first case, an aqueous solution containing TEOS, tetra-*n*-butyl titanate (TBOT), CTAB, TPAOH, HCl and ethanol was sprayed using a TSI atomiser and dried at 200°C. Upon subsequent calcination at 500°C, and thanks to the presence of TPAOH used as a structuring agent, the TS-1 phase could be obtained. In the second approach, TS-1 crystallites were first prepared and then re-dispersed in a precursor solution containing TEOS, TBOT, and CTAB. This suspension was processed in the same way by spray drying. In both cases, only framework Ti species could be observed. The catalysts exhibited both micro- and mesoporosity. Owing to its mesopores allowing facile diffusion paths and thanks to the presence of small TS-1 crystallites exhibiting larger external surface, the catalyst prepared by the first method showed excellent performance in cyclohexene epoxidation.

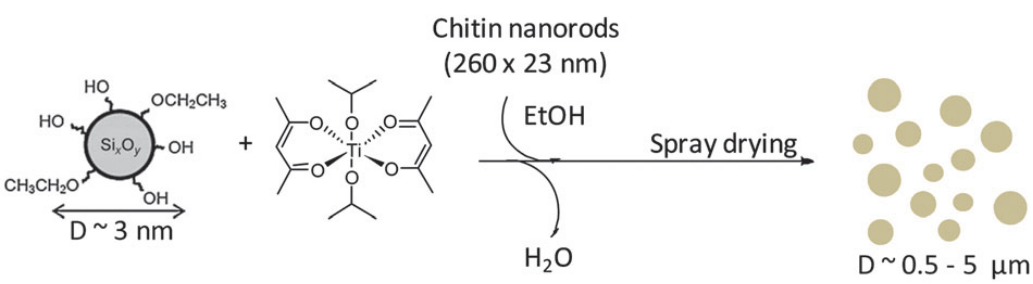

Please do not adjust margins

Please do not adjust margins

Figure 8. Synthesis of silica-titania nano-composites. The obtained spherical particles are porous, as a result of the templating effect of chitin nanorods. Reproduced with authorisation from Sachse *et al.*[175]

3.1.7. Titania microspheres for photocatalytic degradation of organic pollutants

The development of TiO_2-based materials with periodic mesostructured is an intense field of research, especially for photocatalytic applications.[265-267] TiO_2 is the most classical photocatalyst used to degrade organic pollutants.[268, 269] Knowing that the catalytic properties of titania are largely governed by its crystal structure, surface area and particle shape, the aerosol process appears as a powerful tool to design TiO_2-based materials with enhanced performance.

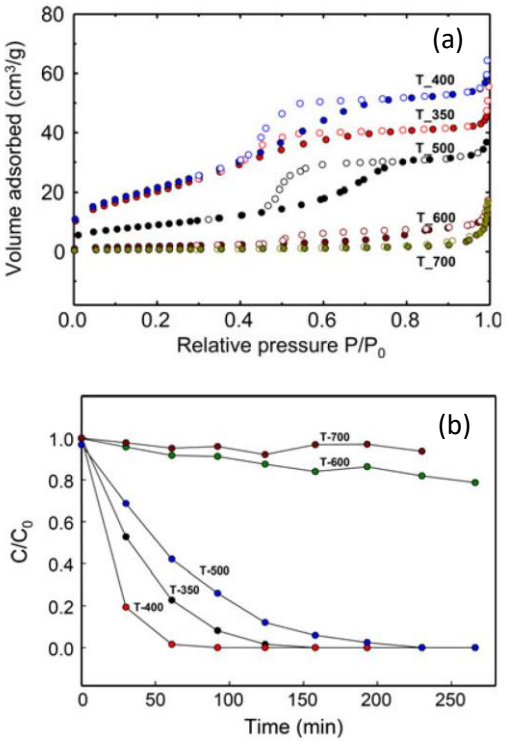

Figure 9. (a) N_2-physisorption isotherms obtained on TiO_2 photocatalysts prepared through an aerosol-assisted sol-gel process and calcined at different temperatures. (b) Performance of the same catalysts in the photocatalytic degradation of acetaldehyde during irradiation at 365 nm (C_0 is the initial acetaldehyde concentration at adsorption equilibrium and C is the remaining acetaldehyde concentration during the reaction). Adapted with authorisation from Oveisi et al.[176]

Oveisi *et al.* have reported on the aerosol-assisted synthesis of mesoporous titania spheres with crystallised anatase domains.[176] Titanium tetraisopropoxide was dissolved and hydrolysed in a highly concentrated HCl solution, which was then added to an ethanol solution containing F127. After 24h ageing, the solution was atomised and dried in an air flow injected at 200°C. To remove the surfactant and enhance crystallinity, the spray-dried products were calcined at various temperatures. Calcination above 350°C was required to remove efficiently the surfactant and release the mesoporosity (Figure 9(a)). Spherical particles were obtained in the 0.5-10 µm range. They showed a very smooth surface before calcination and a rough surface after calcination (at 350°C), indicative of the formation of small anatase crystallites of ~14 nm and of interparticle porosity accompanying the removal of the surfactant (Figure 10). This catalyst exhibit a surface area of 88 $m^2.g^{-1}$, a pore volume of 0.07 $cm^3.g^{-1}$ and an average pore size diameter of 3.5 nm. The onset of anatase crystallites was found at 250°C and the rutile phase was detected from 600°C. As the calcination temperature increases, the specific surface area and the pore volume decrease, while the average pore diameter increases. This can be attributed to the distortion of the mesostructures due to the anatase grain growth and then to the anatase-to-rutile phase transformation.

The photocatalytic properties were tested in the oxidative decomposition of acetaldehyde under UV irradiation (Figure 9(b)).[176] Expectedly, the crystallinity and surface area were found to have a major effect on the photocatalytic performance of the materials. Calcination at 400°C appeared to provide the best compromise to obtain relatively well-crystallised anatase domains while keeping a relatively high specific surface area (80 $m^2.g^{-1}$).

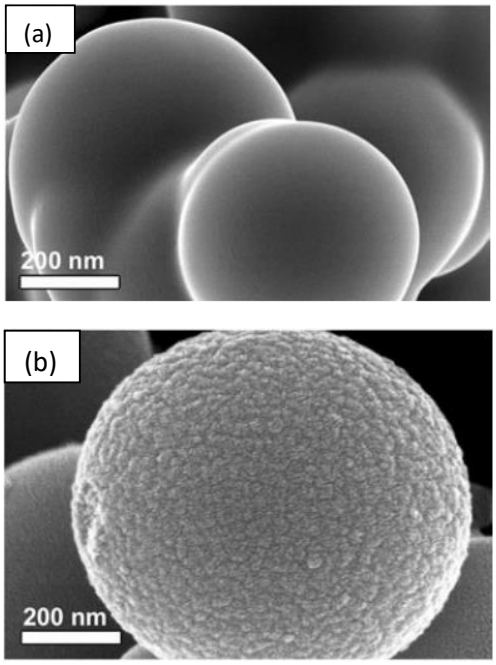

Figure 10. SEM micrographs of TiO_2 micro-spheres obtained by the aerosol process (a) before and (b) after thermal calcination at 350°C. Reproduced with authorisation from Oveisi *et al.*[176]

3.1.8. Metal functionalised periodic mesoporous organosilica

Inorganic-organic hybrid materials find various applications in technology and especially nanotechnology fields.[7, 27] The grafting of organic moieties at the surface of silica-based materials, for example, allows to tune their chemical properties and paves the way to various strategies that are important for

 This journal is © The Royal Society of Chemistry 20xx

Please do not adjust margins

Please do not adjust margins

heterogeneous catalysis, like enzyme immobilisation,[40, 270-273] grafting of organometallic complexes,[274, 275] etc.

About 20 years ago, the first Periodic Mesoporous Organosilica materials, or PMOs, were synthesised.[276-278] In these materials, the organic functionalities are directly incorporated into the silica walls, which reduces pore blockage and confers additional properties to the hybrid, mainly in terms of chemical and thermal stability.[6] Their uniform pore system and their high specific surface area make them excellent candidates for various applications, and especially for heterogeneous catalysis.[6, 279-281]

Aerosol preparation of PMOs was proposed by Yamauchi and co-workers: the aerosol-assisted co-condensation of TEOS and organosilanes lead to ethane and thiol-functionalised spherical mesoporous silica.[282, 283] The incorporation of Fe_3O_4 nanoparticles, in one step, was also demonstrated.[284] More recently, a PMO materials were synthesised by Ide *et al.* using bridging groups bearing a propylene group, which can then be further functionalised.[285] While none of the aforementioned materials were tested as heterogeneous catalysts, these reports should trigger future research work in this direction.

Zhang *et al.* applied an aerosol preparation technique to prepare a new kind of PMO by the co-condensation of TEOS of organometallic silanes, in the presence of CTAB and NaCl double templates. [177] In this case, the final material displays all the features of aerosol-processed PMO – i.e. high surface area, uniform pore structure, spherical particles, etc. – and additionally contains metal centres which can be exploited to generate catalytic active sites. Thus, CTAB, NaCl, ethanol, water, HCl, and TEOS were mixed together, allowing for the pre-hydrolysis of TEOS. Then, a THF solution containing the organometallic-bridged silane was added before atomisation. For comparison, materials were synthesised in the absence of NaCl and/or CTAB, or replacing these templates by P123. Pd, Ru and Rh-based catalysts with the repeating units [-Si-O-Si-CH_2-CH_2-PPh_2-M-PPh_2-CH_2-CH_2-Si-O-Si-] have been prepared in this way (M is the metal). Authors demonstrate the formation of uniform spheres with an average size around 400 nm and mesoporous structure (Figure 11). Cubic cavities of ~60 nm dimension could be formed by the templating effect of NaCl. The metallic species incorporated into the silica walls were shown to act as active sites in an array of catalytic reactions: Water-medium Barbier reaction, Sonogashira reaction, terminal alkyne acylation, Suzuki reaction, isomerisation, and Miyaura-Michael reaction. Activity levels were comparable with the corresponding homogeneous catalysts. Apart from the nature of the metal, the pore structure was shown to play a major role in the level of catalytic performance that could be achieved with the different catalysts. Good recyclability was obtained, owing to the true incorporation of the metal centres in the silica walls, thus not being prone to leaching.

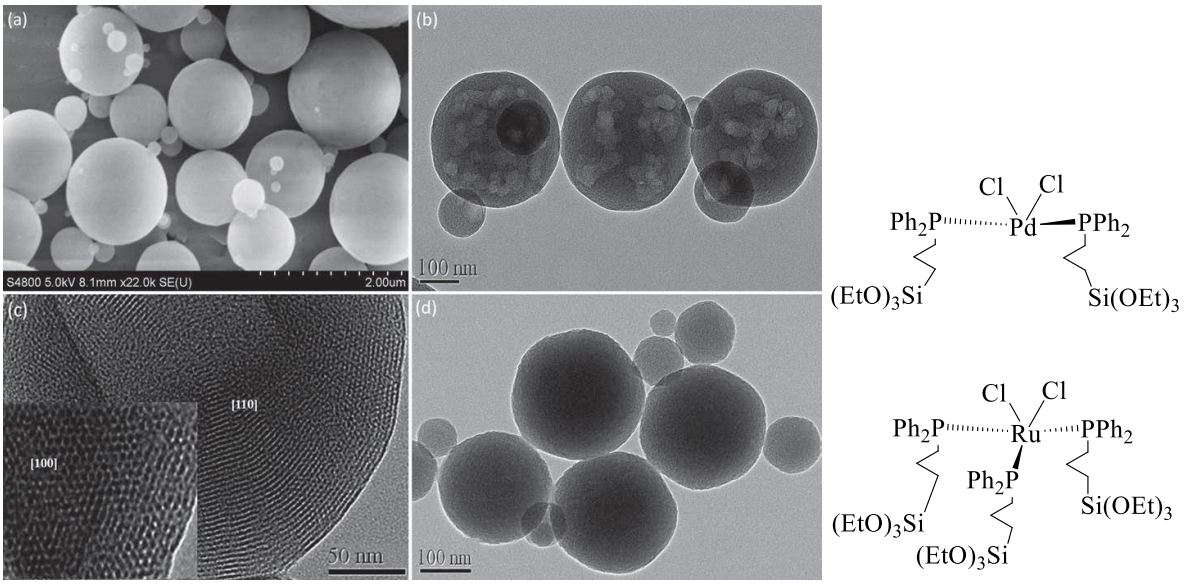

Figure 11. Left: (a) SEM and (b, c) TEM images of a Pd-PPh_2-PMO catalyst prepared with a double template approach (CTAB and NaCl). Spherical organosilica is obtained with (i) cavities in the macropore range due to the templating effect of NaCl and (ii) small mesopores due to the templating effect of CTAB. (d) TEM of a similar catalyst without cavities, prepared in the absence of NaCl. Right: chemical structure of the precursors used in combination with TEOS to produce metal periodic mesoporous organosilica. Adapted with authorisation from Zhang *et al.*[177]

3.1.9. Metal organic frameworks

Metal organic frameworks (MOFs) are a class of porous materials formed by bridging inorganic ions or clusters with organic ligands.[286] MOFs have attracted a lot of attention in the catalysis community because they can combine the benefits of heterogeneous catalysis – easy post reaction separation, reusability, stability – with those of homogeneous catalysis – well-defined active centres, high efficiency and selectivity.[287]

In a recent article, Gholampour *et al.* disclose the one-step preparation of a catalyst consisting in Pd nanoparticles entrapped in the bulk of a MOF structure.[178] The widely studied ZIF-8 structure was selected for this first example of

Please do not adjust margins

Please do not adjust margins

simultaneous fabrication of palladium particles inside a MOF using an aerosol-assisted approach. Inspired by the work of Maspoch and co-workers[55], the authors have prepared an aqueous solution of zinc acetate and methylimidazole, and they have supplemented it with palladium acetate. The solution was processed by spray drying at 180°C. The recovered powder was washed with methanol and dried at room temperature under vacuum. Characterisation confirmed the formation of the ZIF-8 crystalline structure. Bulk Pd was not detected in XRD suggesting a good dispersion. Indeed, electron microscopy studies demonstrated the presence of small (2-10 nm) Pd nanoparticles dispersed within the bulk of the ZIF-8 network (**Figure 12**). XPS revealed that Pd was present in its metallic state, probably because 2-methylimidazol acts both as the organic linker and as reducing agent. The incorporation of Pd did affect the textural properties of the microporous materials, and this was highly dependent on the Pd loading.

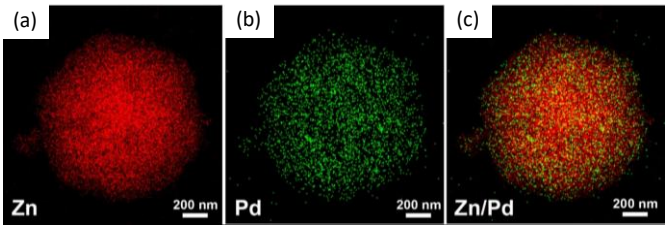

Figure 12. TEM-EDX elemental mapping of the 0.05%Pd@ZIF-8 catalyst showing that Pd is homogeneously dispersed in the ZIF-8 crystal. Adapted with authorisation from Gholampour *et al.*[178]

In the hydrogenation of various akenes, the pristine ZIF-8 was totally inactive, but Pd-loaded samples displayed high activity. Again, this was highly dependent on the Pd loading and the catalyst with 0.05 % Pd content was the most active, outcompeting previously reported catalysts[288, 289] where the Pd nanoparticles were incorporation into the ZIF-8 structure by solution infiltration or encapsulation. The possible occurrence of diffusion limitations is not addressed in the paper.

Regarding the catalyst synthesis, it should be noted that the mixture turns white before atomisation and that a white precipitate forms during the timespan of atomisation. This suggests that the synthesis of the solid is somewhat already triggered at this early stage. Yet, authors have reported that the precipitate was totally amorphous and that the ZIF-8 structure is actually obtained during the aerosol processing. This is why we place this example as a Type IIIc process.

3.1.10. Metal oxide catalysts for electrocatalysis

Electrochemical water splitting is an efficient way to produce 100% pure H_2 without CO_2 rejection.[290, 291] It is therefore being paid considerable attention, since H_2 is currently mainly being produced by the reforming of fossil fuels. Also, electrochemical water splitting allows to timely store sustainable but intermittent energy, like solar energy.[292, 293] The cathodic H_2 evolution reaction (HER) can be catalysed by Pt-based catalysts but can be replaced by cheaper sulphide, carbide, phosphide chalcogenide and even metal-free phases.[174, 294-296] The anodic O_2 Evolution Reaction (OER) can be catalysed by many different metal oxides – especially Co-based and Ni-based catalysts, perovskites, spinels – and hydroxides catalysts like layered double hydroxides.[297]

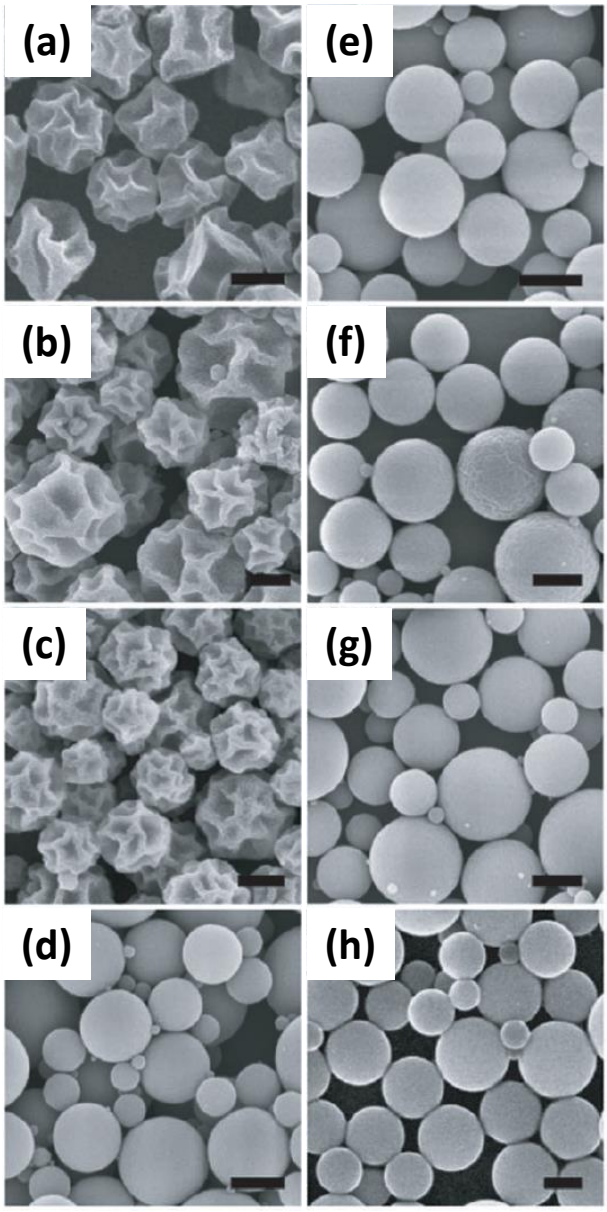

Figure 13. SEM micrographs of (a) NiO, (b) $Fe_1Ni_{10}O_x$, (c) $Fe_2Ni_{10}O_x$, (d) $Fe_6Ni_{10}O_x$, (e) $Fe_{10}Ni_{10}O_x$, (f) $Fe_{10}Ni_6O_x$, (g) $Fe_{10}Ni_2O_x$, and (h) Fe_2O_3 microspheres. Scale bar is 500 nm. Adapted from Kuai *et al.*[179] with authorisation.

Among the studied materials, amorphous metal oxides have shown high OER performances with low overpotential and Tafel slope than crystalline oxides which can be linked to their high capacitance.[298-300] Kuai *et al.* have proposed to screen for amorphous metal oxides using an aerosol-assisted synthesis approach.[179] Their proposition was to take advantage of a Type IIIc aerosol process to prepare formulations from cheap precursors, with adjustable compositions and mesoporous structures. Indeed, the elemental proportion can be accurately controlled from the composition of the mother solution and the

 This journal is © The Royal Society of Chemistry 20xx

Please do not adjust margins

Please do not adjust margins

texture can be controlled by using an appropriate sacrificial templating agent. Ni-Fe mixed oxides were chosen as a case study, starting from an ethanolic precursor solution containing P123, $Fe(NO_3)_3$ and $Ni(NO_3)$. The mist of droplets generated by an ultrasonic humidifier was processed through a tubular furnace heated at 480°C where the salts undergo a fast and partial co-decomposition to yield an amorphous mixed metal oxide. Indeed, the short residence time in the furnace implies that the metal oxides do not have sufficient time to crystallise. The collected powder was washed with ethanol to remove the template before the calcination. Fe-rich formulations yielded solid microspheres, while Ni-rich formulations tended to give concave hollow particles (Figure 13), which was tentatively attributed to a difference in the diffusion rates of Fe^{3+} and Ni^{2+} ions during the thermal processing.

It turned out that $Fe_6Ni_{10}O_x$ was the best catalyst for the electrochemical oxygen reaction with an overpotential of as low as 0.286 V at 10 mA cm^2 and a Tafel slope of 48 mV/decade. Thanks to this aerosol preparation process, it was demonstrated that the homogeneous distribution of Fe into NiO plays a crucial role in the electrochemical water splitting activity. HAADF-STEM-EDX element mapping showed that a remarkable control was achieved in terms of mixed oxides composition and dispersion. Interestingly, the charge-storage capacitance decreased with the calcination temperature, and this aerosol route allowed to keep the calcination temperature low, as compared to other synthesis procedures, thanks to the preliminary short pre-treatment that already occurs in the aerosol furnace.

The same authors have expanded the method to demonstrate its versatility and cost-effectiveness. They prepared a large set of monometallic oxides (Al_2O_3, Cr_2O_3, Mn_3O_4, Fe_2O_3, Co_3O_4, ZnO, Ga_2O_3, ZrO_2 CeO_2, MgO, NiO, CuO, WO_3) and a large series of complex metal oxides starting from metal nitrates salts, and using P123 and F127 as templates.[180] Depending on the formulation different types of complex metal oxides were obtained. For example, starting from Al and Zr nitrates, amorphous mixed oxides were obtained. In contrast, starting from Al and Au nitrates, the obtained solid was composed of AuO crystalline particles dispersed onto an amorphous alumina matrix (Figure 14).

Fe_2O_3 catalysts prepared by this technique were tested in the photocatalytic oxygen evolution reaction (Figure 15). Owing to its higher specific surface area and crystallinity, this catalyst performed better than a reference α-Fe_2O_3 photocatalyst. Moreover, adding Au in the formulation to obtain a Au/Fe_2O_3 formulation enhanced significantly the O_2 evolution rate. This was ascribed to the enhanced charge separation at the interface between the Au nanoparticles and the Fe_2O_3 host, as well as a possible contribution of plasmon-induced light absorbance by Au nanoparticles.

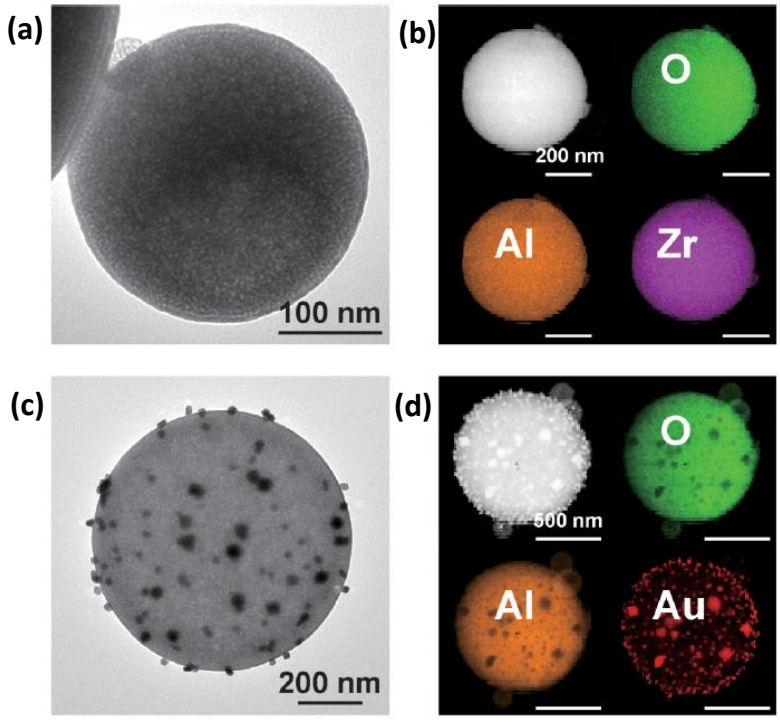

Figure 14. TEM micrographs of (a) mixed Al_2O_3-ZrO_2 amorphous mixed oxide and (c) Al_2O_3 microspheres loaded with gold nanoparticles. Representative complex mesoporous metal oxide products. (b) and (d) show the HAADF-STEM images (top-left corner) and elemental mappings of the corresponding products. Adapted with authorisation from Kuai *et al.*[180]

Please do not adjust margins

Chemical Society Reviews

REVIEW

$NiFe_2O_4$ is often reported as an active hydrogen evolution photocatalyst.[301] Hong *et al.* compared an aerosol-based protocol, using an ethanolic mixture comprised of F127, Fe and Ni nitrates, to a conventional hydrothermal synthesis route.[181] In their Type IIIc aerosol procedure, the droplets first pass through an assembly chamber at 50°C before entering another chamber set at 400°C. Two F127 concentrations were tested (5 $g.L^{-1}$ and 10 $g.L^{-1}$) and the catalysts were further calcined at 300°C or 400°C. Clearly, the texture and crystallinity of the obtained mesoporous nickel ferrites spheres were found to dictate the photocatalytic performance. High crystallinity of semiconductors is known to improve photocatalytic activity due to an enhancement in electron-hole separation.[302, 303] Logically, higher crystallinity resulted in higher catalytic activity for the photocatalytic hydrogen evolution from water with methanol (Figure 16). The surface areas had also an impact and the highest photocatalytic activity and robustness for the H_2 evolution was achieved with the sample exhibited both high crystallinity and surface area.

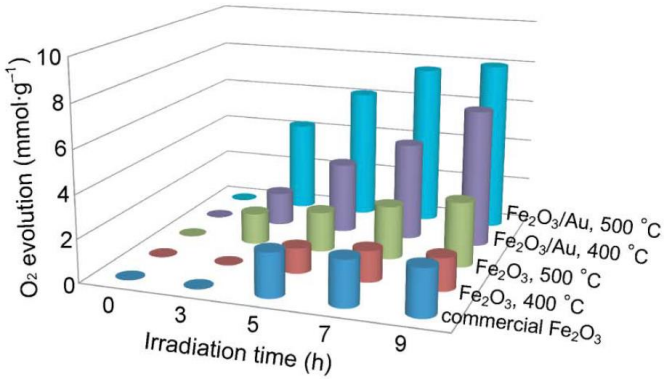

Figure 15. Oxygen evolution rates as a functions of the irradiation time for the different Fe_2O_3-based samples. Reproduced with authorisation from Kuai *et al.*[180]

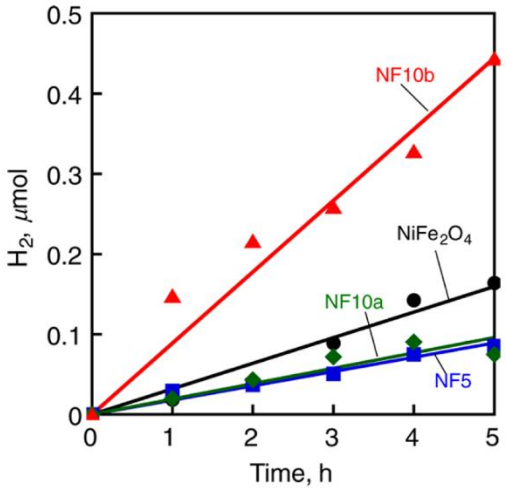

Figure 16. H_2 evolution under visible light irradiation (Xe lamp, $\lambda > 420$ nm) in a reaction suspension (5.0 mL) [methanol/ water, 1/4 (v/v)] containing 2.0 g of photocatalyst; NF5 (blue squares) was amorphous and displayed 235 $m^2.g^{-1}$ surface area; NF10a (green diamonds) was amorphous and displayed 278 $m^2.g^{-1}$ surface area; NF10b (red triangles) was crystalline (spinel nickel ferrite, $NiFe_2O_4$) and displayed 278 $m^2.g^{-1}$ surface area. The catalysts are compared with a reference $NiFe_2O_4$ prepared by a classical hydrothermal method (black dots). Reproduced with authorisation from Hong *et al.*[181]

3.1.11. Supported Au, Pd, Pt nanoparticles for hydrogenation reactions

Noble metals efficiently catalyse hydrogenation reactions and are classically dispersed at the surface of a refractory oxide support to ensure high dispersion and high activity.[304] Hydrogenation reactions are obviously critically important in organic synthesis.[305-307]

Please do not adjust margins

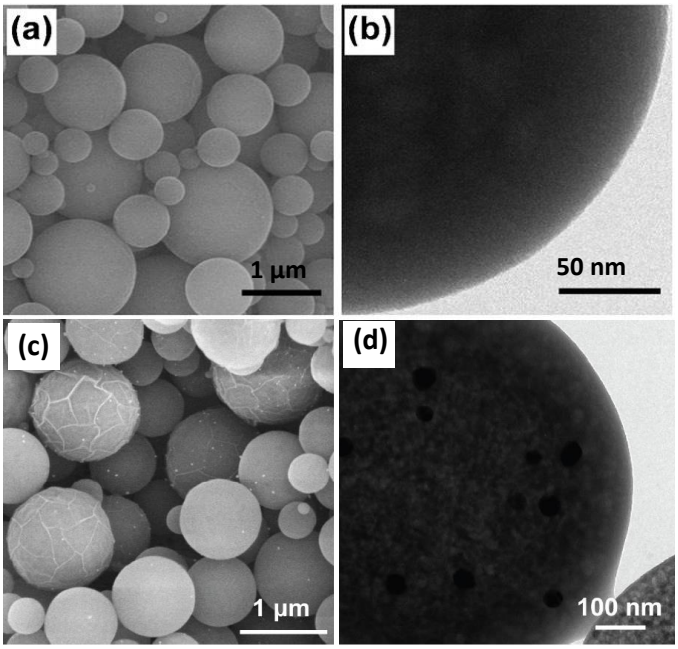

Figure 17. SEM (left) and TEM (right) micrographs of (a, b) 1% Au/Al_2O_3 prepared by the aerosol approach starting from Au colloids and (c, d) 1% Au/Al_2O_3 prepared by the spray method starting from chloroauric acid. Adapted with authorisation from Kan *et al.*[182]

Kan *et al*. proposed an aerosol strategy to support Au, Pd, and Pt nanoparticles onto Al_2O_3 or CeO_2 supports.[182] In this case, a suspension of nanoparticles was preliminarily prepared via $NaBH_4$ reduction of the metal salt in the presence of a capping agent (CTAB, CTAC or CTAB/PVP). The nanoparticles suspension was then mixed with an $Al(NO_3)_2$ or $Ce(NO_3)_3.9H_2O$ solution and a template (P123). The resulting precursor solution was atomised and passed through a tubular furnace set at 480°C. During the drying process, solvent evaporation induced nitrate decomposition and oxide cross-linking, together with the surfactant-directed mesostructure formation. The procedure can therefore be put in the Type IIIc aerosol process category, even if pre-formed metal nanoparticles were also included in the precursor solution. The nanoparticles were trapped in the mesoporous Al_2O_3 or CeO_2 microspheres. For comparison, a $1\%Au/Al_2O_3$ catalyst was synthesised using an aqueous $HAuCl_4$ solution instead of the Au nanoparticles colloidal suspension. In this case, a subsequent thermal treatment in H_2 was required to obtain the metallic Au nanoparticles. According to TEM observations, the final mean Au particle size was ten times smaller on the catalysts prepared via the colloid approach (Figure 17). Thus, this preparation process allows preserving the small size of the pre-formed nanoparticles even at high metal loading because no prolonged thermal treatment in H_2 is required in this case. TEM images also revealed the homogeneous dispersion of the metal active phases on the oxide supports achieved with the aerosol process.

Among the tested catalysts, $1\%Pd/Al_2O_3$ and $1\%Au/Al_2O_3$ showed high reaction rates in the hydrogenation of 4-nitrophenol into 4-aminophenol at 20 °C in water (**Figure 18**). After five successive reaction cycles, the $1\%Au/Al_2O_3$ prepared from Au colloids still exhibited a 96% conversion whereas the conversion obtained with the catalysts prepared from $HAuCl_4$ decreased to 58%. This different behaviour could be explained by the larger nanoparticles generated with the conventional spray method starting from the metal salts. However, the thermal stability of $1\%Au/Al_2O_3$ was not satisfactory: after a 4h treatment at 400°C, 85% of the activity was lost. The coalescence of the Au nanoparticles into large crystals of 100 nm was responsible for the poor thermal stability. Authors found out that CeO_2 was a better support allowing to reach both higher activity and highly improved thermal stability.

Jin *et al.* reported the aerosol preparation of 9 types of catalysts with TiO_2, ZrO_2 and Al_2O_3 as mesoporous microspheres supports and with Au, Pd and Pt as active nanoparticles.[183] Taking inspiration from the work of Tsung *et al.*,[308] they combined the evaporation-induced self-assembly of a templating agent (F127) and the acetic acid-mediated sol-gel chemistry of Ti, Zr and Al alkoxide precursors. A metal salt was added in the starting mixture, which was then atomised and processed at 380°C. The collected powder was calcined and then reduced in flowing H_2. Thus, in this case, the metal salt is directly incorporated along with the precursor solutions in an attempt to enhance the interactions between the metal species and the surrounding matrix. Such direct incorporation of the metal salts in the precursor solutions is indeed often claimed to give rise to synergistic interactions between the metal oxide based active support and the metallic nanoparticles.[309-311] After thermal treatment and reduction, metal nanoparticles were clearly observed in SEM, and the observation of a broken microsphere showed that they are located both on the surface and inside the microsphere.

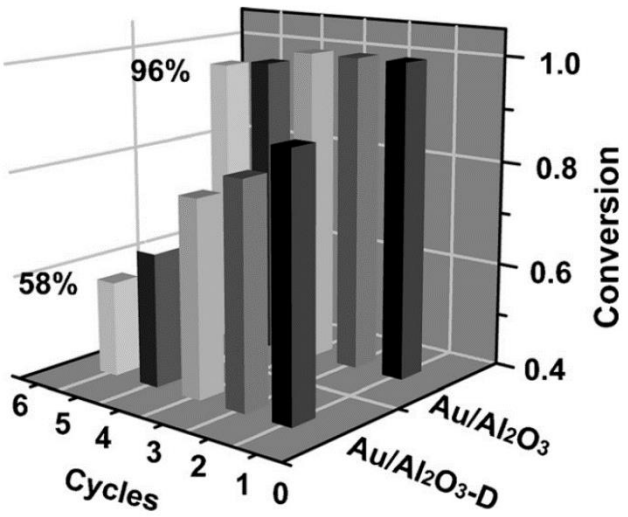

Figure 18. 4-nitrophenol conversion for the 1 % Au/Al_2O_3 (prepared from Au colloids) and 1 % Au/Al_2O_3-D (prepared from chloroauric acid) catalysts for five successive cycles at 5 min reaction time. Reproduced with authorisation from Kan *et al.* [182]

The highest performances in the liquid phase reduction of 4-nitrophenol with sodium borohydride to 4-aminophenol were achieved with the TiO_2 microspheres loaded with Au and Pd (Figure 19). The highest TOFs were generally achieved with the lowest metal loading (0.1 wt.%), and this could be explained by

Please do not adjust margins

Please do not adjust margins

fact that smaller particles are formed at low loading, generating a higher fraction of coordinatively unsaturated surface atoms. Although the recyclability of these catalysts was shown to need further improvement, this work demonstrated that it is possible to prepare highly efficient noble metal-based catalysts via an easy and economical aerosol approach.

To go further, the same authors also investigated a multistep aerosol approach for the preparation of noble-metal nanocrystals embedded into hollow mesoporous microspheres using polystyrene nanospheres as a template.[312] Activity and selectivity in noble metal catalysts are known to be highly dependent on the geometry of the metal particles.[313] Thus, Au nanorods, Pd nanocubes and Au core/Pd shell nanorods were prepared in a first step and then stabilised using methoxypoly(ethyleneglycol) (mPEG). These functionalised metal nanocrystals were adsorbed on preformed polystyrene (PS) beads of ~270 nm. These particles were then added to an acidic sol-gel solution containing a surfactant and Ti, Zr or Si alkoxides. The mixture was spray dried in an oven set at 380°C and the collected powder was calcined at 400°C to remove the surfactant, mPEG, and PS beads. The process is illustrated in Figure 20 in the case of metallic nanorods incorporated into hollow mesoporous zirconia microspheres, but similar results have been obtained with Au nanorods and Pd nanocubes, embedded into titania or zirconia microspheres. The embedding of the metal nanocrystals into the hollow mesoporous metal oxide microspheres was shown to prevent the aggregation of the metal nanocrystals. For example, in the catalytic reduction of 4-nitrophenol to 4-aminophenol, the Pd nanocube-embedded ZrO_2 microspheres were found to exhibit a much higher catalytic activity and a superior recyclability in comparison with a commercial Pd/C catalyst.

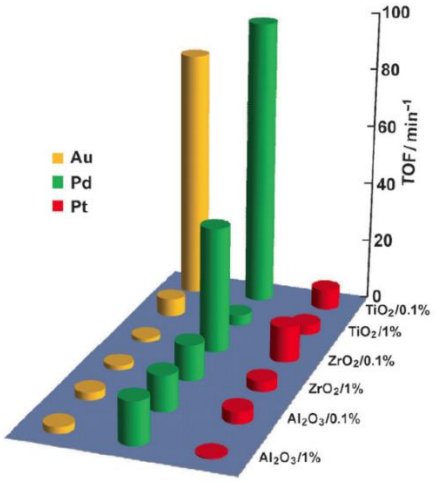

Figure 19. Turnover frequencies obtained in the catalytic reduction of 4-nitrophenol to 4-aminophenol using various metal-based catalysts prepared by an aerosol process. Percentages indicate the molar metal loadings. Reproduced with authorisation from Jin *et al.*[183]

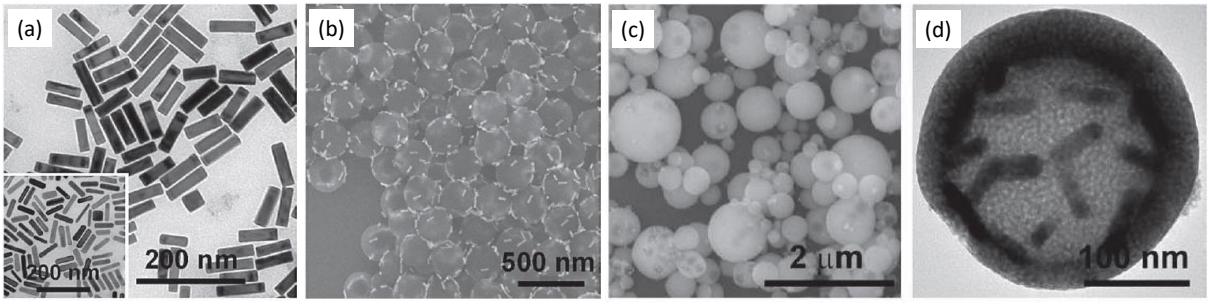

Figure 20. The different steps of the preparation of mesoporous oxide hollow microspheres embedded with metal nanocrystals. In this case, Au core / Pd shell nanorods (a) are adsorbed onto polystyrene beads (b) and theses particles are sprayed together with a zirconium butoxide solution to yield spherical microspheres from which the polymer template is removed by calcination (c and d). Images (a) and (d) were obtained in TEM, Images (b) and (c) were obtained in SEM. Adapted with authorisation from Jin *et al.*[312]

3.1.12. Supported Au nanoparticles for CO oxidation

Supported gold nanoparticles constitute one of the major objects of investigation in catalysis,[314-316] in particular in environmental catalysis, owing to their high activity of CO oxidation.[317] It is well documented that the activity of gold nanoparticles is mainly dictated by their size and one of the challenges is to develop catalysts in which sintering of gold nanoparticles is avoided.[305, 318] Interestingly, Gabaldon *et al.* have used an aerosol process to produce porous silica materials subsequently used as support for gold nanoparticles.[184] In their study, an aqueous solution of TEOS containing CTAB as a templating agent was sprayed and dried rapidly to generate mesoporous silica microspheres (Type IIIc aerosol process). Gold was incorporated in a second step by the deposition-precipitation method and then reduced in flowing H_2 at 200°C. Other classical mesoporous silica materials were used as supports as well. One of their significant findings is that the nanoparticles formed at the surface of aerosol-made silica are much more stable towards sintering during the reduction treatment, as compared to the nanoparticles on all other supports (Figure 21). In fact, 3-D pores like those found in SBA-11, SBA-12, and HMM-2 have great interconnectivity which favours particle sintering via the Otswald ripening mechanism. Aerosol-made silica, on the other hand, displays 1-D pores – like those found in MCM-41 – with limited connectivity. Moreover, the pores in the aerosol-made support are tortuous, because 1-D micelles of surfactant don't have the time to align during the fast synthesis process. Resulting tortuosity also hampers the Otswald ripening. Thus, the catalysts based on the supports made by the aerosol process exhibited smaller gold nanoparticles with narrower size distribution and generally

 This journal is © The Royal Society of Chemistry 20xx

Please do not adjust margins

Please do not adjust margins

performed better in the oxidation of CO. Further catalyst improvement has been obtained by modifying the silica supports with amino groups or by incorporating TiO_2, further enhancing the stability of small gold nanoparticles.

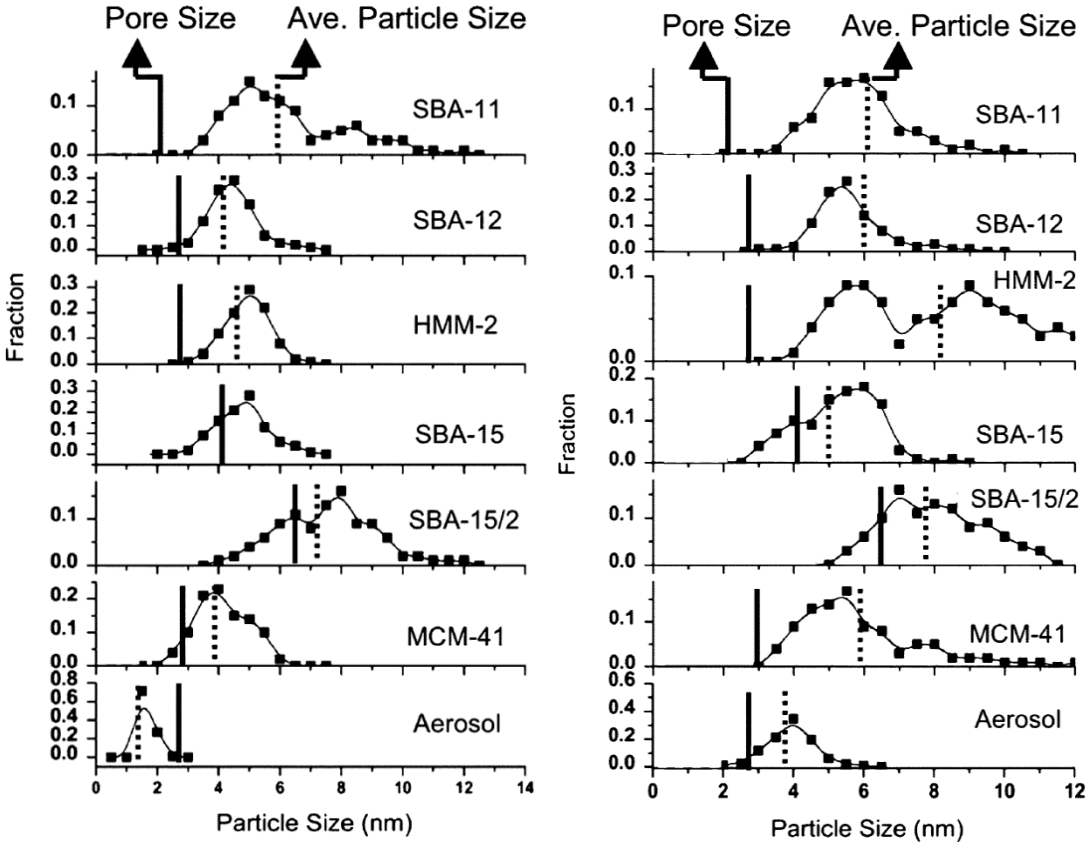

Figure 21. Size distribution of Au nanoparticles deposited onto various mesoporous silica supports after (left) reduction under H_2 at 200°C for 2h or (Right) reaction up to 400°C under flowing 20% CO, 10% CO and He. The solid line represents the pore diameter; the dotted line represents the mean particle size of Au. Reproduced with permission from Gabaldon *et al.*[184]

3.2. Thermal decomposition towards non-porous oxides particles and supported metal nanoparticles

In Type IIIb aerosol methods (Scheme 4), the processing temperature is high, leading to the decomposition of the precursors (alkoxides, salts, chlorides, etc.). In this case, no organic sacrificial templating agent is used, and therefore the obtained elementary particles are typically non-porous. The latter are often aggregated together, thereby generating interparticle mesoporosity. Non-porous elementary particles can also form a spherical crust during processing, generating hollow particles. Two main families of catalysts can be obtained in this case (Table 2): (i) bulk metal oxides or mixed metal oxides and (ii) supported metals or metal oxides.

The case of bulk oxide is illustrated by TiO_2 photocatalysts, obtained from the high temperature decomposition of Ti precursors. In this case, performance will be dictated by the crystallinity of the formed particles and by their specific surface area. Also, the process can be used to insert dopants in the photocatalyst. Such doping can be effectively achieved using aerosol preparation routes.

The case of supported catalysts is exemplified by noble metal-based hydrogenation catalysts supported on alumina. Dispersing highly active and stable metal nanoparticles onto a metal oxide support is an important challenge in catalysis science.[63, 319-321] In conventional preparation methods, a metal salt is impregnated onto a support and then thermally treated – often reduced – into its active form.[322] Alternative procedures include the "deposition-precipitation" methods[323] as well as colloidal methods where the metal nanoparticles are pre-formed before being deposited onto – or trapped into – a suitable support.[324, 325] In general, one major issue in the synthesis of oxides catalysts loaded with metal nanoparticles is to allow the diffusion of the metal species into the nanometre scale pore channels, to ensure high metal dispersion and also to prevent them from blocking the pore openings.[326]

Aerosol methods can be used for the preparation of supported nanoparticles. In some cases (discussed in the following sub-sections), the metal salt is directly incorporated in a precursor solution and both the support and the nanoparticles are obtained in a one-step bottom up approach using the aerosol process. In other cases, only the support is built via the aerosol process, but preformed metal or metal oxide nanoparticles are introduced in the starting solution. A successful example is the preparation of mesoporous TiO_2 microspheres doped with preformed Fe_2O_3 nanoparticles.[331] Another innovative strategy was demonstrated by Backman *et*

Please do not adjust margins

Please do not adjust margins

al. for the synthesis of Ag/TiO_2 materials.[332] They used a particular one-step aerosol process that allowed avoiding the drying and the calcination steps used in wet processes. In this case, the heated zone consisted in two separate zones. Titanium tetra-isopropoxide (TTIP) was used as a precursor for the TiO_2 and nebulised before passing through the first portion of the heated tubular reactor. The thermal decomposition of the TTIP gave rise to the TiO_2 supporting material. The latter was carried through a second zone heated at 1100°C where silver (particles of less than 250 µm in size) was evaporated from a ceramic crucible. This ensures that the TiO_2 particles are already formed before they reach the Ag deposition zone. The finely dispersed silver nanoparticles had a mean particles size of 1.1 nm, according to TEM observations. They could be interesting in photocatytic applications, or in organic synthesis for dearomatisation or epoxidation reactions, for example.[333-335] Aerosol methods were also used to prepare tailored metal particles, including for example core-shell nanoparticles.[336] The materials listed in this paragraph, appear highly interesting in the perspective of applications as heterogeneous catalysts but they have not been tested as catalysts. In the next sections, we present an overview of materials prepared by aerosol processing at high temperature (Type IIIb), which have been successfully applied as heterogeneous catalysts.

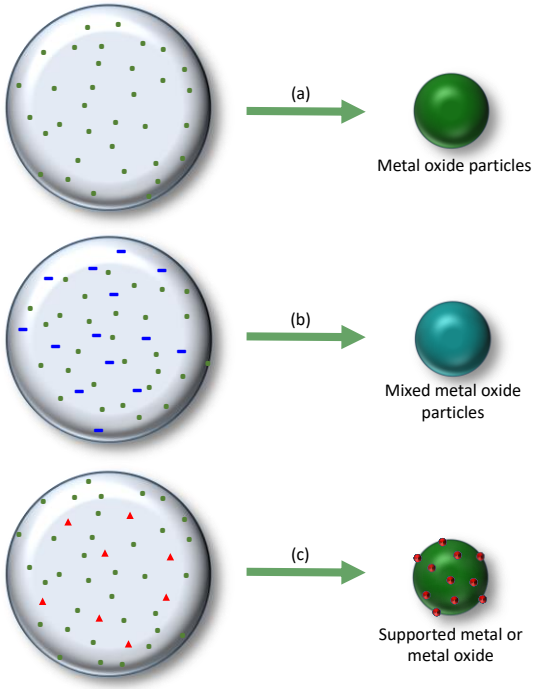

Scheme 4. Thermal decomposition of aerosol droplets to heterogeneous catalysts. In route (a) the starting solution contains a molecular precursor for a metal (i.e. the green dots represent a metal alkoxide, or chloride, etc.) which is thermally decomposed to give non porous metal oxide particles (the latter can be found in various sizes and forms of aggregation). A typical example is the preparation of TiO_2 photocatalysts. In route (b) the same process is carried out in the presence of two (or more) different molecular precursors which decompose together to give mixed oxide particles. A typical example is the preparation of Bi-doped TiO_2 photocatalysts. In route (c) the starting solution contains a molecular precursor that will decompose to form non porous metal oxide particles (or carbon microspheres from organic sources in some examples) and a metal salt (depicted as red triangles) which does not react simultaneously during the thermal process and is deposited at the surface of the support typically in the form of dispersed nanoparticles. An example is that of Ru/Al_2O_3 methanation catalyst.

Table 2. Thermal decomposition towards non porous oxides particles and supported metal nanoparticles (Type IIIb)

Catalyst	Pore diameter (nm)	Specific surface area ($m^2.g^{-1}$)	Pore volume ($cm^3.g^{-1}$)	Reaction	Key chemical property	Reference
$Ti_{1-x}Zr_xO_2$	0.45-3.68	39-96	0.23-0.45	Photocatalytic degradation of Rhodamine B	Core-shell microspherical solid-solution	132
Ni and B-doped TiO_2	3.8-7.3	39-106	0.08-0.16	Photocatalytic removal of NO	Hollow structure favour NO transportation	327
Fe/C nanocomposites	n.r.	n.r.	n.r.	Remediation of chlorinated hydrocarbons (TCE)	Fe nanoparticles accessibility and stability	328
Fe nanoparticles / Carbon matrix	3-5	14-118	0.0284-0.2324	Water treatment	Controlled Fe nanoparticles placement on carbon microspheres	167
Ru/TiO_2 coating	n.r.	n.r.	n.r.	Electrocatalytic activity for OER and CER evolution	Highly porous coating obtained by ordered packing of sub-micron spheres	329
(Li, Na, K, Rb, Cs) Ru/Al_2O_3	n.r.	25-27	n.r.	CO_2 hydrogenation	Activity higher than with conventional impregnation	330

This journal is © The Royal Society of Chemistry 20xx

Please do not adjust margins

Please do not adjust margins

Ru/TiO_2	n.r.	10-15	n.r.	CO_2 hydrogenation	Activity higher than with conventional impregnation	[131]

n.r. stands for "not reported".

3.2.1. TiO_2 and doped TiO_2 for water decontamination (photocatalysis)

TiO_2-based materials are extensively used in the field of environmental photocatalysis, for example for the degradation of organic dyes in industrial wastewater.[337-341] The challenge is to extend the optical absorption of titania from the UV to the visible light region, for example using dopants,[342-346] so that solar light can be used directly as the excitation source. In addition, producing smaller TiO_2 particles with higher crystallinity allows reducing recombination rate of photo-produced electron-hole while accelerating charge transfer.

Huang *et al.* have used an aerosol process to produce a series of $Ti_{1-x}Zr_xO_2$ photocatalysts made of spherical particles, starting from aqueous solutions of $TiCl_4$ and $ZrOCl_2.8H_2O$ solutions sprayed and processes at 600°C in a tubular furnace.[132] No template was used and the texture was simply dictated by the agglomeration of non-porous elementary particles. Among the tested catalysts, the formulation where 9 wt. % of Ti was replaced by Zr showed the best photocatalytic activity in the photocatalytic degradation of rhodamine B, outcompeting the commercial P25 TiO_2. Later on, the same research group extended the method to produce pure and boron and nickel doped TiO_2 microspheres.[327] The synthesis was performed via the nebulisation of an aqueous solution of $TiCl_4$ supplemented with H_3BO_3 and/or $NiCl_2.2H_2O$, followed by rapid thermal decomposition. Microspheres, in the ~100 nm range (Figure 22), were formed by the aggregation of elementary crystalline particles ranging between 7 and 11 nm. In particular, they observed the formation of hollow spheres when the synthesis was performed in the presence of H_3BO_3. This was tentatively explained by the emission of gaseous HBO_2 during the drying process. The materials were tested in the photocatalytic removal of NO and the aerosol-made catalysts performed significantly better than the commercial Degussa P25 photocatalyst (Figure 22).

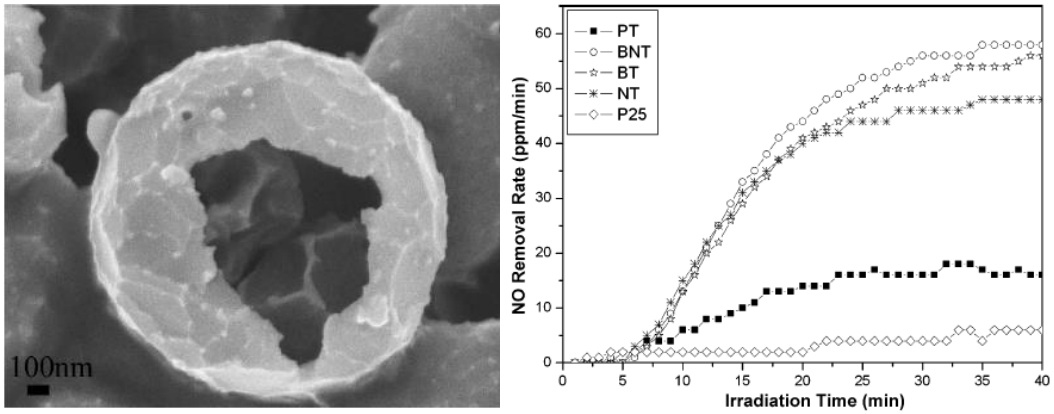

Figure 22. (left) SEM micrograph of a B-doped TiO_2 microsphere obtained by the aerosol process and (right) catalyst performance of aerosol-made photocatalysts as compared to the reference Degussa P25 in the photocatalytic removal of NO (PT=pure titania, BNT = B,Ni-doped titania, BT = B-doped titania, NT = Ni-doped titania). Reproduced with permission from Huang *et al.* [327]

3.2.2. Iron nanoparticles supported on carbon for the remediation of chlorinated organics

Chlorinated organics such as trichloroethylene are classical contaminants in groundwater and are difficult to remediate. Zero valent iron nanoparticles can be used directly in contaminated underground water to convert these chlorinated hydrocarbons into less harmful hydrocarbons via reductive dechlorination.[347] The efficiency of these nanoparticles can be enhanced if they are immobilised onto a carrier. Using an aerosol process, Zhan *et al.* obtained micrometric Fe/C particles (100-800 nm), starting from a solution of sucrose – used as the carbon source – and $FeCl_3.6H_2O$.[328] The solution is atomised to form aerosol droplets which were then carried by an inert gas (N_2) through a heating zone where solvent evaporation and carbonisation occurred. H_2SO_4 was added to the starting solution, as a catalyst for sucrose carbonisation. Interestingly, sucrose carbonisation and iron salt precipitation are competitive phenomena which can be tuned by changing the temperature of the heating zone. This, in turn, allows controlling the position of the Fe nanoparticles with respect to the carbon matrix: embedded inside or dispersed at the surface of the carbon spheres (Figure 23).[167] The composites exhibited excellent performance in the remediation of chlorinated carbons. The carbon matrix plays the role of the adsorbent for the pollutant, facilitating the action of the iron nanoparticles. In this application, the composite is not a true catalyst since iron acts as a reactant and is not recycled. However, the materials developed by Zhan *et al.* look very promising in the perspective of other heterogeneous catalysis processes (e.g. for Fischer-Tropsch synthesis).[348, 349]

Please do not adjust margins

Chemical Society Reviews

REVIEW

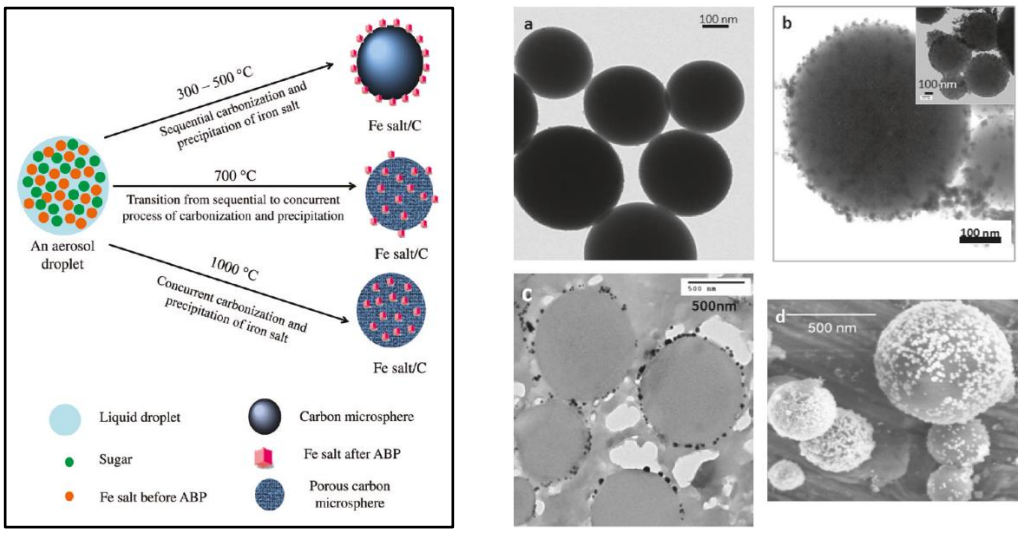

Figure 23. (left) Proposed mechanism of morphological changes and metal nanoparticle placement with temperature (reproduced with authorisation from Sunkara *et al.*[167]). (right) (a) TEM of carbon spheres prepared by an aerosol-based process. (b) TEM, (c) cut-section TEM, and (d) SEM of a Fe/C catalyst (the inset in (b) is the low magnification TEM of Fe/C). Reproduced with authorisation from Zhan *et al.* [328]

3.2.3. RuO_2/TiO_2 for electrocatalysis

Chlor-alkali electrolysis process is an important bulk processes in modern electrochemical industry.[350, 351] Electrodes consisting of Ti coated by a combination of TiO_2 and a noble metal oxide are the most investigated electrocatalysts for the chlorine evolution reaction.[352, 353 291] In this context, aerosol techniques have been proposed to prepare a variety of promising materials. For example, TiO_2 core/RuO_2 shell particles have been prepared using a multistep ultrasonic spray set-up.[354]

Koševic *et al.*[329] have recently proposed the continuous synthesis of spherical RuO_2/TiO_2 particles coupled with their deposition as a coating onto expanded titanium substrate. In their process, tetra-*n*-butylorthotitanate is hydrolysed in a first step, then mixed with $RuCl_3$ and finally dispersed in the form of an aerosol via an ultrasonic atomiser using O_2 as a carrier gas (Figure 24-top). RuO_2/TiO_2 particles form when the aerosol is carried through a tubular furnace set at 800°C. During this thermal process, both TiO_2 and RuO_2 formation and crystallisation occur. The gas-transported particles are electrostatically collected at the surface of expanded titanium by the application of a high-intensity electrostatic field. The titanium plate is maintained at 500°C to trigger an immediate thermal treatment which favours the adhesion of the particles. The particles were shown to adhere to the surface and to form a thick coating of ca. 20 µm, with some cracks (Figure 24-bottom). The anodes showed good electrocatalytic activity for oxygen and chlorine evolution reactions, as well as acceptable stability in the conditions used for the electrolysis of dilute chloride solutions.

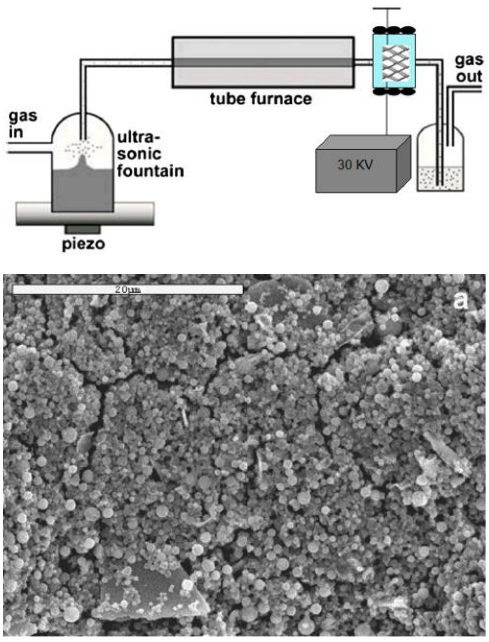

Figure 24. (top) Schematic representation of the setup used to synthesise RuO_2/TiO_2 particles and their deposition onto expanded Ti by an electrostatic field. (bottom) SEM micrograph of a Ti rod with the RuO_2/TiO_2 coating (scale bar is 20 µm). Reproduced with authorisation from Koševic *et al.*[329]

Please do not adjust margins

3.2.4. Ru-based catalysts for CO_2 methanation

With the urgent need we face mitigating our impact on the climate,[355, 356] important efforts are being made to curve net CO_2 emissions. In the perspective of CO_2 utilisation, the Sabatier reaction is a currently vibrant field of research in which a large variety of heterogeneous catalysts are being investigated.[313, 357-364] Among those, Ru-based catalysts are recognised as the most active CO_2 methanation catalysts and is intensely studied.[357, 360, 365-371]

Li *et al.* prepared Ru/Al_2O_3 methanation catalysts via a one-pot aerosol method.[330] An aqueous solution of $RuCl_3.3H_2O$ and $Al(NO_3)_3.9H_2O$ was atomised using an ultrasonic device and then passed through a quartz tube reactor heated by two furnaces connected in series and set at 600°C and 1000°C. The residence time for the droplets in the heated reactor was about one second. Interestingly, authors also prepared alumina supports by the aerosol method and then impregnated the latter with $RuCl_3.3H_2O$ to study the interest on the one-pot approach versus the impregnation method. Prior to use in the methanation reaction, all catalysts were oxidised under oxygen (400°C) and then reduced under hydrogen (400°C). The high temperature encountered during spray drying provoked the crystallisation of the alumina support in the alpha phase and the formation of relatively large RuO_2 crystals. The latter were in strong interaction with the alumina support, as attested by the relatively high reduction temperature observed in TPR for the catalysts prepared through spray.

Spray-dried Ru/Al_2O_3 catalysts outcompeted markedly the impregnated catalysts, both in terms of specific activity and in terms of TOF (Figure 25). Authors put forward that the higher performance of sprayed catalysts could be attributed to a more intimate interaction between the active phase and the support. Possibly, the lower chlorine contamination in the sprayed catalyst could also have led to higher methanation activity. It can be noted that promotion with alkali metals could be achieved easily by simply adding an appropriate salt (e.g. KNO_3) in the precursor solution. The addition of alkaline salts promoted the catalytic activity of Ru/Al_2O_3, irrespective of the preparation methods employed. It may be noted that such formulation should be highly active in the mild condition synthesis of ammonia, which is also of great current interest.[372]

A similar approach was used to prepare Ru/TiO_2 methanation catalysts, using $TiCl_4$ as the titania precursor.[131] Again, the catalysts prepared by the spray technique were much more active than those prepared by the impregnation method, which was rationalised by the formation of additional active sites at the boundaries between the metal and the support and by the inhibition of the so-called strong metal support interaction (SMSI) effect. Apart from the aerosol synthesis itself, an important parameter was found to be the temperature of the reductive pre-treatment.

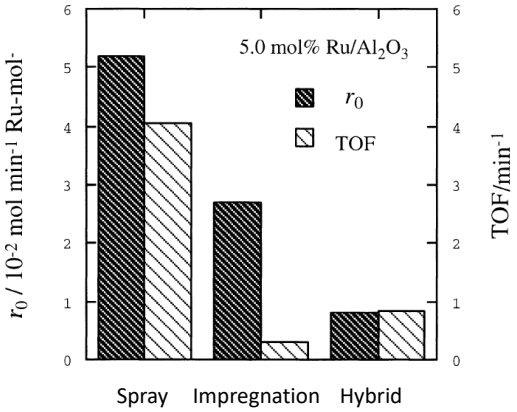

Figure 25. Effect of the preparation methods on the activity (rate and TOF) of 5.0 mol.% Ru/Al_2O_3 catalysts in the methanation of CO_2 at 300°C. (Spray) catalyst prepared in one-pot by atomisation of a $RuCl_3.3H_2O$ and $Al(NO_3)_3.9H_2O$ solution, (Impregnation) catalyst obtained by the impregnation of a commercial alumina support with $RuCl_3.H_2O$, (Hybrid) catalyst obtained by the $RuCl_3.H_2O$ impregnation of an alumina support prepared by spray drying. Adapted with authorisation from Li *et al.*[330]

Table 3. Catalysts prepared by an aerosol-mediated precipitation (Type II).

Catalyst	Specific surface area ($m^2.g^{-1}$)	Pore volume ($cm^3.g^{-1}$)	Reaction	Key chemical property	Reference
$NaAlO_2$	n.r.	n.r.	Glycerol transesterification with DMC	High surface basicity	117
MoVTeNb	2.5-88	0.014-0.084	Selective oxidation of propane to acrylic acid	Controlled synthesis of phase-pure mixed oxides	118
Bi-Mo	4.1-12.2	n.r. [a]	Selective oxidation of propylene into acrolein	High purity and stoichiometric ions interaction	373
Bi-Mo	1.4-3.5	n.r. [a]		Higher SSA by coupling complexation and spray drying	374
Ce-Co/Si-Al papers	n.r. [a]	n.r. [a]	Diesel soot oxidation	Smaller NPs and lower soot combustion T°C than with conventional drip method	375
$ZnAl_2O_4$	90	1	Photo degradation of MO/MB to MO	Good interaction between basic Mo molecules and acidic-sites of $ZnO/ZnAl_2O_4$	376
Nano-sized ZSM-5 aggregates	413.3	0.3251	Catalytic cracking of 1,3,5-triisopropylbenzene	Uniform pore channels, high thermal stability, acidity, good Al species distribution	377

Please do not adjust margins

Please do not adjust margins

Pd/ferrierite	n.r. [a]	0.22	Hydrogenation of propyne (alkyne)	Higher Pd dispersion	378

n.r. stands for "not reported".

3.3. Catalysts prepared by an aerosol-mediated precipitation from salts

In this category, the Type II aerosol processing is used to trigger the precipitation of molecular or ionic species initially present in solution (Scheme 5 and Table 3). Owing to the fact that the precipitation is confined into the aerosol droplets and occurs very rapidly, the solid formed particles can exhibit particular crystallites size and shape, very different from what can be obtained by classical precipitation processes triggered by (slow) evaporation or pH change. The possibility of mixing different salts is an interesting feature of such process. Also, the gas transported particles can advantageously be deposited onto suitable structured supports.

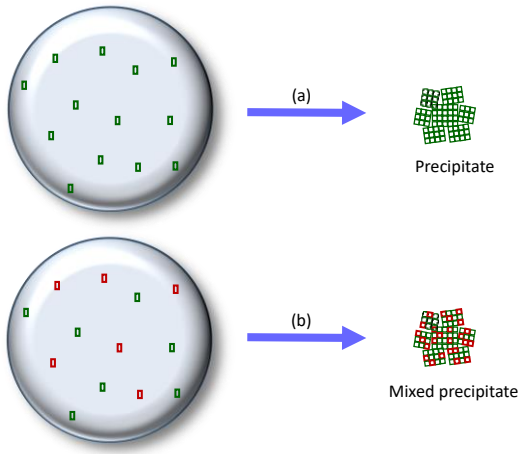

Scheme 5. Aerosol-mediated precipitation from salts (Type II process). In route (a) one type of salt (depicted as small green rectangles) is spray dried to yield a precipitate. In route (b) a mixture of two or more different salts is spray dried to yield a new crystalline compound.

3.3.1. $NaAlO_2$ microspheres for the synthesis of glycerol carbonate

One of the economically attractive way to upgrade glycerol is to convert it into glycerol carbonate.[379-381] By using dialkylcarbonates (preferentially dimethyl carbonate, DMC) and a basic heterogeneous catalyst, a truly green process can be designed.[382-385] For example, good yields of glycerol carbonate were obtained with CaO, MgO, and various hydrotalcite catalysts.[386-392]

A less common basic heterogeneous catalyst is $NaAlO_2$, which is highly soluble in water but can be used in its solid form in most organic solvents.[385, 393, 394] In a recent communication, $NaAlO_2$ was shown to exhibit high activity in the transesterification of DMC with glycerol to provide glycerol carbonate in high yield, even at room temperature.[117] Interestingly, solid $NaAlO_2$ was even more active when prepared from the solution state by drying through atomisation, as compared to the commercial solid or the solid obtained by simple vacuum drying. In the aerosol-assisted precipitation technique, an aqueous or hydro-alcoholic solution of $NaAlO_2$ was simply spray-dried in a tubular furnace maintained at 700°C. The dried solid was composed of spherical particles of sodium aluminate (Figure 26). Interestingly, the $NaAlO_2$ crystallites constituting these spherical aggregates were relatively small, accounting for a higher number of strong basic sites, as compared to the commercial or to the vacuum dried catalysts. In turn, this exalted basicity resulted in significantly enhanced catalytic activity, as measured in the most classical reaction conditions (excess DMC, 90°C). A significant finding is that this highly active catalyst can also catalyse the reaction in high yield at room temperature. Using only 3 wt.% catalyst (with respect to glycerol) and a DMC to glycerol ratio of 2, the equilibrium conversion of 75% was reached in only 30 min. A clear correlation was established between the size of the $NaAlO_2$ crystallites in the different catalysts tested, the basicity, and the catalytic activity in the synthesis of glycerol carbonate (Figure 26). In this respect, aerosol-made catalysts had a clear advantage over those made by simple drying. A similar aerosol-precipitation synthesis strategy was recently reported to prepare hollow Na_2ZrO_3 microspheres with high surface area, successfully exploited for CO_2 capture.[395]

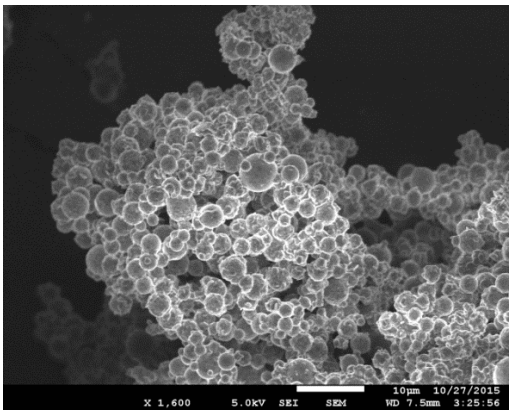

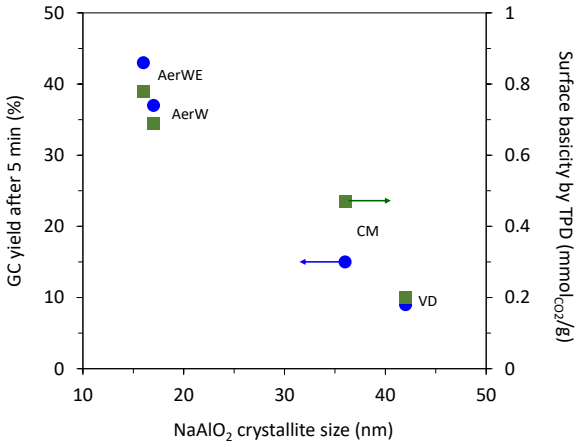

Figure 26. (top) SEM micrograph of the $NaAlO_2$ microspheres obtained by spray drying; (bottom) correlation between crystallite size, basicity and intrinsic activity in the room-temperature synthesis of glycerol carbonate from glycerol and dimethyl carbonate (3 wt.% of catalyst, 1:2 mol ratio of glycerol:DMC at 30 °C). AerW = $NaAlO_2$ prepared by spray drying starting from an aqueous solution, AerWE = $NaAlO_2$ prepared by spray

 This journal is © The Royal Society of Chemistry 20xx

Please do not adjust margins

Please do not adjust margins

drying starting from a hydro-aloholic solution, CM = commercial $NaAlO_2$ powder, VD = $NaAlO_2$ prepared by vacuum drying starting from an aqueous solution. Reproduced with authorisation from Ramesh and Debecker.[117]

3.3.2. Complex Oxide Catalysts for the selective oxidation of light hydrocarbons

Complex multicationic oxides are intensely investigated as catalysts for alkane activation.[396] [397-400] In particular, the catalytic properties of MoVTeNb oxide catalysts have captured the interest of researchers for the selective oxidation of propane to acrylic acid.[401-404] The performance of such selective oxidation catalysts are dictated by the crystallinity and by the specific surface area of the solid. The crystalline structure is particularly crucial because these catalyst work via a Mars and van Krevelen mechanism where oxygen atoms diffuse from the bulk of the crystal towards the surface to oxidise the organic substrate (and the vacancies are replaced by oxygen atoms coming from molecular O_2 which diffuse in the opposite direction).[405] Only some specific crystalline structures are efficient in these processes, like the well-known "M1" phase. To obtain such active phase, a specific calcination procedure is usually employed but the latter also favour the formation of particles with low specific surface area.

Kolen'Ko *et al.* compared three different solution-based methods with multistep approaches.[118] In particular, they report two preparation methods based on aerosol processing. In the first one, the precursor solid is obtained by spray drying an aqueous solution containing $(NH_4)_6Mo_7O_{24}.4H_2O$, NH_4VO_3, $Te(OH)_6$ and $NH_4[NbO(C_2O_4)_2].xH_2O$ with a nominal molar composition Mo/V/Te/Nb of 1:0.3:0.23:0.125. The solid was mainly formed by the concomitant precipitation of the three salts even if partial transformation to the mixed oxide probably occurs already at this early stage. The precursor solid was calcined in air (275°C) and then annealed in Ar (600°C) to yield a mixture of the crystalline M1 and M2 MoVTeNb oxide phases. The M1 phase was then isolated using a dedicated washing route.[406] The spherical particles obtained initially have short-range structural ordering with a week XRD signal for the M1 phase. Upon thermal treatment and washing, the particles morphology and crystallinity are strongly affected. The M2 phase is effectively eliminated by the washing and small rod-like crystals of the M1 phase are obtained. The final product exhibits a specific surface area of 9 $m^2.g^{-1}$.

The second aerosol method is based on the spray drying of a homogeneous complex solution, followed by a superheated water vapour treatment. MoO_3 was dissolved in water along with $C_2H_2O_4.2H_2O$ and then $Te(OH)_6$. A V-containing solution was prepared by dissolution of V_2O_5 in an aqueous $C_2H_2O_4.2H_2O$ solution. Both solutions were mixed together and $NH_4[NbO(C_2O_4)_2].xH_2O$ was added to yield an oxalic complex solution with a nominal ratio 1:0.225:0.15:0.1535. The solid product collected after spray drying was immediately calcined at 275°C in air, treated in superheated water vapour (500°C, 20 MPa) and then annealed at 600°C in Ar (Figure 27-A). In this case, the catalyst precursor (before thermal treatments) is essentially amorphous. The superheated water vapour treatment yields a single-phase M1 catalyst, with relatively low crystallinity. After annealing in Ar, the catalysts consist of cylindrical structures on a sub-micrometer scale and faceted, elongated nanoparticles, exhibiting moderate aggregation (Figure 27-B). This method yields relatively small M1 nanocrystals, as compared to those produced by a classical hydrothermal method. Specific surface area reaches 13 $m^2.g^{-1}$.

Both catalysts prepared by an aerosol-assisted method were more active than reference catalysts prepared by hydrothermal method. This can be rationalised by the lower specific surface area of the latter (6 $m^2.g^{-1}$), even if the density of active sites also seems to be different in the different catalysts.

Bismuth molybdates exhibit good catalytic activity for the selective oxidation of light hydrocarbons, yielding for example acrolein, metacrolein, butadiene, etc.[126, 407-411] "BiMo" catalysts can be found in α, β, or γ phases, with the formula $Bi_2O_3.nMoO_3$, where n = 3, 2, or 1 respectively. Activity and selectivity of these phases are different for each reaction and it is therefore interesting to master the synthesis of pure phases of bismuth molybdates or at least their mixtures in controlled ratios.[412]

Please do not adjust margins

Chemical Society Reviews

REVIEW

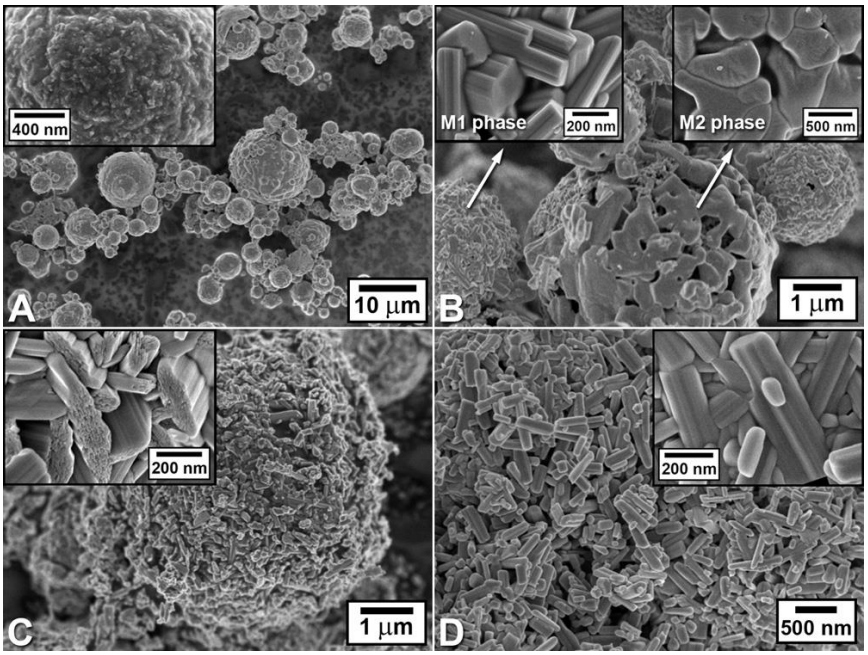

Figure 27. SEM micrographs of the MoVTeNb oxide catalyst obtained by the spray drying of a salt solution. (A) spray-dried and calcined, (B) after annealing in Ar, (C) washed in H_2O_2 and (D) heat activated in Ar. Reproduced with authorisation from Kolen'Ko *et al.*[118]

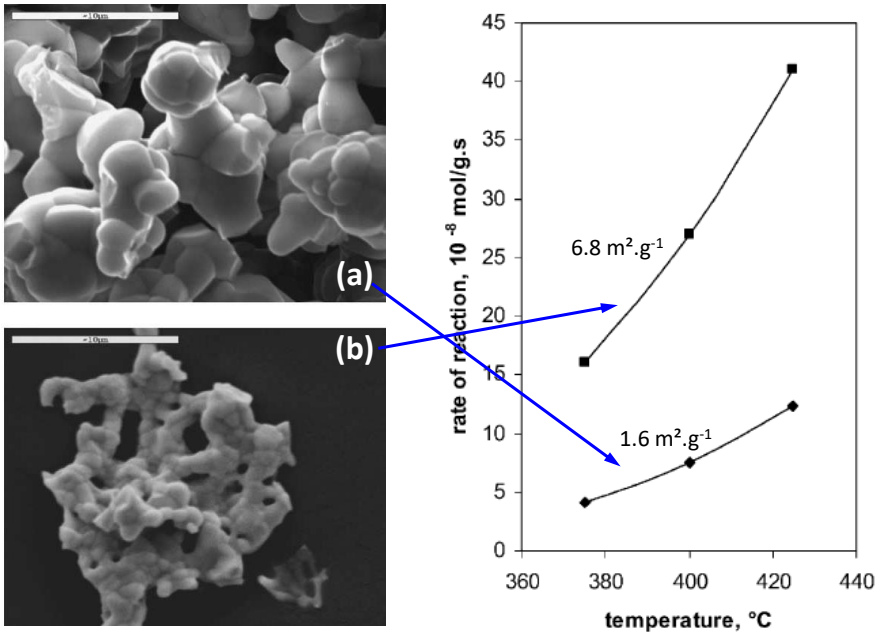

Figure 28. SEM micrograph and rate of acrolein formation with α-$Bi_2Mo_3O_{12}$ phase obtained by spray drying (a) without or (b) with citric acid (citric acid/Bi molar ratio = 3). (scale bar = 40 µm) Adapted from Le *et al.*[374]

Chemical Society Reviews

REVIEW

Van Driessche *et al.* have used a spray drying technique to synthesise a range of multi-metal oxides with interesting properties.[413] Based on this method, BiMo catalysts have been obtained by the rapid drying of an aerosol generated from an acidic aqueous solution of $(NH_4)_6MoO_{24}.4H_2O$ and $Bi(NO_3)_3.5H_2O$.[373] The collected powders were amorphous, indicating that intermediate crystallisation or phase segregation did not occur during drying. Depending on the Bi/Mo atomic ratios introduced in the synthesis and on the calcination temperature, pure α, β, and γ phases could be obtained. In terms of specific activity for the oxidation of propylene to acrolein, the spray dried samples compared well with catalysts prepared by classical precipitation method. This was not surprising because the specific surface area of the obtained materials remained very low (< 2 $m^2.g^{-1}$). The aerosol method was subsequently improved by the same authors,[374] by combining it with a complexation method based on the use of citric acid.[414] The latter method is known to favour a gelation with better intermixed oxides through a three-dimensional organic network of metallic components, and to yield materials with enhanced surface area due to the organic additive burning off.[415] Again, pure α, β, and γ bismuth molybdate phases could be obtained when the spray drying method was applied in the presence of citric acid. Expectedly, the materials had a more divided structure, higher surface area and this resulted in an increase in catalytic activity while selectivity for acrolein was preserved (**Figure 28**). Dimethyl oxalate, malic acid, and malonic acid were tested as well as organic additives and showed to have a similar effect.

3.3.3. Structured catalytic filters for soot oxidation

Soot particles coming from diesel engines are classically abated by catalytic filters based on SiC monoliths promoted with active elements.[416-421] Ceramic papers have recently emerged as a suitable alternative to monoliths, allowing accommodating flexible structured catalysts for diesel filters.[422-427] Catalytic components are incorporated into the filter to permit the passive regeneration of the filter.[428] This can be done by drip impregnation of metal salts, followed by calcination.

Trying to achieve a better distribution of the catalytic components throughout the filter, Tuler *et al.* have proposed the direct spray deposition of Ce and Co onto Ce-promoted aluminosilicate ceramic papers.[375] An aerosol generated from an aqueous solution of $Ce(NO_3)_3$ and $Co(NO_3)_2$ was treated in a tubular oven in which the formed droplets were dried rapidly. The air-borne particles were directly sprayed onto a ceramic paper disc inserted in the collecting filter. By comparison with wet preparation techniques, it was shown that the dispersion of the active elements was highly improved (Figure 29). Drip impregnation shows agglomerates of catalytic particles larger than 5 μm resulting from the active elements accumulation at the fibres crossings due to capillary forces exerted during the drying. On the contrary, when using the spray deposition method smaller agglomerates are formed (< 1 μm), distributed throughout the filter. This resulted in a significant improvement of the soot oxidation activity, with a light-off curve shifted by about 30°C. One remaining challenge in the case of such structured catalyst is the stability of the interaction between the sprayed particles and the support.

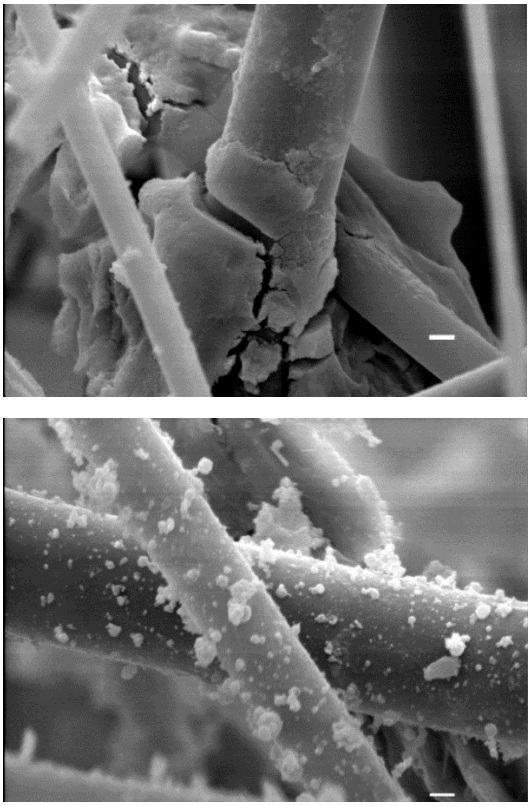

Figure 29. SEM micrograph of ceramic filter fibres after Ce and Co deposition by (top) drip impregnation and (bottom) aerosol spray deposition. The filter catalysts are calcined at 600°C. Scale bars represent 1 μm. Adapted with authorisation from Tuler *et al.*[375]

3.4. Drying of preformed particles

3.4.1. Drying preformed catalyst particles to form aggregates (shaping)

Type I aerosol processes can be advantageously exploited to aggregate pre-formed fine catalysts powders. Considering the fact that such processes do not belong to catalysts synthesis methods – but rather shaping – they are not covered

Please do not adjust margins

systematically and exhaustively in the present review. Only a handful of representative examples are provided below. Nevertheless, particle aggregation is crucial for many catalytic processes, where the size of the catalyst particles dictates the practicality of the process. For examples, catalyst recovery through filtration, sedimentation or centrifugation will be made easier with larger particles. Also, aggregated particles allow for the design of flow processes where the reactants mixture has to pass through a fixed bed of particles, without excessive pressure drop. Finally, aerosol processes usually yield spherical particles – potentially featuring good attrition resistance – making them particularly well-suited for applications in fluidised bed reactors.

Kim *et al*. showed how spray drying reprocessing enables to achieve spherical particles with increased attrition resistance.[429] Fine powdery SAPO-34 catalysts have been prepared by a hydrothermal method before being introduced into a slurry solution containing binders. The slurry was spray-dried to yield SAPO-34 microspheres of 60-65 microns. The latter showed good yields in the methanol-to-olefins (MTO) process. More importantly, they had highly improved attrition resistance, as they were able to withstand the rapid flow velocity in circulating fluidised bed reactors.

Liu and Zhou have reported on the preparation of Cu-incorporated TiO_2 granules used in the photocatalytic degradation of an azo dye.[430] A slurry was prepared from commercial TiO_2 and CuO powders and simply spray-dried to yield spheres of 40-80 µm.

Attrition-resistant Ni-Mg/Al_2O_3 catalysts have been synthesised by Cui *et al*. via spray-granulation.[431] Such catalyst formulation is important nowadays because nickel – combining relatively low price and good activity – is the most classical CO_2 methanation active phase.[432-434] The purpose of this work was to determine the influence of the combination of the spray drying process with two types and amounts of binders (silica sol or alumina sol) on their mechanical strength. The catalysts were tested a fluidised bed methanation reactor. Characterisations revealed that their attrition resistance was in correlation with their microstructures: the higher the pore volumes, the lower the attrition resistance.

3.4.2. Preparation form preformed colloids (followed by thermal treatments)

One interesting example of Type I process for heterogeneous catalyst preparation is that of hydrotalcite (or layered double hydroxides, LDH) microspheres. LDH feature a unique bi-dimensional layered structure, able to adsorb, intercalate and immobilise species of interest.[435, 436] LDH have attracted increasing attention in the last decades, with the emergence of a range of applications in the fields of adsorption, catalysis, drug carriers, energy production, storage and conversion.[437-441] In particular, the basic properties and the interesting textures of LDH make these materials highly interesting in heterogeneous catalysis.[442-446] In a recent review, Prevot and Tokudome covered the synthesis and applications of 3D hierarchical and porous LDH structures.[447] Spray drying was highlighted as an efficient means to obtain such structures, starting from LDH colloidal suspensions, which can be obtained either by the polyol method[448] or by designing the LDH preparation as to separate the nucleation and aging steps.[449] Upon solvent evaporation, spherical microparticles are readily formed in which the layered structure of the LDH is preserved.[450] Such LDH particles feature accessible diffusion pathways in the macropore domain; they have been obtained with a wide range of compositions.[451]

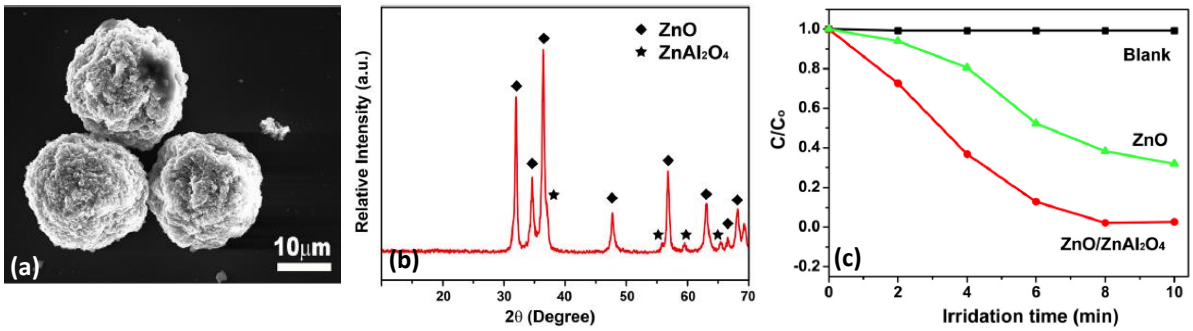

Figure 30. (a) SEM micrograph and (b) XRD patterns of the ZnO/$ZnAl_2O_4$ photocatalyst obtained by the spray drying method (Type I) followed by calcination. (c) photocatalytic performance in the degradation of MB (1.2×10^{-6} M) at 25°C under mercury lamp, compared to a blank experiment (no catalyst) and to a commercial ZnO powder. Upon calcination, topotactic transformations occur, the layered double structure collapses and ZnO and $ZnAl_2O_4$ phases are formed. Yet, the hierarchically spherical morphology of the particles is preserved and the final texture remains advantageous (specific surface area of 90 $m^2.g^{-1}$ and pore volume of 1.0 $cm^3.g^{-1}$). Adapted with authorisation from Huo *et al.*[376]

This method has been exploited by Huo *et al.* for the preparation of a hierarchical ZnO/$ZnAl_2O_4$ photocatalyst.[376] Nano-sized ZnAl-LDH powder was prepared by mixing a salt solution containing $Zn(NO_3)_2.6H_2O$and $Al(NO_3)_3.9H_2O$ (with a Zn^{2+}/Al^{3+} ratio of 2) with a base solution containing NaOH and Na_2CO_3. After ageing, the slurry was washed and filtered. The filter cake was re-dispersed in water to form the precursor slurry (3 wt.% of ZnAl-LDH nano-platelets). At this stage, ZnAl-LDH nano-platelets are obtained with a mean size of 140 nm. The slurry was atomised, dried in hot air (150°C) and the obtained powder was collected in a cyclone. Spherical particles with dimensions in the 1-20 µm range were obtained, with a specific surface area of 100 $m^2.g^{-1}$ and a pore volume of 0.65 $cm^3.g^{-1}$ (Figure 30). Finally, the ZnO/$ZnAl_2O_4$ composite

 This journal is © The Royal Society of Chemistry 20xx

Please do not adjust margins

Please do not adjust margins

photocatalyst was obtained by calcination in air at 800°C. Upon such thermal treatment, topotactic transformations occur, the layered double structure collapses and ZnO and $ZnAl_2O_4$ phases are formed. Yet, the hierarchically spherical morphology of the particles was preserved and the final texture remained advantageous (specific surface area of 90 $m^2.g^{-1}$ and pore volume of 1.0 $cm^3.g^{-1}$). Photocatalytic activity of the composites was assessed in the degradation of methylene blue (MB) and of methyl orange (MO). The $ZnO/ZnAl_2O_4$ photocatalyst proved to be much more active than the commercial ZnO powder (**Figure 30**).

Another example of Type I process based on the use of colloidal suspensions is that of acidic alumino-silicates. In the petrochemical industry, nano-sized ZSM-5 catalysts have shown outstanding performances for naphtha cracking, methanol to gasoline (MTG), ethanol to gasoline (ETG), and acetone to olefin (ATO) in comparison to microporous ZSM-5, by reducing both diffusive constraints and the deactivating effect of coke.[379, 452-454] However, the synthesis process – based on the silanisation of protozeolitic seeds[455-459] – usually requires large quantity of solvents and achieves only low product yield.

Xiong *et al.* have proposed a two-step aerosol-assisted synthesis of nano-sized ZSM-5 zeolite from an aqueous solution of silicon and aluminum precursors.[377] In this case, the aerosol process is only used for the first step of the material synthesis and is not sufficient to obtain the final active catalyst. First, an aqueous precursor solution containing a silica source (colloidal silica, Ludox®) and $NaAlO_2$ is sprayed and dried by passing through an oven set at 230°C to form an amorphous SiO_2-Al_2O_3-Na_2O powder. No organic template was used. The obtained powder was further dried at 120°C overnight to eliminate residual water. Then, the material was crystallised in an autoclave after addition of an aqueous TPAOH solution, used as a structure directing agent to form MFI aggregates. The obtained catalyst was composed of MFI nanocrystals (50-100 nm) and had improved textural properties as compared to those of a ZSM-5 zeolite synthesised by a conventional hydrothermal method.

Their catalytic performances have been compared in the cracking of 1,2,5-triisopropylbenzene, which requires strong acid sites.[182] The higher stability and activity (Figure 32) achieved by the nano-sized ZSM-5 (noted AZ-5) in the catalytic cracking of 1,3,5-TIPB are related to the improved interconnectivity of the mesopores and to the higher amount of acidic centres exposed, due to the larger external surface area (73 $m^2.g^{-1}$) as compared to the reference catalyst (noted HZ-5). This aerosol-assisted synthesis of nano-sized ZSM-5 aggregates appears to be more effective than the conventional hydrothermal method to ensure a good distribution of the Al species in the network and to generate slightly stronger acidic sites.[377] According to the authors, the aerosol route favours the crystal nucleation thanks to the high supersaturation of the precursor solution achieved in this dense system.

A similar strategy was applied by the same authors[460] to prepare zeolitic titanosilicates, and in particular TS-1, which is known to find various important applications in heterogeneous catalysis, like olefin epoxidation.[461-465] It should be noted however that with such two-step procedures – i.e. (i) aerosol preparation of an amorphous material and (ii) further crystallisation of the zeolite in hydrothermal conditions in the presence of structure directing agent – the shape and size of the initial particles are lost. Instead of small and spherical particles, zeolite crystals are obtained after re-dissolution and crystallisation; their shape and size are governed by the parameters of the crystallisation step.

Nandiyanto *et al*. proposed an elegant method to prepare large macroporous anatase TiO_2 particles, successfully used as photocatalyst for the degradation of rhodamine-B.[466] A colloidal suspension of small anatase particles (~5 nm) was mixed to a suspension of polystyrene beads (~200 nm), sprayed using an ultrasonic nebuliser, and thermally treated in a tubular furnace. The aerosol processing involved two heated zones set respectively at 200°C and 500°C. Solvent evaporation in the first zone resulted in the formation of large particles of titania/polystyrene composite. Interestingly, despite a short residence time of ~3 seconds, the treatment at 500°C allowed to remove the polymer beads and directly reveal the macroporosity. At the same time, this thermal treatment did not trigger any significant sintering of the TiO_2 nanoparticles, ensuring that the intrinsic photocatalytic activity was preserved. Thus, a hierarchical photocatalyst was obtained in one step, exhibiting much higher photocatalytic activity than the reference catalyst prepared in the absence of polystyrene template, and almost as active as the free nanoparticles. Additionally, the particle outer diameter could be tuned in the 0.2-1 µm range simply by adjusting the concentration of the starting suspension.

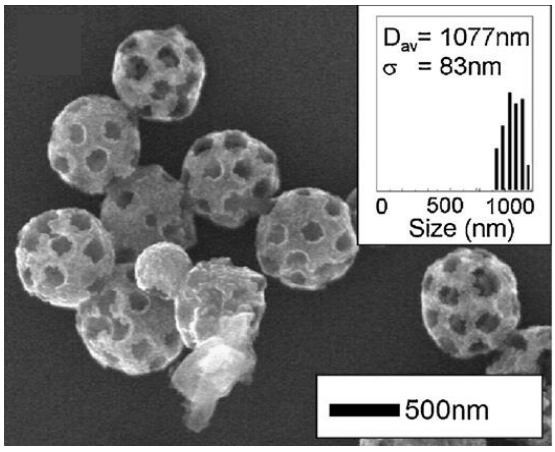

Figure 31. Macroporous photocatalyst made of small anatase TiO_2 particles sprayed together with polystyrene beads which served as a template for the macropores. Reproduced with authorisation from Nandiyanto et al.[466]

3.4.3. Impregnation via aerosol processing

Drying preformed particles via an aerosol process can also give a convenient opportunity to supplement the materials with additional components. For examples, additives may be included in the process to modify the surface properties of the catalyst (binders for adhesion, mineral acids or bases for the formation of corresponding surface sites, etc.). Interestingly, a catalytically active phase can be added on the surface of

Please do not adjust margins

Please do not adjust margins

preformed support particles to yield a supported catalyst. The method can be seen as an alternative to classical impregnation techniques.

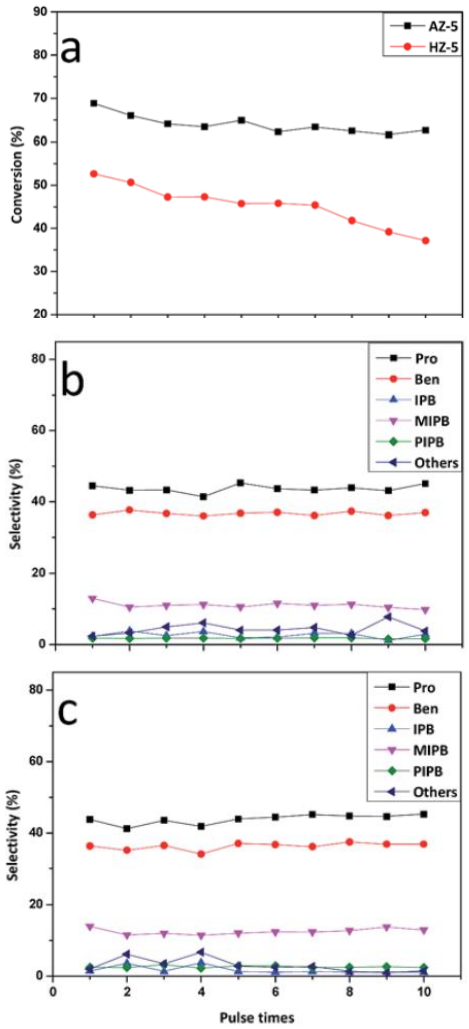

Figure 32. Cracking of 1,3,5-triisopropylbenzene with a reference ZSM-5 catalyst obtained by conventional hydrothermal method (HZ-5) and with a nano-sized ZSM-5 catalyst prepared by a two-steps aerosol process (AZ-5): (a) conversion, (b) selectivity of AZ-5, (c) selectivity of HZ-5 for the different products (propylene (Pro), m-diisopropylbenzene (MIPB), isopropylbenzene (IPB), benzene (Ben), p-diisopropylbenzene (PIPB)). Adapted from Xiong *et al.*[377] with authorisation.

Santiago *et al.*[378] highlighted the benefits of aerosol processing in the preparation of Pd/ferrierite catalysts. Starting from preformed a ferrierite powder, they compared four methods for the deposition of Pd: wet impregnations, dry impregnations, freeze-drying and aerosol spray deposition. For the latter, a ferrierite powder was dispersed in a palladium nitrates solution and sprayed using a spray dryer device from Büchi. During drying, supersaturation of Pd was reached in the droplets and crystallisation of Pd was triggered at the surface of the zeolitic particles, resulting in ferrierite-supported Pd nanoparticles. According to the TEM observations (Figure 33), wet and dry impregnation methods did not allow to control the distribution and homogeneity of the Pd nanoparticles unlike the freeze and spray drying methods. Also, the freeze-drying generated larger nanoparticles compared to the spray-deposition method. By modifying the flow rate, the droplets size could be modified and the nanoparticles distribution and their potential re-agglomeration during the crystallisation could be studied. Reduced Pd-ferrierite catalysts prepared by aerosol were highly active in the gas-phase partial hydrogenation of propyne at 75°C, with high alkene selectivity. In HRTEM, the used catalyst was not significantly altered, indicating good sintering resistance.

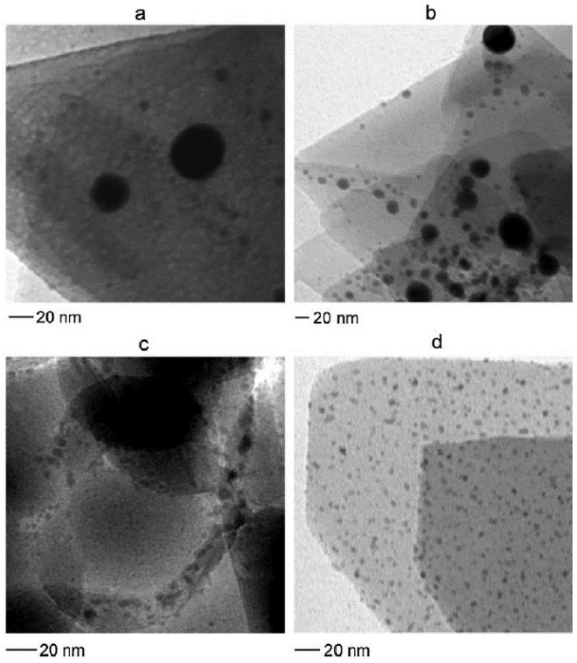

Figure 33. TEM micrographs of the Pd/ferrierite samples obtained by (a) wet impregnation, (b) dry impregnation, (c) freeze drying, and (d) aerosol spray deposition. The samples were calcined in static air at 573 K for 2 h. Reproduced with authorisation from Santiago *et al.*[378]

4. Transfer to industrial applications

The aerosol production of solid particles can be envisaged at various scales. A small lab-scale atomizer (e.g. from TSI Incorporated[467]) can produce a few gram of dry materials per hour. A popular lab-scale device is the Mini Spray Dryer B-290 from Büchi[468] which can deliver typically 10 to 50 g of dry solid in an hour. In the examples described above from the scholarly literature, the production rates are rarely provided by the authors. At the pilot scale, production rate typically range between 1 kg and 100 kg per hour (e.g. with a GEA spray drier equipped with a high speed turbine[469]). Large scale industrial spray dryers, like for example those commercialised by Dorst[470] typically deliver several hundreds of kg per hour. Thus, small scale research on the preparation of heterogeneous catalysts via aerosol process can be expected to transfer to the industrial scale, at least in terms of production capacity. The remaining challenge is to master the details of particle formation and final chemical and physical properties of the solid particles formed at the different production scales.

This journal is © The Royal Society of Chemistry 20xx

Please do not adjust margins

Please do not adjust margins

From an industrial point of view, spray drying has been a catalyst processing technique used for nearly a century. A research on an international patent database with the keywords "spray drying catalyst" resulted in more than 1400 hits, illustrating that spray drying is indeed a major processing technique for producing catalysts at the industrial scale. The first report in patent bibliography can be found as early as 1923 (published in 1924) and was described by Francis X. Govers.[100] From a chemical point of view, this process was used to produce SiO_2 particles (or other mixed metal oxide/SiO_2 particles) from colloidal silicic acid suspensions (or from other mixed metal oxide/colloidal silicic acid suspensions). The suspensions were atomised before any gelation could occur so that the gelation is actually triggered during the drying. In the classification that we propose for aerosol processes, this corresponds to materials prepared according to the Type I or Type IIIc processes, depending on whether the particles are pre-formed before atomisation or being formed during the processing. Targeted applications were adsorptive agents, catalysts or catalyst supports.

The next remarkable patent was deposited by Gen Zeolite Company in 1930 for the preparation of silica or mixed SiO_2/MO_x materials, produced by mixing a silicic acid suspension (resulting from the reaction between sodium silicate and an inorganic acid) with salts of transition metals like iron, aluminium, etc.[101] The gelation was then induced by adding a base to the mixture. Atomisation is mentioned as a potential drying method provided that the gel formed is sufficiently fluid (i.e. Type I process following our classification).

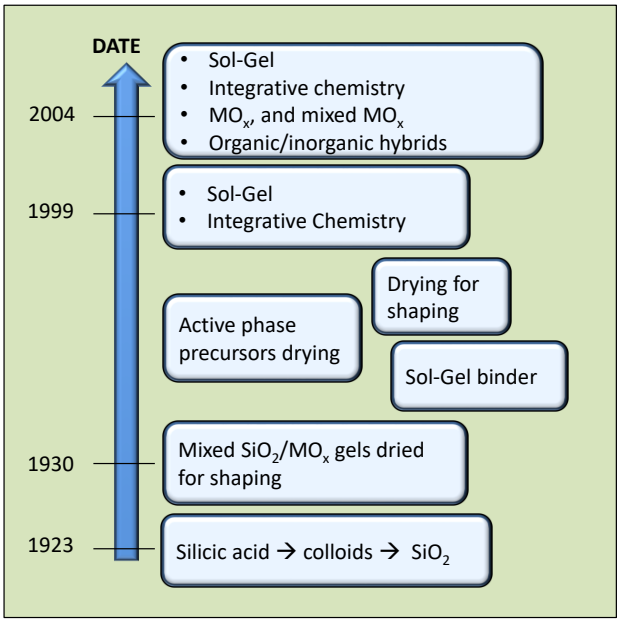

Figure 34. Chronology of patents of catalysts made by aerosol processes since 1923

Since then, and until the 1990's, between 5 and 10 patents can be found on average every year. Most patents were filed to protect methods for aggregation, drying of gels, drying of slurries made of particles (catalyst supports), bonding catalysts support particles with sol-gel binders and/or loading suspended particles with active phase precursors (Figure 34). In almost all cases, as-made materials are calcined for decomposing active phase precursors.

From this body of literature, the sol-gel chemist can be somehow frustrated. Indeed, apart from silica chemistry that was well understood before the 1960's, it is difficult to determine the part of sol-gel chemistry (involving the polycondensation of molecular precursors) from the mere drying of catalysts precursors followed by a calcination (i.e. oxidation or reduction in a furnace) that leads to the final catalyst. Apart from this, the patent literature clearly shows that many variations of catalyst supports / active phases were addressed, either for petrochemical industry, or fine chemistry, or environmental chemistry. Yet, no conceptual breakthrough was reported until the end of the 1990's.

In 1999, a revolution was patented by Bruinsma and co-workers who introduced integrative chemistry concepts for the design of silica-based catalysts made by aerosol.[471] They used supramolecular assembly of surfactant as a template for creating very high surface area catalysts supports, thereby inventing the first mesostructured materials made by aerosol using the evaporation-induced self-assembly (only six years after the first communication of Kuroda *et al.* on mesoporous molecular sieves[472]). Since then, this pioneering approach was further developed and led to numerous advanced formulations with superior catalytic activities, such as those we proposed from 2004 for various applications,[473-479] from hydrotreatment to olefin metathesis (some of them being described in this manuscript).

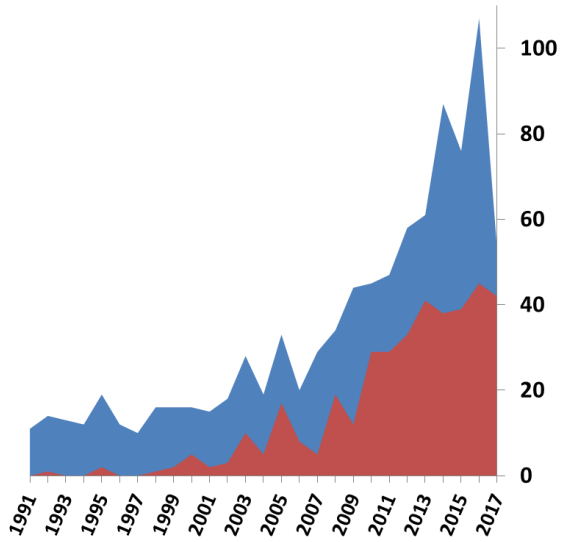

Figure 35. Evolution of patent number from 1991 to 2017 (blue: total number; red: from China researchers and industry)

Looking at the evolution of the number of patent since 1990 (Figure 35), an intense boost in the patenting activity is observed in the beginning of this century. A closer look shows that the subjects of these patents are similar to those of the 20th century with no major additional concept. Indeed, the reason of

Please do not adjust margins

Please do not adjust margins

this recent boost in patent activity has to be put in parallel with the current dynamism of Chinese research and industry sector. In 2017, Chinese patents represent more than 50% of the world patenting publications.

5. Prospects & conclusions

The catalysis scientists are currently facing important challenges mainly related to the pressing need we have to envisage a more sustainable chemical industry – in the broader context of a more sustainable society. Challenges in chemistry are often solved by catalysis, and it seems reasonable to state that our ability to build new types of catalytic materials with new properties will help us build what Taarning *et al.*[222] call the "renewable chemical industry". New solid catalysts will be used to convert lignocellulose or its fractionation products into a range of useful chemicals and materials,[480, 481] to synthesise bioplastics,[226, 482] to perform organic synthesis in cascade reactions,[483, 484] to combine the action of inorganic functions with organometallics or enzymes,[485] etc. To proceed, one will need to design inorganic and hybrid solid materials with a new level of control on composition, homogeneity, special dispersion and distribution the active elements, speciation, surface functionalities, hydrothermal stability, hydrophobic/hydrophilic balance, texture, structure, etc.

This review demonstrates through a large range of practical examples that aerosol processes have decisive technical features which make them highly attractive to address such an ambitious agenda. Aerosol preparation techniques should be looked at with an opportunistic eye, in the perspective of new technology breakthroughs in chemical science. The most important of those features can be summed up by looking at the key properties which dictate the performance of heterogeneous catalysts. We also look into the unresolved issues of aerosol preparation techniques and we identify the most promising areas of development for innovative catalytic materials.

5.1. Technical upsides of aerosol processing

Aerosol processes offer a good control on the composition and homogeneity of the produced materials, as long as the properties of the starting solution or suspension are controlled and kept constant over the timespan of atomisation. As demonstrated in this review, the use of sacrificial templating agents offers a very broad spectrum of textures with tuneable and uniform pore size and shape. This is obviously a key parameter for heterogeneous catalysts.

The tuneable contact time in the reactive zone offers a range of possibilities. If it is short, the process can yield metastable states involving species with very different reactivity. This cannot be achieved via conventional precipitation or gelation based routes. A long processing time can also offer some flexibility and allow the formation of more complex structures, including clays, hybrid and hierarchical structures (vide infra).

In principle, aerosol preparation techniques are continuous and scalable. Each droplet should be seen as an individual micro-reactor where chemical and physical transformations occur during drying. In this sense, simply feeding the atomiser for longer timespans allows accumulating larger quantities of the same desired materials. If larger production equipment is needed to increase productivity, the scalability will mainly be governed by the ability of the engineer to maintain similar atomisation and drying parameters at different production scale (vide infra).

5.2. Technical issues and related opportunities

The particle size distribution is largely dictated by the spraying nozzle. Intrinsically, small-scale atomisers generate droplets in a relatively broad range of sizes which results in particle size polydispersity. When it comes to heterogeneous catalysis applications, this can be an issue. Post-synthesis separation is usually used to select the particles with the appropriate size (centrifugation, cycloning, etc.). Large-scale atomisers are less sensitive to this issue. Also, it should be noted that many technical options are available regarding the type and geometry of atomisation devices (ultrasonic nozzles, pressure nozzles, two-fluid nozzles, rotary atomisers, piezoelectric nebulisers, etc.).[142, 486, 487] This can offer the engineer a way to control size polydispersity to a certain extent.

The actual size of the spherical particles can also be crucial for application in heterogeneous catalysis. While some processes can use directly small particles size (e.g. around 50 micrometers for fluid catalytic cracking), many other applications and reactor geometries (including fixed bed or moving reactors) require larger particles. Thus, the possibility to obtain relatively large solid particles would allow to proceed directly to the application, without further shaping (pelletizing, extrusion, etc.). Obviously, the atomisation mode has a direct impact on the aerosol droplet size and therefore on the size of the final solid particles. However, the size also depends on the composition of the starting sol. On the one hand, it is easy to obtain relatively large aggregates of preformed smaller particles, simply by playing on the concentration of the slurry that is atomised. On the other hand, when the solid has to be formed during the aerosol processing, starting from a precursor solution, the size of the elementary particles tends to remain small. It is actually limited by the concentration of the precursor solution, which is itself limited by stability and/or homogeneity issues. Two-step procedures may be applied in which small elementary particles are synthesised first, exploiting for example the aerosol-assisted sol-gel process, and then re-suspended and aggregated together in a second "shaping" step via spray drying.

Energy consumption may be pointed as a potential shortcoming of aerosol processes, because large amounts of solvents have to be vaporized and possibly re-condensed. Yet, many aerosol processes also allow to shorten and simplify significantly the catalyst preparation, and to obtain improved catalyst formulations. Therefore, the comparison between competing preparation procedures should be done carefully, taking into account all the economic and environmental aspects.

 This journal is © The Royal Society of Chemistry 20xx

Please do not adjust margins

Please do not adjust margins

When sacrificial templating agents are being used, their cost should be taken into account. Most heterogeneous catalysts with tailor-made textural properties – as described in this review – have been obtained using block copolymer templates, the price of which can be prohibitive for large scale industrial production. These solids might make it to commercial application only if they offer a significant performance breakthrough in the application in which they are subsequently exploited.

Managing the kinetics of surfactant micelle formation and inorganic polycondensation is a challenge. In order to fully benefit from the templating effect of the surfactant, its evaporation-induced self-assembly must occur before the inorganic network is completely formed. Obviously, complex formulations involving several inorganic precursors and/or several templating agents will be trickier to control. On the one hand, it must be recalled that the precursors which undergo fast polycondensation reactions are expected to trap the other precursors, resulting in rather homogeneous formulations. The formation, under kinetic control, of multi-components catalytic materials with high surface areas allows to quench original metastable phases trapped inside new architectures broadening the scope of possibilities for the design and production of new catalysts. On the other hand, it may be envisaged to slow down the drying process, to generate tuneable gradients in composition or in porosity. In fact, the resulting hierarchical or core-shell materials would have tremendous potential for application as heterogeneous catalysts.

5.3. Future trends

We believe the future of aerosol processes for the preparation of heterogeneous catalysts will deal with (i) hybrid catalytic materials and (ii) coupling with smart engineering strategies.

Short processing times coupled with moderate heating temperatures and volatile solvents should allow to process fragile components such as organic moieties and even enzymes. Thus, it is expected that a wide range of catalytic materials will be developed in the near future, including oxides bearing organic functions at their surface, metal organic frameworks (MOFs), covalent organic frameworks (COFs), periodic mesoporous silicas (PMOs), entrapped enzymes, etc.

A first example of silica-based hybrid materials was obtained by the aerosol-assisted sol-gel method, using organosilanes to insert thiol surface functions.[488] The latter were converted to sulfonate groups by chemical modification, to generate materials with high surface acidity. Depending on the nature of the organosilane, materials could be obtained with varying degrees of mesostructuration and proton exchange capacity. These hybrids could be applied in various acid catalysed reactions. Along these lines, much is still to be discovered. The scope is very large if we simply envisage to combine the synthesis of porous silica with the range of available organosilane precursors. It is even broader when it comes to expanding the strategy to other oxides and mixed oxides.

As we have seen above, PMOs can be prepared by the AASG route and their use as heterogeneous catalysts was demonstrated for a range of organic reactions. There is no doubt that the technical and economic advantages of aerosol processing, coupled with the large variety of chemical functions that can be accommodated within such structure will give rise to important applications in heterogeneous catalysis.

The same holds for MOFs and COFs which have long attracted the interest of the catalysis science community.[489, 490] MOFs, in particular, have shown tantalizing potential for commercial applications as heterogeneous catalysts.[287, 491] The synthesis of MOFs is progressively being coupled with interesting processing techniques which allow either to enable large-scale production or to design specific materials architectures.[492] Very recently, several reports were published on the synthesis of MOFs via aerosol processes.[55, 178, 493-497] Successful application as heterogeneous catalyst was only demonstrated in the case of Pd@ZIF-8.[178] The other examples however undoubtedly validate the versatility of the method to synthesise such complex hybrid materials and other examples of applications in heterogeneous catalysis should flourish in the coming years.

The coupling of aerosol synthesis with advanced processing techniques and smart engineering strategies will be an important driver for future innovations in the field of heterogeneous catalysis. Yet, this field is still in its infancy. Implementing multi-nozzle injection for example (e.g. the mist at the exit of a first atomisation module is combined with colloidal matter coming from a second nozzle) will probably initiate a new wave of innovation in the synthesis of catalytic materials with complex, hierarchical or core-shell structure. Also, aerosol processing can be used to design “spray coating” techniques[51] leading to transparent or coloured surfaces with functional coatings. The latter can have photocatalytic properties, to be exploited in environmental applications.

5.4. To conclude

Aerosol- or spray-processed materials have already strongly impacted many sectors such as nano-medicine, pharmacy, cosmetic, food, etc. In these fields aerosol-made materials are an industrial reality. Today, the scholarly literature related to the field of spray synthesis for the preparation of heterogeneous catalysts is relatively abundant and promising. Yet, it only represents the tip of the iceberg as compared to the tremendous application potential of aerosol techniques for the preparation of heterogeneous catalysts. In particular aerosol-based integrative strategies combined with hybridisation will allow to tailor make original catalysts and will open new areas using the so-called “chemistry of shape” concept. Such approaches rely on two pillars: miniaturisation and hybridisation. Miniaturisation aims at housing a large number of elementary functions in small volumes. Hybridisation – in particular between mineral and organic components – enriches the whole by association of functions selected from the best of both worlds. The confinement of solid materials synthesis in small aerosol droplets can offer a decisive advantage. Moreover

Please do not adjust margins

Please do not adjust margins

the processing of complex mixtures containing colloidal nano or microparticles, templating agents, molecular precursors, organometallic complexes, bioactive species, dopants, etc. allows envisaging the synthesis of heterogeneous catalysts in a sort of "Lego-like" approach starting from a myriad of potential nano-building blocks. The obtained catalysts will be hierarchical, multifunctional, and well-defined down to the actual structure of the active site. These will pave the way to new chemical processes and to a more sustainable chemical industry and society.

Conflicts of interest

There are no conflicts to declare.

Notes and references

1. S. Mann, S. L. Burkett, S. A. Davis, C. E. Fowler, N. H. Mendelson, S. D. Sims, D. Walsh and N. T. Whilton, *Chem. Mater.*, 1997, **9**, 2300.
2. G. J. d. A. A. Soler-Illia, C. Sanchez, B. Lebeau and J. Patarin, *Chem. Rev.*, 2002, **102**, 4093.
3. G. A. Ozin, *Chem. Commun.*, 2000, 419.
4. C. Sanchez, H. Arribart and M. M. Giraud Guille, *Nat. Mater.*, 2005, **4**, 277.
5. E. Prouzet, S. Ravaine, C. Sanchez and R. Backov, *New J. Chem.*, 2008, **32**, 1284.
6. P. Van Der Voort, D. Esquivel, E. De Canck, F. Goethals, I. Van Driessche and F. J. Romero-Salguero, *Chem. Soc. Rev.*, 2013, **42**, 3913.
7. B. Arkles, *MRS Bull.*, 2011, **26**, 402.
8. C. Sanchez and F. Ribot, *New J. Chem.*, 1994, **18**, 1007.
9. M.-H. Sun, S.-Z. Huang, L.-H. Chen, Y. Li, X.-Y. Yang, Z.-Y. Yuan and B.-L. Su, *Chem. Soc. Rev.*, 2016, **45**, 3479.
10. C. Sanchez, P. Belleville, M. Popall and L. Nicole, *Chem. Soc. Rev.*, 2011, **40**, 696.
11. O. D. Velev, T. A. Jede, R. F. Lobo and A. M. Lenhoff, *Nature*, 1997, **389**, 447.
12. B. T. Holland, C. F. Blanford and A. Stein, *Science*, 1998, **281**, 538.
13. P. Yang, T. Deng, D. Zhao, P. Feng, D. Pine, B. F. Chmelka, G. M. Whitesides and G. D. Stucky, *Science*, 1998, **282**, 2244.
14. S. A. Davis, S. L. Burkett, N. H. Mendelson and S. Mann, *Nature*, 1997, **385**, 420.
15. A. B. Sanghvi, K. P. H. Miller, A. M. Belcher and C. E. Schmidt, *Nat. Mater.*, 2005, **4**, 496.
16. K. T. Nam, R. Wartena, P. J. Yoo, F. W. Liau, Y. J. Lee, Y.-M. Chiang, P. T. Hammond and A. M. Belcher, *Proc. Natl. Acad. Sci.*, 2008, **105**, 17227.
17. C. Mao, D. J. Solis, B. D. Reiss, S. T. Kottmann, R. Y. Sweeney, A. Hayhurst, G. Georgiou, B. Iverson and A. M. Belcher, *Science*, 2004, **303**, 213.
18. U. H. F. Bunz, *Adv. Mater.*, 2006, **18**, 973.
19. Y. Sakatani, C. Boissière, D. Grosso, L. Nicole, G. J. A. A. Soler-Illia and C. Sanchez, *Chem. Mater.*, 2007, **20**, 1049.
20. K. J. C. van Bommel, A. Friggeri and S. Shinkai, *Angew. Chem. Int. Ed.*, 2003, **42**, 980.
21. M. Llusar and C. Sanchez, *Chem. Mater.*, 2008, **20**, 782.
22. K. Nakanishi and N. Tanaka, *Acc. Chem. Res.*, 2007, **40**, 863.
23. K. Kanamori and K. Nakanishi, *Chem. Soc. Rev.*, 2011, **40**, 754.
24. F. Schüth, *Chem. Mater.*, 2001, **13**, 3184.
25. R. Backov, *Soft Matter*, 2006, **2**, 452.
26. C. Sanchez, L. Rozes, F. Ribot, C. Laberty-Robert, D. Grosso, C. Sassoye, C. Boissiere and L. Nicole, *C. R. Chimie*, 2010, **13**, 3.
27. L. Nicole, L. Rozes and C. Sanchez, *Adv. Mater.*, 2010, **22**, 3208.
28. H. Fan, Y. Lu, A. Stump, S. T. Reed, T. Baer, R. Schunk, V. Perez-Luna, G. P. Lopez and C. J. Brinker, *Nature*, 2000, **405**, 56.
29. M. Mougenot, M. Lejeune, J. F. Baumard, C. Boissiere, F. Ribot, D. Grosso, C. Sanchez and R. Noguera, *J. Am. Ceram. Soc.*, 2006, **89**, 1876.
30. B. Fousseret, M. Mougenot, F. Rossignol, J.-F. Baumard, B. Soulestin, C. Boissière, F. Ribot, D. Jalabert, C. Carrion, C. Sanchez and M. Lejeune, *Chem. Mater.*, 2010, **22**, 3875.
31. O. De Los Cobos, B. Fousseret, M. Lejeune, F. Rossignol, M. Dutreilh-Colas, C. Carrion, C. Boissière, F. Ribot, C. Sanchez, X. Cattoën, M. Wong Chi Man and J.-O. Durand, *Chem. Mater.*, 2012, **24**, 4337.
32. P. Calvert, *Chem. Mater.*, 2001, **13**, 3299.
33. S. Madhugiri, W. Zhou, J. P. Ferraris and K. J. Balkus Jr, *Microporous Mesoporous Mater.*, 2003, **63**, 75.
34. S. Madhugiri, B. Sun, P. G. Smirniotis, J. P. Ferraris and K. J. Balkus Jr, *Microporous Mesoporous Mater.*, 2004, **69**, 77.
35. L. D. Santos, M. Maréchal, A. Guillermo, S. Lyonnard, S. Moldovan, O. Ersen, O. Sel, H. Perrot and C. Laberty-Robert, *Adv. Funct. Mater.*, 2016, **26**, 594.
36. D. P. Debecker, C. Boissiere, G. Laurent, S. Huet, P. Eliaers, C. Sanchez and R. Backov, *Chem. Commun.*, 2015, **51**, 14018.
37. N. Brun, S. Ungureanu, H. Deleuze and R. Backov, *Chem. Soc. Rev.*, 2011, **40**, 771.
38. F. Carn, A. Colin, M. F. Achard, H. Deleuze, Z. Saadi and R. Backov, *Adv. Mater.*, 2004, **16**, 140.
39. N. Brun, A. Babeau-Garcia, M.-F. Achard, C. Sanchez, F. Durand, G. Laurent, M. Birot, H. Deleuze and R. Backov, *Energ. Env. Sci.*, 2011, **4**, 2840.
40. L. van den Biggelaar, P. Soumillion and D. P. Debecker, *Catalysts*, 2017, **7**, 54.
41. P. Innocenzi, T. Kidchob, P. Falcaro and M. Takahashi, *Chem. Mater.*, 2007, **20**, 607.
42. R. Houbertz, L. Fröhlich, M. Popall, U. Streppel, P. Dannberg, A. Bräuer, J. Serbin and B. N. Chichkov, *Adv. Eng. Mater.*, 2003, **5**, 551.
43. C. J. Brinker, Y. Lu, A. Sellinger and H. Fan, *Adv. Mater.*, 1999, **11**, 579.
44. C. Sanchez, C. Boissière, D. Grosso, C. Laberty and L. Nicole, *Chem. Mater.*, 2008, **20**, 682.

 This journal is © The Royal Society of Chemistry 20xx

Please do not adjust margins

Please do not adjust margins

45. M. C. Fuertes, F. J. López-Alcaraz, M. C. Marchi, H. E. Troiani, V. Luca, H. Míguez and G. J. A. A. Soler-Illia, *Adv. Funct. Mater.*, 2007, **17**, 1247.
46. M. N. Ghazzal, D. P. Debecker and E. M. Gaigneaux, *Thin Solid Films*, 2016, **611**, 117.
47. A. Chiappone, E. Fantino, I. Roppolo, M. Lorusso, D. Manfredi, P. Fino, C. F. Pirri and F. Calignano, *ACS Applied Materials & Interfaces*, 2016, **8**, 5627.
48. E. B. Duoss, M. Twardowski and J. A. Lewis, *Adv. Mater.*, 2007, **19**, 3485.
49. B. C. Gross, J. L. Erkal, S. Y. Lockwood, C. Chen and D. M. Spence, *Anal. Chem.*, 2014, **86**, 3240.
50. Y. F. Lu, H. Y. Fan, A. Stump, T. L. Ward, T. Rieker and C. J. Brinker, *Nature*, 1999, **398**, 223.
51. J. Pang, J. N. Stuecker, Y. Jiang, A. J. Bhakta, E. D. Branson, P. Li, J. Cesarano, D. Sutton, P. Calvert and C. J. Brinker, *Small*, 2008, **4**, 982.
52. W. Wang, D. Grozea, A. Kim, D. D. Perovic and G. A. Ozin, *Adv. Mater.*, 2010, **22**, 99.
53. K. Okuyama, M. Abdullah, I. Wuled Lenggoro and F. Iskandar, *Adv. Powder Technol.*, 2006, **17**, 587.
54. C. Boissiere, D. Grosso, A. Chaumonnot, L. Nicole and C. Sanchez, *Adv. Mater.*, 2011, **23**, 599.
55. A. Carné-Sánchez, I. Imaz, M. Cano-Sarabia and D. Maspoch, *Nat. Chem.*, 2013, **5**, 203.
56. B. Buesser and S. E. Pratsinis, *Annu. Rev. Chem. Biomol. Eng.*, 2012, **3**, 103.
57. M. T. Bore, S. B. Rathod, T. L. Ward and A. K. Datye, *Langmuir*, 2003, **19**, 256.
58. P. J. Bruinsma, A. Y. Kim, J. Liu and S. Baskaran, *Chem. Mater.*, 1997, **9**, 2507.
59. I. Shyjumon, M. Rappolt, B. Sartori, H. Amenitsch and P. Laggner, *Rev. Sci. Instrum.*, 2008, **79**.
60. S. Pega, C. Boissiere, D. Grosso, T. Azais, A. Chaumonnot and C. Sanchez *Angew. Chem. Int. Ed.*, 2009, **48**, 2784.
61. D. P. Debecker, *Chem. Record*, 2018, In Press DOI:10.1002/tcr.201700068.
62. A. T. Bell, *Science*, 2003, **299**, 1688.
63. R. J. White, R. Luque, V. L. Budarin, J. H. Clark and D. J. Macquarrie, *Chem. Soc. Rev.*, 2009, **38**, 481.
64. D. E. De Vos, M. Dams, B. F. Sels and P. A. Jacobs, *Chem. Rev.*, 2002, **102**, 3615.
65. L.-B. Sun, X.-Q. Liu and H.-C. Zhou, *Chem. Soc. Rev.*, 2015, **44**, 5092.
66. C. Perego and R. Millini, *Chem. Soc. Rev.*, 2013, **42**, 3956.
67. D. P. Debecker, V. Hulea and P. H. Mutin, *Appl. Catal. A*, 2013, **451**, 192.
68. F. Zaera, *Chem. Soc. Rev.*, 2013, **42**, 2746.
69. N. Pal and A. Bhaumik, *RSC Adv.*, 2015, **5**, 24363.
70. W. R. Marshall, *Atomization and spray drying*, American Institute of Chemical Engineers, 1954.
71. K. Masters, *Spray drying handbook*, Halsted Press, 1979.
72. A. H. Lefebvre and V. G. McDonell, *Atomization and Sprays, Second Edition*, CRC Press, 2017.
73. M. I Ré, *Drying Technol.*, 1998, **16**, 1195.
74. G. A. Reineccius, in *Flavor Encapsulation*, American Chemical Society, 1988, vol. 370, ch. 7, pp. 55.
75. L. L. Balassa, G. O. Fanger and O. B. Wurzburg, *C R C Critical Reviews in Food Technology*, 1971, **2**, 245.
76. G. A. Rocha, C. S. Fávaro-Trindade and C. R. F. Grosso, *Food Bioprod. Process.*, 2012, **90**, 37.
77. S. M. Jafari, E. Assadpoor, B. Bhandari and Y. He, *Food Res. Int.*, 2008, **41**, 172.
78. H. C. F. Carneiro, R. V. Tonon, C. R. F. Grosso and M. D. Hubinger, *J. Food Eng.*, 2013, **115**, 443.
79. P. Schuck, *Lait*, 2002, **82**, 375.
80. B. R. Bhandari, A. Senoussi, E. D. Dumoulin and A. Lebert, *Drying Technol.*, 1993, **11**, 1081.
81. E. H. J. Kim, X. D. Chen and D. Pearce, *J. Food Eng.*, 2009, **94**, 169.
82. A. M. Goula and K. G. Adamopoulos, *Innov. food Sci. Emerg. Technol.*, 2010, **11**, 342.
83. C. A. Morgan, N. Herman, P. A. White and G. Vesey, *J. Microbiol. Methods*, 2006, **66**, 183.
84. S. H. Peighambardoust, A. Golshan Tafti and J. Hesari, *Trends Food Sci. Tech.*, 2011, **22**, 215.
85. B. Riveros, J. Ferrer and R. Bórquez, *Drying Technol.*, 2009, **27**, 123.
86. J. Silva, R. Freixo, P. Gibbs and P. Teixeira, *Int. J. Dairy Technol.*, 2011, **64**, 321.
87. J. Guerin, J. Petit, J. Burgain, F. Borges, B. Bhandari, C. Perroud, S. Desobry, J. Scher and C. Gaiani, *J. Food Eng.*, 2017, **193**, 10.
88. C. M. Librán, S. Castro and J. M. Lagaron, *Innov. food Sci. Emerg. Technol.*, 2017, **39**, 216.
89. D. A. LeClair, E. D. Cranston, Z. Xing and M. R. Thompson, *Pharm. Res.*, 2016, **33**, 2763.
90. J. Broadhead, S. K. Edmond Rouan and C. T. Rhodes, *Drug Dev. Ind. Pharm.*, 1992, **18**, 1169.
91. M. W. Woo, M. G. Lee, S. Shakiba and S. Mansouri, *Expert Opin. Drug Del.*, 2017, **14**, 1315.
92. A. Langford, B. Bhatnagar, R. Walters, S. Tchessalov and S. Ohtake, *Drying Technol.*, 2017, 1.
93. M. L. Eggersdorfer, V. Koren, E. Stolovicki, E. Amstad and D. A. Weitz, *Cryst. Growth Des.*, 2017, **17**, 2046.
94. W.-y. Zhao, T.-l. Zhang, L.-n. Zhang, L. Yang and Z.-n. Zhou, *J. Ind. Eng. Chem.*, 2016, **38**, 73.
95. M. Tong and D. J. Browne, *J. Mater. Process. Technol.*, 2008, **202**, 419.
96. S. J. Savage and F. H. Froes, *JOM*, 1984, **36**, 20.
97. C. Si, X. Tang, X. Zhang, J. Wang and W. Wu, *Mater. Des.*, 2017, **118**, 66.
98. P. Sun, Z. Z. Fang, Y. Zhang and Y. Xia, *JOM*, 2017, **69**, 1853.
99. C. Song, K. Li, K. Xie, W. Lu, S. Zhao, Q. Han and Q. Zhai, *Powder Technol.*, 2014, **263**, 31.
100. F. X. Govers, US1506118, 1924, Method of preparing siliceous material.
101. S. Behrman Abraham, US1755496, 1930, Process of preparing siliceous materials
102. K. Ebner, US2155119, 1939, Process of and apparatus for the thermal decomposition of substances or mixtures of same.
103. S. J. Lukasiewicz, *J. Am. Ceram. Soc.*, 1989, **72**, 617.

Please do not adjust margins

Please do not adjust margins

104. R. M. Laine, in *Ceramics Science and Technology*, Wiley-VCH Verlag GmbH & Co. KGaA, 2012, DOI: 10.1002/9783527631957.ch4, pp. 97.
105. B. Schimmoeller, S. E. Pratsinis and A. Baiker, *ChemCatChem*, 2011, **3**, 1234.
106. A. E. Danks, S. R. Hall and Z. Schnepp, *Mater. Horiz.*, 2016, **3**, 91.
107. J. Livage and C. Sanchez, *J. Non-Cryst. Solids*, 1992, **145**, 11.
108. A. Corma, *Chem. Rev.*, 1997, **97**, 2373.
109. D. Grosso, G. J. de A.A. Soler-Illia, E. L. Crepaldi, B. Charleux and C. Sanchez, *Adv. Funct. Mater.*, 2003, **13**, 37.
110. C. Boissiere, D. Grosso, H. Amenitsch, A. Gibaud, A. Coupe, N. Baccile and C. Sanchez, *Chem. Commun.*, 2003, 2798.
111. G. Bertrand, P. Roy, C. Filiatre and C. Coddet, *Chem. Eng. Sci.*, 2005, **60**, 95.
112. N. Saadatkhah, M. G. Rigamonti, D. C. Boffito, H. Li and G. S. Patience, *Powder Technol.*, 2017, **316**, 434.
113. D. Cui, J. Liu, J. Yu, F. Su and G. Xu, *Int. J. Hydrogen Energy*, 2017, **42**, 4987.
114. R. Vehring, *Pharm. Res.*, 2008, **25**, 999.
115. A. Gharsallaoui, G. Roudaut, O. Chambin, A. Voilley and R. Saurel, *Food Res. Int.*, 2007, **40**, 1107.
116. A. Sosnik and K. P. Seremeta, *Adv. Colloid Interface Sci.*, 2015, **223**, 40.
117. S. Ramesh and D. P. Debecker, *Catal. Commun.*, 2017, **97**, 102.
118. Y. V. Kolen'ko, W. Zhang, R. N. d'Alnoncourt, F. Girgsdies, T. W. Hansen, T. Wolfram, R. Schlögl and A. Trunschke, *ChemCatChem*, 2011, **3**, 1597.
119. W. Y. Teoh, R. Amal and L. Madler, *Nanoscale*, 2010, **2**, 1324.
120. R. Strobel and S. E. Pratsinis, *J. Mater. Chem.*, 2007, **17**, 4743.
121. M. Høj, K. Linde, T. K. Hansen, M. Brorson, A. D. Jensen and J.-D. Grunwaldt, *Appl. Catal. A*, 2011, **397**, 201.
122. S. Li, Y. Ren, P. Biswas and S. D. Tse, *Prog. Energy Combust. Sci.*, 2016, **55**, 1.
123. B. Buesser and S. E. Pratsinis, *Annu. Rev. Chem. Biomol. Eng.*, 2012, **3**, 103.
124. L. Mädler, H. K. Kammler, R. Mueller and S. E. Pratsinis, *J. Aerosol Sci*, 2002, **33**, 369.
125. B. Schimmoeller, R. Delaigle, D. P. Debecker and E. M. Gaigneaux, *Catal. Today*, 2010, **157**, 198.
126. K. Schuh, W. Kleist, M. Hoj, V. Trouillet, A. D. Jensen and J. D. Grunwaldt, *Chem. Commun.*, 2014, **50**, 15404.
127. D. P. Debecker, B. Schimmoeller, M. Stoyanova, C. Poleunis, P. Bertrand, U. Rodemerck and E. M. Gaigneaux, *J. Catal.*, 2011, **277**, 154.
128. S. Pisduangdaw, J. Panpranot, C. Methastidsook, C. Chaisuk, K. Faungnawakij, P. Praserthdam and O. Mekasuwandumrong, *Appl. Catal. A*, 2009, **370**, 1.
129. R. Strobel, W. J. Stark, L. Mädler, S. E. Pratsinis and A. Baiker, *J. Catal.*, 2003, **213**, 296.
130. O. Mekasuwandumrong, S. Somboonthanakij, P. Praserthdam and J. Panpranot, *Ind. Eng. Chem. Res.*, 2009, **48**, 2819.
131. D. Li, N. Ichikuni, S. Shimazu and T. Uematsu, *Appl. Catal. A*, 1999, **180**, 227.
132. Y. Huang, Z. Zheng, Z. Ai, L. Zhang, X. Fan and Z. Zou, *J. Phys. Chem. B*, 2006, **110**, 19323.
133. D. P. Debecker, M. Stoyanova, F. Colbeau-Justin, U. Rodemerck, C. Boissière, E. M. Gaigneaux and C. Sanchez, *Angew. Chem. Int. Ed.*, 2012, **51**, 2129.
134. E. Belamie, M. Y. Boltoeva, K. Yang, T. Cacciaguerra and B. Alonso, *J. Mater. Chem.*, 2011, **21**, 16997.
135. A. Lawley, *JOM*, 1981, **33**, 13.
136. A. M. Mullis, T. D. Bigg and N. J. Adkins, *J. Alloys Compd.*, 2015, **648**, 139.
137. A. M. Mullis, T. D. Bigg and N. J. Adkins, *Intermetallics*, 2015, **67**, 63.
138. F. Devred, A. H. Gieske, N. Adkins, U. Dahlborg, C. M. Bao, M. Calvo-Dahlborg, J. W. Bakker and B. E. Nieuwenhuys, *Appl. Catal. A*, 2009, **356**, 154.
139. F. Devred, G. Reinhart, G. N. Iles, B. van der Klugt, N. J. Adkins, J. W. Bakker and B. E. Nieuwenhuys, *Catal. Today*, 2011, **163**, 13.
140. D. Tourret, G. Reinhart, C. A. Gandin, G. N. Iles, U. Dahlborg, M. Calvo-Dahlborg and C. M. Bao, *Acta Mater.*, 2011, **59**, 6658.
141. Y. F. Zhao, J. J. Si, J. G. Song, Q. Yang and X. D. Hui, *Mater. Sci. Eng. B*, 2014, **181**, 46.
142. A. B. D. Nandiyanto and K. Okuyama, *Adv. Powder Technol.*, 2011, **22**, 1.
143. A. J. Hewitt, *J. Aerosol Sci*, 1993, **24**, 155.
144. F. Iskandar, *Adv. Powder Technol.*, 2009, **20**, 283.
145. W.-N. Wang, A. Purwanto, I. W. Lenggoro, K. Okuyama, H. Chang and H. D. Jang, *Ind. Eng. Chem. Res.*, 2008, **47**, 1650.
146. F. Iskandar, L. Gradon and K. Okuyama, *J. Colloid Interface Sci.*, 2003, **265**, 296.
147. N. Godard, X. Collard, A. Vivian, L. A. Bivona, S. Fiorilli, L. Fusaro and C. Aprile, *Appl. Catal. A*, 2018, DOI: https://doi.org/10.1016/j.apcata.2018.02.014.
148. Y. De Vos, M. Jacobs, P. Van Der Voort, I. Van Driessche, F. Snijkers and A. Verberckmoes, *Chem. Eng. J.*, 2017, **309**, 824.
149. R. Strobel, A. Baiker and S. E. Pratsinis, *Adv. Powder Technol.*, 2006, **17**, 457.
150. R. Koirala, S. E. Pratsinis and A. Baiker, *Chem. Soc. Rev.*, 2016, **45**, 3053.
151. A. Ishihara, T. Wakamatsu, H. Nasu and T. Hashimoto, *Appl. Catal. A*, 2014, **478**, 58.
152. M. Caillot, A. Chaumonnot, M. Digne, C. Poleunis, D. P. Debecker and J. A. van Bokhoven, *Microporous Mesoporous Mater.*, 2014, **185**, 179.
153. K. Sabyrov, N. Musselwhite, G. Melaet and G. A. Somorjai, *Catal. Sci. Technol.*, 2017, **7**, 1756.
154. K. Yamaguchi, K. Ebitani, T. Yoshida, H. Yoshida and K. Kaneda, *J. Am. Chem. Soc.*, 1999, **121**, 4526.
155. C. Noda Pérez, C. A. Pérez, C. A. Henriques and J. L. F. Monteiro, *Appl. Catal. A*, 2004, **272**, 229.
156. L. Hora, V. Kelbichová, O. Kikhtyanin, O. Bortnovskiy and D. Kubička, *Catal. Today*, 2014, **223**, 138.
157. R. Hutter, T. Mallat and A. Baiker, *J. Catal.*, 1995, **153**, 177.

 This journal is © The Royal Society of Chemistry 20xx

Please do not adjust margins

Please do not adjust margins

158. Z. Zhang, Z. Jiang and W. Shangguan, *Catal. Today*, 2016, **264**, 270.
159. V. Smeets, L. Ben Mustapha, J. Schnee, E. M. Gaigneaux and D. P. Debecker, *ChemRxiv - DOI: 10.26434/chemrxiv.6002354.v1*, 2018.
160. C. Evangelisti, M. Guidotti, C. Tiozzo, R. Psaro, N. Maksimchuk, I. Ivanchikova, A. N. Shmakov and O. Kholdeeva, *Inorg. Chim. Acta*, 2018, **470**, 393.
161. G. J. Hutchings, *J. Mater. Chem.*, 2009, **19**, 1222.
162. J. R. H. Ross, *Heterogeneous Catalysis Fundamentals and Applications*, Elsevier, Amsterdam, The Netherlands, 2012.
163. M. Campanati, G. Fornasari and A. Vaccari, *Catal. Today*, 2003, **77**, 299.
164. A. Chaumonnot, F. Tihay, A. Coupé, S. Pega, C. Boissière, D. Grosso and C. Sanchez, *Oil Gas Sci. Technol.*, 2009, **64**, 681.
165. Z. Guo, G. Xiong, L. Liu, P. Li, L. Hao, Y. Cao and F. Tian, *J. Porous Mater.*, 2016, **23**, 407.
166. F. Colbeau-Justin, C. Boissière, A. Chaumonnot, A. Bonduelle and C. Sanchez, *Adv. Funct. Mater.*, 2014, **24**, 233.
167. B. Sunkara, J. Zhan, I. Kolesnichenko, Y. Wang, J. He, J. E. Holland, G. L. McPherson and V. T. John, *Langmuir*, 2011, **27**, 7854.
168. S. Pega, C. Boissière, A. Chaumonnot and C. Sanchez, in *Stud. Surf. Sci. Catal.*, eds. A. Gédéon, P. Massiani and F. Babonneau, Elsevier, 2008, vol. 174, pp. 471.
169. D. P. Debecker, M. Stoyanova, U. Rodemerck, F. Colbeau-Justin, C. Boissère, A. Chaumonnot, A. Bonduelle and C. Sanchez, *Appl. Catal. A*, 2014, **470**, 458.
170. S. Maksasithorn, P. Praserthdam, K. Suriye and D. P. Debecker, *Microporous Mesoporous Mater.*, 2015, **213**, 125.
171. N. Godard, A. Vivian, L. Fusaro, L. Cannavicci, C. Aprile and D. P. Debecker, *ChemCatChem*, 2017, **9**, 2211.
172. C. Wang and H. Bai, *Ind. Eng. Chem. Res.*, 2011, **50**, 3842.
173. C. Y. Wang and H. Bai, *Catal. Today*, 2011, **174**, 70.
174. K. Y. Jung, Y. R. Jung, J.-K. Jeon, J. H. Kim, Y.-K. Park and S. Kim, *J. Ind. Eng. Chem.*, 2011, **17**, 144.
175. A. Sachse, V. Hulea, K. L. Kostov, N. Marcotte, M. Y. Boltoeva, E. Belamie and B. Alonso, *Chem. Commun.*, 2012, **48**, 10648.
176. H. Oveisi, N. Suzuki, A. Beitollahi and Y. Yamauchi, *J. Sol-Gel Sci. Technol.*, 2010, **56**, 212.
177. F. Zhang, C. Kang, Y. Wei and H. Li, *Adv. Funct. Mater.*, 2011, **21**, 3189.
178. N. Gholampour, S. Chaemchuen, Z.-Y. Hu, B. Mousavi, G. Van Tendeloo and F. Verpoort, *Chem. Eng. J.*, 2017, **322**, 702.
179. L. Kuai, J. Geng, C. Chen, E. Kan, Y. Liu, Q. Wang and B. Geng, *Angew. Chem. Int. Ed.*, 2014, **53**, 7547.
180. L. Kuai, J. Wang, T. Ming, C. Fang, Z. Sun, B. Geng and J. Wang, *Sci. Rep.*, 2015, **5**, 9923.
181. D. Hong, Y. Yamada, M. Sheehan, S. Shikano, C.-H. Kuo, M. Tian, C.-K. Tsung and S. Fukuzumi, *ACS Sus. Chem. Eng.*, 2014, **2**, 2588.
182. E. Kan, L. Kuai, W. Wang and B. Geng, *Chem. Eur. J.*, 2015, **21**, 13291.
183. Z. Jin, M. Xiao, Z. Bao, P. Wang and J. Wang, *Angew. Chem. Int. Ed.*, 2012, **51**, 6406.
184. J. P. Gabaldon, M. Bore and A. K. Datye, *Top. Catal.*, 2007, **44**, 253.
185. A. Primo and H. Garcia, *Chem. Soc. Rev.*, 2014, **43**, 7548.
186. R. Mokaya, *Angew. Chem. Int. Ed.*, 1999, **38**, 2930.
187. Z. Zhang, Y. Han, L. Zhu, R. Wang, Y. Yu, S. Qiu, D. Zhao and F.-S. Xiao, *Angew. Chem. Int. Ed.*, 2001, **40**, 1258.
188. K. Li, J. Valla and J. Garcia-Martinez, *ChemCatChem*, 2014, **6**, 46.
189. S. Fiorilli, V. Cauda, L. Pontiroli, C. Vitale-Brovarone and B. Onida, *New J. Chem.*, 2016, **40**, 4420.
190. H. Liu, H.-M. Kao and C. P. Grey, *The Journal of Physical Chemistry B*, 1999, **103**, 4786.
191. R. Ryoo, K. Cho and F. M. Mota, in *Zeolites in Sustainable Chemistry*, Springer, 2016, pp. 101.
192. Z. Zhang, Y. Han, F.-S. Xiao, S. Qiu, L. Zhu, R. Wang, Y. Yu, Z. Zhang, B. Zou and Y. Wang, *J. Am. Chem. Soc.*, 2001, **123**, 5014.
193. K. S. Triantafyllidis, E. F. Iliopoulou, E. V. Antonakou, A. A. Lappas, H. Wang and T. J. Pinnavaia, *Microporous Mesoporous Mater.*, 2007, **99**, 132.
194. S. Zeng, J. Blanchard, M. Breysse, Y. Shi, X. Su, H. Nie and D. Li, *Appl. Catal. A*, 2005, **294**, 59.
195. A. Aerts, A. van Isacker, W. Huybrechts, S. P. Kremer, C. E. Kirschhock, F. Collignon, K. Houthoofd, J. F. Denayer, G. V. Baron and G. B. Marin, *Appl. Catal. A*, 2004, **257**, 7.
196. J. C. Mol, *J. Mol. Catal. A*, 2004, **213**, 39.
197. X. Zhu, X. Li, S. Xie, S. Liu, G. Xu, W. Xin, S. Huang and L. Xu, *Catalysis Surveys from Asia*, 2008, **13**, 1.
198. S. Lwin and I. E. Wachs, *ACS Catal.*, 2014, **4**, 2505.
199. J.-F. Wu, A. Ramanathan and B. Subramaniam, *J. Catal.*, 2017, **350**, 182.
200. K. Amakawa, S. Wrabetz, J. Kröhnert, G. Tzolova-Müller, R. Schlögl and A. Trunschke, *J. Am. Chem. Soc.*, 2012, **134**, 11462.
201. H. Balcar and J. Čejka, *Coord. Chem. Rev.*, 2013, **257**, 3107.
202. K. Bouchmella, P. Hubert Mutin, M. Stoyanova, C. Poleunis, P. Eloy, U. Rodemerck, E. M. Gaigneaux and D. P. Debecker, *J. Catal.*, 2013, **301**, 233.
203. S. Maksasithorn, D. P. Debecker, P. Praserthdam, J. Panpranot, K. Suriye and S. K. N. Ayudhya, *Chin. J. Catal.*, 2014, **35**, 232.
204. K. Ding, A. Gulec, A. M. Johnson, T. L. Drake, W. Wu, Y. Lin, E. Weitz, L. D. Marks and P. C. Stair, *ACS Catal.*, 2016, **6**, 5740.
205. K. Bouchmella, M. Stoyanova, U. Rodemerck, D. P. Debecker and P. Hubert Mutin, *Catal. Commun.*, 2015, **58**, 183.
206. D. P. Debecker, M. Stoyanova, U. Rodemerck, A. Leonard, B.-L. Su and E. M. Gaigneaux, *Catal. Today*, 2011, **169**, 60.
207. J. Handzlik, J. Ogonowski, J. Stoch and M. Mikołajczyk, *Appl. Catal. A*, 2004, **273**, 99.
208. D. P. Debecker, M. Stoyanova, U. Rodemerck, P. Eloy, A. Leonard, B. L. Su and E. M. Gaigneaux, *J. Phys. Chem. C*, 2010, **114**, 18664.

This journal is © The Royal Society of Chemistry 20xx

Please do not adjust margins

Please do not adjust margins

209. D. P. Debecker, D. Hauwaert, M. Stoyanova, A. Barkschat, U. Rodemerck and E. M. Gaigneaux, *Appl. Catal. A*, 2011, **391**, 78.
210. J. Handzlik, J. Ogonowski, J. Stoch, M. Mikolajczyk and P. Michorczyk, *Appl. Catal. A*, 2006, **312**, 213.
211. S. Liu, S. Huang, W. Xin, J. Bai, S. Xie and L. Xu, *Catal. Today*, 2004, **93-95**, 471.
212. D. P. Debecker, K. Bouchmella, M. Stoyanova, U. Rodemerck, E. M. Gaigneaux and P. H. Mutin, *Catal. Sci. Technol.*, 2012, **2**, 1157.
213. D. P. Debecker, K. Bouchmella, C. Poleunis, P. Eloy, P. Bertrand, E. M. Gaigneaux and P. H. Mutin, *Chem. Mat.*, 2009, **21**, 2817.
214. D. P. Debecker, M. Stoyanova, U. Rodemerck and E. M. Gaigneaux, *J. Mol. Catal. A: Chem.*, 2011, **340**, 65.
215. S. Maksasithorn, P. Praserthdam, K. Suriye, M. Devillers and D. P. Debecker, *Appl. Catal. A*, 2014, **488**, 200.
216. B. Delmon, *Catalysis Letters*, 1993, **22**, 1.
217. S. T. Oyama, T. Gott, H. Zhao and Y.-K. Lee, *Catal. Today*, 2009, **143**, 94.
218. M. Breysse, P. Afanasiev, C. Geantet and M. Vrinat, *Catal. Today*, 2003, **86**, 5.
219. A. M. Maitra, N. W. Cant and D. L. Trimm, *Appl. Catal.*, 1989, **48**, 187.
220. M. Breysse, C. Geantet, P. Afanasiev, J. Blanchard and M. Vrinat, *Catal. Today*, 2008, **130**, 3.
221. L. Coulier, V. H. J. de Beer, J. A. R. van Veen and J. W. Niemantsverdriet, *Top. Catal.*, 2000, **13**, 99.
222. P. N. R. Vennestrøm, C. M. Osmundsen, C. H. Christensen and E. Taarning, *Angew. Chem. Int. Ed.*, 2011, **50**, 10502.
223. R. A. Gross and B. Kalra, *Science*, 2002, **297**, 803.
224. L. T. Lim, R. Auras and M. Rubino, *Prog. Polym. Sci.*, 2008, **33**, 820.
225. F. H. Isikgor and C. R. Becer, *Polym. Chem.*, 2015, **6**, 4497.
226. R. De Clercq, M. Dusselier and B. F. Sels, *Green Chem.*, 2017, **19**, 5012.
227. M. Dusselier, P. Van Wouwe, A. Dewaele, E. Makshina and B. F. Sels, *Energ. Env. Sci.*, 2013, **6**, 1415.
228. A. Engin, H. Haluk and K. Gurkan, *Green Chem.*, 2003, **5**, 460.
229. S. Tolborg, I. Sádaba, C. M. Osmundsen, P. Fristrup, M. S. Holm and E. Taarning, *ChemSusChem*, 2015, **8**, 613.
230. L. Li, X. Collard, A. Bertrand, B. F. Sels, P. P. Pescarmona and C. Aprile, *J. Catal.*, 2014, **314**, 56.
231. L. Li, C. Stroobants, K. Lin, P. A. Jacobs, B. F. Sels and P. P. Pescarmona, *Green Chem.*, 2011, **13**, 1175.
232. Q. Guo, F. Fan, E. A. Pidko, W. N. P. van der Graaff, Z. Feng, C. Li and E. J. M. Hensen, *ChemSusChem*, 2013, **6**, 1352.
233. P. Y. Dapsens, C. Mondelli and J. Perez-Ramirez, *Chem. Soc. Rev.*, 2015, **44**, 7025.
234. K. Chaudhari, T. K. Das, P. R. Rajmohanan, K. Lazar, S. Sivasanker and A. J. Chandwadkar, *J. Catal.*, 1999, **183**, 281.
235. P. Shah, A. V. Ramaswamy, K. Lazar and V. Ramaswamy, *Microporous Mesoporous Mater.*, 2007, **100**, 210.
236. M. S. Kamal, S. A. Razzak and M. M. Hossain, *Atmos. Environ.*, 2016, **140**, 117.
237. .
238. C. Du, S. Lu, Q. Wang, A. G. Buekens, M. Ni and D. P. Debecker, *Chem. Eng. J.*, 2018, **334**, 519.
239. L. F. Liotta, *Appl. Catal. B*, 2010, **100**, 403.
240. J. M. Toledo, J. Corella and A. Sanz, *Environ. Prog.*, 2001, **20**, 167.
241. W. B. Li, J. X. Wang and H. Gong, *Catal. Today*, 2009, **148**, 81.
242. H. Huang, Y. Xu, Q. Feng and D. Y. C. Leung, *Catal. Sci. Technol.*, 2015, **5**, 2649.
243. A. Aranzabal, B. Pereda-Ayo, M. González-Marcos, J. González-Marcos, R. López-Fonseca and J. González-Velasco, *Chem. Pap.*, 2014, **68**, 1169.
244. D. P. Debecker, R. Delaigle, P. Eloy and E. M. Gaigneaux, *J. Mol. Catal. A*, 2008, **289**, 38.
245. D. P. Debecker, R. Delaigle, P. C. Hung, A. Buekens, E. M. Gaigneaux and M. B. Chang, *Chemosphere*, 2011, **82**, 1337.
246. M. Paulis, L. M. Gandía, A. Gil, J. Sambeth, J. A. Odriozola and M. Montes, *Appl. Catal. B*, 2000, **26**, 37.
247. B. Miranda, E. Díaz, S. Ordóñez, A. Vega and F. V. Díez, *Chemosphere*, 2007, **66**, 1706.
248. R. Delaigle, D. P. Debecker, F. Bertinchamps and E. M. Gaigneaux, *Top. Catal.*, 2009, **52**, 501.
249. C.-H. Cho and S.-K. Ihm, *Env. Sci. Technol.*, 2002, **36**, 1600.
250. D. P. Debecker, K. Bouchmella, R. Delaigle, P. Eloy, C. Poleunis, P. Bertrand, E. M. Gaigneaux and P. H. Mutin, *Appl. Catal. B*, 2010, **94**, 38.
251. E. Finocchio, M. Baldi, G. Busca, C. Pistarino, G. Romezzano, F. Bregani and G. P. Toledo, *Catal. Today*, 2000, **59**, 261.
252. D. P. Debecker, F. Bertinchamps, N. Blangenois, P. Eloy and E. M. Gaigneaux, *Appl. Catal. B*, 2007, **74**, 223.
253. C. Gannoun, R. Delaigle, P. Eloy, D. P. Debecker, A. Ghorbel and E. M. Gaigneaux, *Catal. Commun.*, 2011, **15**, 1.
254. B. M. Weckhuysen and D. E. Keller, *Catal. Today*, 2003, **78**, 25.
255. S. Chin, J. Jurng, J.-H. Lee and S.-J. Moon, *Chemosphere*, 2009, **75**, 1206.
256. D. R. C. Huybrechts, L. D. Bruycker and P. A. Jacobs, *Nature*, 1990, **345**, 240.
257. J. S. Reddy and R. Kumar, *J. Catal.*, 1991, **130**, 440.
258. T. Blasco, A. Corma, M. Navarro and J. P. Pariente, *J. Catal.*, 1995, **156**, 65.
259. P. T. Tanev, M. Chibwe and T. J. Pinnavaia, *Nature*, 1994, **368**, 321.
260. A. Corma, M. Domine, J. A. Gaona, J. L. Jordá, M. T. Navarro, F. Rey, J. Pérez-Pariente, J. Tsuji, B. McCulloch and L. T. Nemeth, *Chem. Commun.*, 1998, 2211.
261. N. Ravasio, F. Zaccheria, M. Guidotti and R. Psaro, *Top. Catal.*, 2004, **27**, 157.
262. M. Guidotti, C. Pirovano, N. Ravasio, B. Lázaro, J. M. Fraile, J. A. Mayoral, B. Coq and A. Galarneau, *Green Chem.*, 2009, **11**, 1421.
263. M. Andrianainarivelo, R. Corriu, D. Leclercq, P. H. Mutin and A. Vioux, *J. Mater. Chem.*, 1996, **6**, 1665.
264. B. Alonso and E. Belamie, *Angew. Chem. Int. Ed.*, 2010, **49**, 8201.
265. J. G. Yu, Y. R. Su and B. Cheng, *Adv. Funct. Mater.*, 2007, **17**, 1984.

 This journal is © The Royal Society of Chemistry 20xx

Please do not adjust margins

Please do not adjust margins

266. M. N. Ghazzal, H. Kebaili, M. Joseph, D. P. Debecker, P. Eloy, J. De Coninck and E. M. Gaigneaux, *Appl. Catal. B*, 2012, **115**, 276.
267. C. Guo, M. Ge, L. Liu, G. Gao, Y. Feng and Y. Wang, *Env. Sci. Technol.*, 2010, **44**, 419.
268. J. Schneider, M. Matsuoka, M. Takeuchi, J. Zhang, Y. Horiuchi, M. Anpo and D. W. Bahnemann, *Chem. Rev.*, 2014, **114**, 9919.
269. S. G. Kumar and L. G. Devi, *J. Phys. Chem. A*, 2011, **115**, 13211.
270. U. T. Bornscheuer, *Angew. Chem. Int. Ed.*, 2003, **42**, 3336.
271. R. A. Sheldon and S. van Pelt, *Chem. Soc. Rev.*, 2013, **42**, 6223.
272. I. González-Delgado, Y. Segura, A. Martín, M.-J. López-Muñoz and G. Morales, *Microporous Mesoporous Mater.*, 2018, **257**, 51.
273. F. Tian, Y. Guo, F. Lin, Y. Zhang, Q. Yuan and H. Liang, *Int. J. Biol. Macromol.*, 2016, **87**, 191.
274. F. Hoffmann, M. Cornelius, J. Morell and M. Fröba, *Angew. Chem. Int. Ed.*, 2006, **45**, 3216.
275. A. P. Wight and M. E. Davis, *Chem. Rev.*, 2002, **102**, 3589.
276. T. Asefa, M. J. MacLachlan, N. Coombs and G. A. Ozin, *Nature*, 1999, **402**, 867.
277. S. Inagaki, S. Guan, Y. Fukushima, T. Ohsuna and O. Terasaki, *J. Am. Chem. Soc.*, 1999, **121**, 9611.
278. B. J. Melde, B. T. Holland, C. F. Blanford and A. Stein, *Chem. Mater.*, 1999, **11**, 3302.
279. N. Mizoshita, T. Tani and S. Inagaki, *Chem. Soc. Rev.*, 2011, **40**, 789.
280. Q. Yang, J. Liu, L. Zhang and C. Li, *J. Mater. Chem.*, 2009, **19**, 1945.
281. A. Modak, J. Mondal and A. Bhaumik, *Green Chem.*, 2012, **14**, 2840.
282. Y. Yusuke, S. Norihiro, G. Prashant, S. Keisuke, F. Naoki, M. Miwa, S. Tadashi, I. Satoru and K. Tatsuo, *Sci. Technol. Adv. Mater.*, 2009, **10**, 025005.
283. N. Suzuki and Y. Yamauchi, *J. Nanosci. Nanotechnol.*, 2010, **10**, 5759.
284. N. Suzuki, P. Gupta, H. Sukegawa, K. Inomata, S. Inoue and Y. Yamauchi, *J. Nanosci. Nanotechnol.*, 2010, **10**, 6612.
285. M. Ide, E. De Canck, I. Van Driessche, F. Lynen and P. Van Der Voort, *RSC Adv.*, 2015, **5**, 5546.
286. H. Li, M. Eddaoudi, M. O'Keeffe and O. M. Yaghi, *Nature*, 1999, **402**, 276.
287. J. Lee, O. K. Farha, J. Roberts, K. A. Scheidt, S. T. Nguyen and J. T. Hupp, *Chem. Soc. Rev.*, 2009, **38**, 1450.
288. L. Lin, T. Zhang, H. Liu, J. Qiu and X. Zhang, *Nanoscale*, 2015, **7**, 7615.
289. M. Sabo, A. Henschel, H. Frode, E. Klemm and S. Kaskel, *J. Mater. Chem.*, 2007, **17**, 3827.
290. A. J. Bard and M. A. Fox, *Acc. Chem. Res.*, 1995, **28**, 141.
291. M. Jiang, H. Wang, Y. Li, H. Zhang, G. Zhang, Z. Lu, X. Sun and L. Jiang, *Small*, 2017, **13**, 1602240.
292. M. G. Walter, E. L. Warren, J. R. McKone, S. W. Boettcher, Q. Mi, E. A. Santori and N. S. Lewis, *Chem. Rev.*, 2010, **110**, 6446.
293. A. Vojvodic and J. K. Nørskov, *Science*, 2011, **334**, 1355.
294. D. Merki, S. Fierro, H. Vrubel and X. Hu, *Chem. Sci.*, 2011, **2**, 1262.
295. J. D. Benck, T. R. Hellstern, J. Kibsgaard, P. Chakthranont and T. F. Jaramillo, *ACS Catal.*, 2014, **4**, 3957.
296. P. C. K. Vesborg, B. Seger and I. Chorkendorff, *Journal of Physical Chemistry Letters*, 2015, **6**, 951.
297. X. Li, X. Hao, A. Abudula and G. Guan, *J. Mater. Chem. A*, 2016, **4**, 11973.
298. M. W. Kanan and D. G. Nocera, *Science*, 2008, **321**, 1072.
299. E. Tsuji, A. Imanishi, K.-i. Fukui and Y. Nakato, *Electrochim. Acta*, 2011, **56**, 2009.
300. R. D. Smith, M. S. Prévot, R. D. Fagan, S. Trudel and C. P. Berlinguette, *J. Am. Chem. Soc.*, 2013, **135**, 11580.
301. T. Peng, X. Zhang, H. Lv and L. Zan, *Catal. Commun.*, 2012, **28**, 116.
302. K. Shankar, J. I. Basham, N. K. Allam, O. K. Varghese, G. K. Mor, X. Feng, M. Paulose, J. A. Seabold, K.-S. Choi and C. A. Grimes, *J. Phys. Chem. C*, 2009, **113**, 6327.
303. W. Lubberhuizen, D. Vanmaekelbergh and E. Van Faassen, *J. Porous Mater.*, 2000, **7**, 147.
304. M. Boudart, in *Adv. Catal.*, eds. D. D. Eley, H. Pines and P. B. Weisz, Academic Press, 1969, vol. 20, pp. 153.
305. A. Corma and H. Garcia, *Chem. Soc. Rev.*, 2008, **37**, 2096.
306. H. Wei, X. Liu, A. Wang, L. Zhang, B. Qiao, X. Yang, Y. Huang, S. Miao, J. Liu and T. Zhang, *Nat. Commun.*, 2014, **5**, 5634.
307. L. Bai, X. Wang, Q. Chen, Y. Ye, H. Zheng, J. Guo, Y. Yin and C. Gao, *Angew. Chem. Int. Ed.*, 2016, **55**, 15656.
308. C.-K. Tsung, J. Fan, N. Zheng, Q. Shi, A. J. Forman, J. Wang and G. D. Stucky, *Angew. Chem. Int. Ed.*, 2008, **47**, 8682.
309. A. Corma and P. Serna, *Science*, 2006, **313**, 332.
310. D. I. Enache, J. K. Edwards, P. Landon, B. Solsona-Espriu, A. F. Carley, A. A. Herzing, M. Watanabe, C. J. Kiely, D. W. Knight and G. J. Hutchings, *Science*, 2006, **311**, 362.
311. J. H. Kwak, J. Hu, D. Mei, C.-W. Yi, D. H. Kim, C. H. F. Peden, L. F. Allard and J. Szanyi, *Science*, 2009, **325**, 1670.
312. Z. Jin, F. Wang, F. Wang, J. Wang, J. C. Yu and J. Wang, *Adv. Funct. Mater.*, 2013, **23**, 2137.
313. J. Martins, N. Batail, S. Silva, S. Rafik-Clement, A. Karelovic, D. P. Debecker, A. Chaumonnot and D. Uzio, *Catal. Commun.*, 2015, **58**, 11.
314. G. C. Bond, L. C. and D. T. Thompson, *Catalysis by Gold*, Imperial College Press, 2006.
315. A. S. K. Hashmi and G. J. Hutchings, *Angew. Chem. Int. Ed.*, 2006, **45**, 7896.
316. B. K. Min and C. M. Friend, *Chem. Rev.*, 2007, **107**, 2709.
317. J. Saavedra, H. A. Doan, C. J. Pursell, L. C. Grabow and B. D. Chandler, *Science*, 2014, **345**, 1599.
318. M. Haruta, *Chem. Record*, 2003, **3**, 75.
319. D. P. Debecker, C. Faure, M. E. Meyre, A. Derre and E. M. Gaigneaux, *Small*, 2008, **4**, 1806.
320. G. Prieto, J. Zečević, H. Friedrich, K. P. de Jong and P. E. de Jongh, *Nat. Mater.*, 2013, **12**, 34.
321. R. Delaigle, M. M. F. Joseph, D. P. Debecker, P. Eloy and E. M. Gaigneaux, *Top. Catal.*, 2013, **56**, 1867.
322. J. A. Anderson and M. Fernandez Garcia, *Supported Metals in Catalysis*, Imperial College Press, London, 2012.

This journal is © The Royal Society of Chemistry 20xx

Please do not adjust margins

Please do not adjust margins

323. J. R. Regalbuto, *Catalyst Preparation: Science and Engineering*, CRC Press, Boca Raton, 2016.
324. C. Sassoye, G. Muller, D. P. Debecker, A. Karelovic, S. Cassaignon, C. Pizarro, P. Ruiz and C. Sanchez, *Green Chem.*, 2011, **13**, 3230.
325. N. Zheng and G. D. Stucky, *J. Am. Chem. Soc.*, 2006, **128**, 14278.
326. F. Pinna, *Catal. Today*, 1998, **41**, 129.
327. Y. Huang, W. Ho, Z. Ai, X. Song, L. Zhang and S. Lee, *Appl. Catal. B*, 2009, **89**, 398.
328. J. Zhan, I. Kolesnichenko, B. Sunkara, J. He, G. L. McPherson, G. Piringer and V. T. John, *Env. Sci. Technol.*, 2011, **45**, 1949.
329. M. Košević, S. Stopic, A. Bulan, J. Kintrup, R. Weber, J. Stevanović, V. Panić and B. Friedrich, *Adv. Powder Technol.*, 2017, **28**, 43.
330. D. Li, N. Ichikuni, S. Shimazu and T. Uematsu, *Appl. Catal. A*, 1998, **172**, 351.
331. M. Pal, L. Wan, Y. Zhu, Y. Liu, Y. Liu, W. Gao, Y. Li, G. Zheng, A. A. Elzatahry, A. Alghamdi, Y. Deng and D. Zhao, *J. Colloid Interface Sci.*, 2016, **479**, 150.
332. U. Backman, U. Tapper and J. K. Jokiniemi, *Synthetic Metals*, 2004, **142**, 169.
333. F. Schröder, U. K. Sharma, M. Mertens, F. Devred, D. P. Debecker, R. Luque and E. V. V. d. Eycken, *ACS Catal.*, 2016, **6**, 8156.
334. X. Wang, J. Xue, X. Wang and X. Liu, *PLOS ONE*, 2017, **12**, e0176332.
335. Y. Choi, H.-i. Kim, G.-h. Moon, S. Jo and W. Choi, *ACS Catal.*, 2016, **6**, 821.
336. K. C. Pingali, S. Deng and D. A. Rockstraw, *Powder Technol.*, 2008, **183**, 282.
337. D. F. Ollis and H. Al-Ekabi, *Photocatalytic purification and treatment of water and air: proceedings of the 1st International Conference on TiO2 Photocatalytic Purification and Treatment of Water and Air, London, Ontario, Canada, 8-13 November, 1992*, Elsevier Science Ltd, 1993.
338. M. A. Fox and M. T. Dulay, *Chem. Rev.*, 1993, **93**, 341.
339. A. Linsebigler, G. Lu and J. Yates, *Chem. Rev*, 1995, **95**, 735.
340. H. Herrmann, S. T. Martin and M. R. Hoffmann, *J. Phys. Chem.*, 1995, **99**, 16641.
341. D. F. Ollis, E. Pelizzetti and N. Serpone, *Env. Sci. Technol.*, 1991, **25**, 1522.
342. S. U. Khan, M. Al-Shahry and W. B. Ingler, *science*, 2002, **297**, 2243.
343. S. Sakthivel and H. Kisch, *Angew. Chem. Int. Ed.*, 2003, **42**, 4908.
344. C. Burda, Y. Lou, X. Chen, A. Samia and J. Stout, *Nano Lett.*, 2003, **3**, 1049.
345. T. Murase, H. Irie and K. Hashimoto, *J. Phys. Chem. B*, 2004, **108**, 15803.
346. J. L. Gole, J. D. Stout, C. Burda, Y. Lou and X. Chen, *J. Phys. Chem. B*, 2004, **108**, 1230.
347. T. Phenrat, N. Saleh, K. Sirk, R. D. Tilton and G. V. Lowry, *Env. Sci. Technol.*, 2006, **41**, 284.
348. H. Xiong, M. Moyo, M. A. M. Motchelaho, L. L. Jewell and N. J. Coville, *Appl. Catal. A*, 2010, **388**, 168.
349. G. Yu, B. Sun, Y. Pei, S. Xie, S. Yan, M. Qiao, K. Fan, X. Zhang and B. Zong, *J. Am. Chem. Soc.*, 2010, **132**, 935.
350. B. Huskinson, J. Rugolo, S. K. Mondal and M. J. Aziz, *Energ. Env. Sci.*, 2012, **5**, 8690.
351. K. Cho and M. R. Hoffmann, *Chem. Mater.*, 2015, **27**, 2224.
352. K. S. Exner, J. Anton, T. Jacob and H. Over, *Angew. Chem. Int. Ed.*, 2014, **53**, 11032.
353. V. V. Panić, A. Dekanski, S. K. Milonjić, R. T. Atanasoski and B. Ž. Nikolić, *Colloids Surf. A*, 1999, **157**, 269.
354. S. Stopic, B. Friedrich, M. Schroeder and T. E. Weirich, *Mater. Res. Bull.*, 2013, **48**, 3633.
355. T. M. L. Wigley, R. Richels and J. A. Edmonds, *Nature*, 1996, **379**, 240.
356. P. Friedlingstein, R. M. Andrew, J. Rogelj, G. P. Peters, J. G. Canadell, R. Knutti, G. Luderer, M. R. Raupach, M. Schaeffer, D. P. van Vuuren and C. Le Quéré, *Nat. Geosci.*, 2014, **7**, 709.
357. M. A. A. Aziz, A. A. Jalil, S. Triwahyono and A. Ahmad, *Green Chem.*, 2015, **17**, 2647.
358. G. Gouget, D. P. Debecker, A. Kim, G. Olivieri, J.-J. Gallet, F. Bournel, C. Thomas, O. Ersen, S. Moldovan, C. Sanchez, S. Carenco and D. Portehault, *Inorg. Chem.*, 2017, **56**, 9225.
359. A. Kim, D. P. Debecker, F. Devred, V. Dubois, C. Sanchez and C. Sassoye, *Appl. Catal. B*, 2018, **220**, 615.
360. P. Frontera, A. Macario, M. Ferraro and P. Antonucci, *Catalysts*, 2017, **7**, 59.
361. C. V. Picasso, D. A. Safin, I. Dovgaliuk, F. Devred, D. Debecker, H.-W. Li, J. Proost and Y. Filinchuk, *Int. J. Hydrogen Energy*, 2016, **41**, 14377.
362. H. H. Shin, L. Lu, Z. Yang, C. J. Kiely and S. McIntosh, *ACS Catal.*, 2016, **6**, 2811.
363. R. Lippi, S. C. Howard, H. Barron, C. D. Easton, I. C. Madsen, L. J. Waddington, C. Vogt, M. R. Hill, C. J. Sumby, C. J. Doonan and D. F. Kennedy, *J. Mater. Chem. A*, 2017, **5**, 12990.
364. W. Wang, S. Wang, X. Ma and J. Gong, *Chem. Soc. Rev.*, 2011, **40**, 3703.
365. W. Wei and G. Jinlong, *Frontiers Chem. Sci. Eng.*, 2011, **5**, 2.
366. J. A. Mieth and J. A. Schwarz, *J. Catal.*, 1989, **118**, 203.
367. G. D. Weatherbee and C. H. Bartholomew, *J. Catal.*, 1984, **87**, 352.
368. S. Carenco, C. Sassoye, M. Faustini, P. Eloy, D. P. Debecker, H. Bluhm and M. Salmeron, *J. Phys. Chem. C*, 2016, **120**, 15354.
369. F. Solymosi, A. Erdohelyi and M. Kocsis, *J. Chem. Soc. Faraday Trans.*, 1981, **77**, 1003.
370. F. Wang, S. He, H. Chen, B. Wang, L. Zheng, M. Wei, D. G. Evans and X. Duan, *J. Am. Chem. Soc.*, 2016, **138**, 6298.
371. A. Kim, C. Sanchez, G. Patriarche, O. Ersen, S. Moldovan, A. Wisnet, C. Sassoye and D. P. Debecker, *Catal. Sci. Technol.*, 2016, **6**, 8117.
372. C. Fernández, C. Sassoye, D. P. Debecker, C. Sanchez and P. Ruiz, *Appl. Catal. A*, 2014, **474**, 194.
373. M. T. Le, J. Van Craenenbroeck, I. Van Driessche and S. Hoste, *Appl. Catal. A*, 2003, **249**, 355.

 This journal is © The Royal Society of Chemistry 20xx

Please do not adjust margins

Please do not adjust margins

374. M. T. Le, W. J. M. Van Well, I. Van Driessche and S. Hoste, *Appl. Catal. A*, 2004, **267**, 227.
375. F. E. Tuler, E. M. Gaigneaux, E. E. Miró, V. G. Milt and D. P. Debecker, *Catal. Commun.*, 2015, **72**, 116.
376. R. Huo, Y. Kuang, Z. Zhao, F. Zhang and S. Xu, *J. Colloid Interface Sci.*, 2013, **407**, 17.
377. G. Xiong, J. Yin, J. Liu, X. Liu, Z. Guo and L. Liu, *RSC Adv.*, 2016, **6**, 101365.
378. M. Santiago, A. Restuccia, F. Gramm and J. Pérez-Ramírez, *Microporous and Mesoporous Mater.*, 2011, **146**, 76.
379. G. M. Lari, A. B. L. de Moura, L. Weimann, S. Mitchell, C. Mondelli and J. Perez-Ramirez, *J. Mater. Chem. A*, 2017, **5**, 16200.
380. M. Pagliaro, R. Ciriminna, H. Kimura, M. Rossi and C. Della Pina, *Angew. Chem. Int. Ed.*, 2007, **46**, 4434.
381. A. Galadima and O. Muraza, *Waste Biomass Valorization*, 2017, **8**, 141.
382. J. R. Ochoa-Gómez, O. Gómez-Jiménez-Aberasturi, B. Maestro-Madurga, A. Pesquera-Rodríguez, C. Ramírez-López, L. Lorenzo-Ibarreta, J. Torrecilla-Soria and M. C. Villarán-Velasco, *Appl. Catal. A*, 2009, **366**, 315.
383. W. K. Teng, G. C. Ngoh, R. Yusoff and M. K. Aroua, *Energy Convers. Manage.*, 2014, **88**, 484.
384. M. O. Sonnati, S. Amigoni, E. P. Taffin de Givenchy, T. Darmanin, O. Choulet and F. Guittard, *Green Chem.*, 2013, **15**, 283.
385. S. Ramesh, L. van den Biggelaar, F. Devred and D. P. Debecker, *ChemCatChem*, 2018, In press.
386. F. S. H. Simanjuntak, T. K. Kim, S. D. Lee, B. S. Ahn, H. S. Kim and H. Lee, *Appl. Catal. A*, 2011, **401**, 220.
387. J. Li and T. Wang, *React. Kinet. Mech. Catal.*, 2011, **102**, 113.
388. P. Liu, M. Derchi and E. J. M. Hensen, *Appl. Catal. B*, 2014, **144**, 135.
389. P. Liu, M. Derchi and E. J. M. Hensen, *Appl. Catal. A*, 2013, **467**, 124.
390. A. Kumar, K. Iwatani, S. Nishimura, A. Takagaki and K. Ebitani, *Catal. Today*, 2012, **185**, 241.
391. A. Takagaki, K. Iwatani, S. Nishimura and K. Ebitani, *Green Chem.*, 2010, **12**, 578.
392. X. Zhang, D. Wang, J. Ma and W. Wei, *Catal. Lett.*, 2017, **147**, 1181.
393. A. V. Agafonov, I. A. Yamanovskaya, V. K. Ivanov, G. A. Seisenbaeva and V. G. Kessler, *J. Sol-Gel Sci. Technol.*, 2015, **76**, 90.
394. J. A. Kaduk and S. Pei, *J. Solid State Chem.*, 1995, **115**, 126.
395. F. Bamiduro, G. Ji, A. P. Brown, V. A. Dupont, M. Zhao and S. J. Milne, *ChemSusChem*, 2017, **10**, 2059.
396. J. B. Wagner, O. Timpe, F. A. Hamid, A. Trunschke, U. Wild, D. S. Su, R. K. Widi, S. B. A. Hamid and R. Schlögl, *Top. Catal.*, 2006, **38**, 51.
397. M.-J. Cheng and W. A. Goddard, *J. Am. Chem. Soc.*, 2015, **137**, 13224.
398. M.-J. Cheng and W. A. Goddard, *Top. Catal.*, 2016, **59**, 1506.
399. P. Kube, B. Frank, S. Wrabetz, J. Kröhnert, M. Hävecker, J. Velasco-Vélez, J. Noack, R. Schlögl and A. Trunschke, *ChemCatChem*, 2017, **9**, 573.
400. D. Vitry, J.-L. Dubois and W. Ueda, *J. Mol. Catal. A: Chem.*, 2004, **220**, 67.
401. M. M. Lin, *Appl. Catal. A*, 2003, **250**, 305.
402. P. Beato, A. Blume, F. Girgsdies, R. E. Jentoft, R. Schlögl, O. Timpe, A. Trunschke, G. Weinberg, Q. Basher, F. A. Hamid, S. B. A. Hamid, E. Omar and L. Mohd Salim, *Appl. Catal. A*, 2006, **307**, 137.
403. H. Murayama, D. Vitry, W. Ueda, G. Fuchs, M. Anne and J. L. Dubois, *Appl. Catal. A*, 2007, **318**, 137.
404. T. Ushikubo, K. Oshima, A. Kayou and M. Hatano, *Stud. Surf. Sci. Catal.*, 1997, **112**, 473.
405. D. Weber, P. Weidler and B. Kraushaar-Czarnetzki, *Top. Catal.*, 2017, **60**, 1401.
406. M. Baca and J.-M. M. Millet, *Appl. Catal. A*, 2005, **279**, 67.
407. Y. Moro-Oka and W. Ueda, *Adv. Catal.*, 1994, **40**, 233.
408. K. Schuh, W. Kleist, M. Høj, V. Trouillet, P. Beato, A. Jensen and J.-D. Grunwaldt, *Catalysts*, 2015, **5**, 1554.
409. V. I. Sobolev, K. Y. Koltunov and G. A. Zenkovets, *Catal. Lett.*, 2017, **147**, 310.
410. B. Farin, A. H. A. Monteverde Videla, S. Specchia and E. M. Gaigneaux, *Catal. Today*, 2015, **257**, 11.
411. P. Sprenger, W. Kleist and J.-D. Grunwaldt, *ACS Catal.*, 2017, **7**, 5628.
412. B. Farin, C. Swalus, M. Devillers and E. M. Gaigneaux, *Catal. Today*, 2013, **203**, 24.
413. I. Van Driessche, R. Mouton and S. Hoste, *Mater. Res. Bull.*, 1996, **31**, 979.
414. E. Godard, E. M. Gaigneaux, P. Ruiz and B. Delmon, *Catal. Today*, 2000, **61**, 279.
415. J. A. Schwarz, C. Contescu and A. Contescu, *Chem. Rev.*, 1995, **95**, 477.
416. Y. Wei, J. Liu, Z. Zhao, A. Duan, G. Jiang, C. Xu, J. Gao, H. He and X. Wang, *Energ. Env. Sci.*, 2011, **4**, 2959.
417. B. Guan, R. Zhan, H. Lin and Z. Huang, *J. Env. Manage.*, 2015, **154**, 225.
418. S. Quiles-Diaz, J. Gimenez-Manogil and A. Garcia-Garcia, *RSC Adv.*, 2015, **5**, 17018.
419. E. Aneggi, D. Wiater, C. de Leitenburg, J. Llorca and A. Trovarelli, *ACS Catal.*, 2014, **4**, 172.
420. S. Liu, X. Wu, D. Weng, M. Li and R. Ran, *ACS Catal.*, 2015, **5**, 909.
421. F. E. Tuler, R. Portela, P. Ávila, E. D. Banús, E. E. Miró and V. G. Milt, *Appl. Catal. A*, 2015, **498**, 41.
422. F. E. Tuler, E. D. Banús, M. A. Zanuttini, E. E. Miró and V. G. Milt, *Chem. Eng. J.*, 2014, **246**, 287.
423. H. Koga, S. Fukahori, T. Kitaoka, M. Nakamura and H. Wariishi, *Chem. Eng. J.*, 2008, **139**, 408.
424. H. Ishihara, H. Koga, T. Kitaoka, H. Wariishi, A. Tomoda and R. Suzuki, *Chem. Eng. Sci.*, 2010, **65**, 208.
425. H. Koga, S. Fukahori, T. Kitaoka, A. Tomoda, R. Suzuki and H. Wariishi, *Appl. Catal. A*, 2006, **309**, 263.
426. H. Koga, T. Kitaoka and H. Wariishi, *Chem. Commun.*, 2008, 5616.

Please do not adjust margins

Please do not adjust margins

427. H. Koga, Y. Umemura, H. Ishihara, T. Kitaoka, A. Tomoda, R. Suzuki and H. Wariishi, *Appl. Catal. B*, 2009, **90**, 699.
428. M. Piumetti, S. Bensaid, N. Russo and D. Fino, *Appl. Catal. B*, 2016, **180**, 271.
429. M. Kim, H.-J. Chae, T.-W. Kim, K.-E. Jeong, C.-U. Kim and S.-Y. Jeong, *J. Ind. Eng. Chem.*, 2011, **17**, 621.
430. Z. Liu and C. Zhou, *Prog. Nat. Sci. Mater. Int.*, 2015, **25**, 334.
431. D. Cui, J. Liu, J. Yu, F. Su and G. Xu, *Catal. Sci. Technol.*, 2015, **5**, 3119.
432. C. Mebrahtu, S. Abate, S. Perathoner, S. Chen and G. Centi, *Catal. Today*, 2017.
433. M. C. Bacariza, R. Bértolo, I. Graça, J. M. Lopes and C. Henriques, *J. CO2 Utilization*, 2017, **21**, 280.
434. R. A. Hubble, J. Y. Lim and J. S. Dennis, *Faraday Discuss.*, 2016, **192**, 529.
435. X. Duan and D. G. E. Evans, *Layered double hydroxydes*, Springer, Berlin/Heidelberg, 2006.
436. C. Forano, U. Costantino, V. Prévot and C. T. Gueho, in *Developments in Clay Science*, ed. G. L. E. Faiza Bergaya, Elsevier, 2013, vol. 5, pp. 745.
437. Q. Wang and D. O'Hare, *Chem. Rev.*, 2012, **112**, 4124.
438. S. P. Newman and W. Jones, *New J. Chem.*, 1998, **22**, 105.
439. J. Cornejo, R. Celis, I. Pavlovic and M. A. Ulibarri, *Clay Min.*, 2008, **43**, 155.
440. V. Rives, M. del Arco and C. Martín, *J. Controlled Release*, 2013, **169**, 28.
441. K.-H. Goh, T.-T. Lim and Z. Dong, *Water Res.*, 2008, **42**, 1343.
442. D. P. Debecker, E. M. Gaigneaux and G. Busca, *Chem. Eur. J.*, 2009, **15**, 3920.
443. Z. P. Xu, J. Zhang, M. O. Adebajo, H. Zhang and C. Zhou, *Appl. Clay Sci.*, 2011, **53**, 139.
444. G. Fan, F. Li, D. G. Evans and X. Duan, *Chem. Soc. Rev.*, 2014, **43**, 7040.
445. F. Zhang, X. Xiang, F. Li and X. Duan, *Catal. Surv. Asia*, 2008, **12**, 253.
446. S. He, Z. An, M. Wei, D. G. Evans and X. Duan, *Chem. Commun.*, 2013, **49**, 5912.
447. V. Prevot and Y. Tokudome, *J. Mater. Sci.*, 2017, **52**, 11229.
448. V. Prevot, C. Forano and J. P. Besse, *Chem. Mater.*, 2005, **17**, 6695.
449. Y. Zhao, F. Li, R. Zhang, D. G. Evans and X. Duan, *Chem. Mater.*, 2002, **14**, 4286.
450. V. Prevot, C. Szczepaniak and M. Jaber, *J. Colloid Interface Sci.*, 2011, **356**, 566.
451. Y. Wang, F. Zhang, S. Xu, X. Wang, D. G. Evans and X. Duan, *Ind. Eng. Chem. Res.*, 2008, **47**, 5746.
452. F. Mohammadparast, R. Halladj and S. Askari, *Chem. Eng. Commun.*, 2015, **202**, 542.
453. T. Tago, H. Konno, M. Sakamoto, Y. Nakasaka and T. Masuda, *Appl. Catal. A*, 2011, **403**, 183.
454. N. Viswanadham, S. K. Saxena, J. Kumar, P. Sreenivasulu and D. Nandan, *Fuel*, 2012, **95**, 298.
455. D. P. Serrano, J. Aguado, J. M. Escola, A. Peral, G. Morales and E. Abella, *Catal. Today*, 2011, **168**, 86.
456. D. P. Serrano, J. Aguado, G. Morales, J. M. Rodríguez, A. Peral, M. Thommes, J. D. Epping and B. F. Chmelka, *Chem. Mater.*, 2009, **21**, 641.
457. D. P. Serrano, J. Aguado, J. M. Escola, J. M. Rodriguez and A. Peral, *J. Mater. Chem.*, 2008, **18**, 4210.
458. Y.-P. Guo, H.-J. Wang, Y.-J. Guo, L.-H. Guo, L.-F. Chu and C.-X. Guo, *Chem. Eng. J.*, 2011, **166**, 391.
459. Y. Zhang, K. Zhu, X. Duan, P. Li, X. Zhou and W. Yuan, *RSC Adv.*, 2014, **4**, 14471.
460. Z. Guo, G. Xiong, L. liu, J. Yin, R. Zhao and S. Yu, *RSC Adv.*, 2015, **5**, 71433.
461. K. Lin, O. I. Lebedev, G. Van Tendeloo, P. A. Jacobs and P. P. Pescarmona, *Chem. Eur. J.*, 2010, **16**, 13509.
462. D. Serrano, R. Sanz, P. Pizarro and I. Moreno, *Chem. Commun.*, 2009, 1407.
463. M. G. Clerici and P. Ingallina, *J. Catal.*, 1993, **140**, 71.
464. Z. Deng, Y. Yang, X. Lu, J. Ding, M. He and P. Wu, *Catal. Sci. Technol.*, 2016, **6**, 2605.
465. A.-L. Adedigba, G. Sankar, C. R. A. Catlow, Y. Du, S. Xi and A. Borgna, *Microporous Mesoporous Mater.*, 2017, **244**, 83.
466. A. B. D. Nandiyanto, F. Iskandar and K. Okuyama, *Chem. Eng. J.*, 2009, **152**, 293.
467. TSI Incorporated - Aerosol generators & dispersers, http://www.tsi.com/aerosol-generators-and-dispersers/.
468. Büchi - Spray Drying & Encapsulation Solutions, https://www.buchi.com/en/content/spray-drying-encapsulation-solutions.
469. GEO - Spray driers, https://www.gea.com/en/productgroups/dryers_particle-processing-systems/spray-dryers/index.jsp.
470. Dorst - Spray drying plants, https://www.dorst.de/en/spray-drying-plants.html.
471. P. J. Bruinsma, S. Baskaran, J. R. Bontha and L. J., US5922299 (A), 1999, Mesoporous-silica films, fibers, and powders by evaporation.
472. T. Yanagisawa, *Bull. Chem. Soc. Jpn.*, 1990, **63**, 988.
473. A. Chaumonnot, C. Sanchez, C. Boissiere, F. Colbeau-Justin and A. Bonduelle, WO2012085358, 2012, Method for preparing a spherical materials having a hierarchized porosity and including metal particles trapped in a silicon matrix
474. D. P. Debecker, F. Colbeau-Justin, C. Sanchez and A. Chaumonnot, WO2014202888, 2014, Method for olefin metathesis using a catalyst made from a spherical material having a hierarchised porosity comprising metal oxide partciles trapped in a matrix comprising silicon oxide
475. A. Chaumonnot and A. Fecant, WO2017089110, 2017, Method for synthesizing hydrocarbons from a syngas in the presence of a cobalt catalyst trapped in a mesoporous oxide matrix and obtained from at least one colloidal precursor
476. A. Chaumonnot and A. Fecant, WO2017089111, 2017, Process for synthesizing hydrocarbons from syngas in the presence of a cobalt catalyst trapped in a mesoporous oxide matrix and obtained from at least one monomeric precursor

 This journal is © The Royal Society of Chemistry 20xx

Please do not adjust margins

Please do not adjust margins

477. A. Chaumonnot, C. Sanchez, C. Boissère, F. Colbeau-Justin, K. Marchand, E. Devers, A. Bonduelle, D. Uzio, A. Daudin and B. Guichard, US2014005031, 2014, Spherical material based on heteropolyanions trapped in a mesostructured oxide matric and use thereof as catalyst in hydrocarbon refining processes
478. A. Bonduelle and A. Chaumonnot, US2011073522, 2011, Catalyst based on an amorphous material comprising silicon with a hierarchical and organized porosity, and an improved process for the treatment of hydrocarbon feeds
479. A. Chaumonnot, C. Sanchez, C. Boissère, F. Colbeau-Justin and A. Bonduelle, US2014021096, 2010, Process for preparing a spherical material with a hierarchical porosity comprising metallic particles trapped in a mesostructured Matrix.
480. W. Schutyser, S. Van den Bosch, J. Dijkmans, S. Turner, M. Meledina, G. Van Tendeloo, D. P. Debecker and B. F. Sels, *ChemSusChem*, 2015, **8**, 1805.
481. W. Schutyser, T. Renders, S. Van den Bosch, S. F. Koelewijn, G. T. Beckham and B. F. Sels, *Chem. Soc. Rev.*, 2018, DOI: 10.1039/C7CS00566K.
482. M. N. Rashed, S. M. A. H. Siddiki, M. A. Ali, S. K. Moromi, A. S. Touchy, K. Kon, T. Toyao and K.-i. Shimizu, *Green Chem.*, 2017, **19**, 3238.
483. M. J. Climent, A. Corma and S. Iborra, *ChemSusChem*, 2009, **2**, 500.
484. Christopher M. A. Parlett, Mark A. Isaacs, Simon K. Beaumont, Laura M. Bingham, Nicole S. Hondow, K. Wilson and Adam F. Lee, *Nat. Mater.*, 2015, **15**, 178.
485. A. Corma, *Catal. Rev.*, 2004, **46**, 369.
486. T. Gemci and N. Chigier, in *Production, Handling and Characterization of Particulate Materials*, eds. H. G. Merkus and G. M. H. Meesters, Springer International Publishing, Cham, 2016, DOI: 10.1007/978-3-319-20949-4_7, pp. 201.
487. K. Omer and N. Ashgriz, in *Handbook of Atomization and Sprays: Theory and Applications*, ed. N. Ashgriz, Springer US, Boston, MA, 2011, DOI: 10.1007/978-1-4419-7264-4_24, pp. 497.
488. S. Pega, A. Coupe, C. Boissère, T. Azais, D. Grosso, C. Sanchez, J. Blanchard, D. Massiot and A. Chaumonnot, in *Nanoporous Materials*, WORLD SCIENTIFIC, 2012, DOI: 10.1142/9789812779168_0048, pp. 457.
489. A. Corma, H. García and F. X. Llabrés i Xamena, *Chem. Rev.*, 2010, **110**, 4606.
490. S. Lin, C. S. Diercks, Y.-B. Zhang, N. Kornienko, E. M. Nichols, Y. Zhao, A. R. Paris, D. Kim, P. Yang, O. M. Yaghi and C. J. Chang, *Science*, 2015, **349**, 1208.
491. A. H. Chughtai, N. Ahmad, H. A. Younus, A. Laypkov and F. Verpoort, *Chem. Soc. Rev.*, 2015, **44**, 6804.
492. M. Rubio-Martinez, C. Avci-Camur, A. W. Thornton, I. Imaz, D. Maspoch and M. R. Hill, *Chem. Soc. Rev.*, 2017, **46**, 3453.
493. A. Garcia Marquez, P. Horcajada, D. Grosso, G. Ferey, C. Serre, C. Sanchez and C. Boissiere, *Chem. Commun.*, 2013, **49**, 3848.
494. C. Avci-Camur, J. Troyano, J. Perez-Carvajal, A. Legrand, D. Farrusseng, I. Imaz and D. Maspoch, *Green Chem.*, 2018, DOI: 10.1039/C7GC03132G.
495. M. Kubo, T. Saito and M. Shimada, *Microporous Mesoporous Mater.*, 2017, **245**, 126.
496. H. K. Arslan, O. Shekhah, J. Wohlgemuth, M. Franzreb, R. A. Fischer and C. Wöll, *Adv. Funct. Mater.*, 2011, **21**, 4228.
497. L. Garzón-Tovar, S. Rodríguez-Hermida, I. Imaz and D. Maspoch, *J. Am. Chem. Soc.*, 2017, **139**, 897.

This journal is © The Royal Society of Chemistry 20xx

Please do not adjust margins